The Messenger

No. 139 – March 2010

Laser development at ESO
Progress on KMOS
Black hole mass of Cen-A
A strongly lensed sub-millimetre galaxy

The Visible and Infrared Survey Telescope for Astronomy (VISTA): Looking Back at Commissioning

Jim Emerson[1]
Will Sutherland[1]

[1] Astronomy Unit, Queen Mary University of London, United Kingdom

The ESO near-infrared survey telescope, VISTA, is about to enter operation. Dry runs for VISTA's Public Surveys have been in progress since November 2009 and the full surveys will begin soon. Some points from the VISTA commissioning are outlined.

Introduction

VISTA, the Visible and Infrared Survey Telescope for Astronomy, is a 4.1-metre wide-field survey telescope, equipped with a 1.65-degree field, (67-Mpixel) near-infrared (NIR) camera, for performing extensive surveys of the southern skies with sensitivity matched to the needs of 8-metre-class telescopes. Over its first five years of operations, the majority of VISTA's time will be used for six ESO Public Surveys (Arnaboldi et al., 2007). NIR imaging surveys particularly target the cold, the obscured, and the high redshift Universe, to generate science directly and also in order to select objects worthy of further study by the Very Large Telescope (VLT).

Details of the design of VISTA were given in Emerson et al. (2004), a progress update in Emerson et al. (2006), pictures of the NIR camera in *The Messenger* (131, 6), the site in issue 132 (p. 55), the primary mirror (M1) installation in issues 132 and 133 (p. 6 and 67 respectively), the camera being lifted up through the azimuth floor (138, 2) and the first release of images was also described in *The Messenger* (138, 2). Here we outline some interesting points from the commissioning period.

Credit: S. Beard

Figure 1. VISTA's camera is shown being mounted onto the telescope. The camera (black) has been lifted from the ground floor through a removable sector in the dome floor, using the enclosure crane (yellow at top) and the lifting arm (blue). The enclosure is rotated to place the camera behind the telescope (this picture). Next the camera is moved into the M1 hole and bolted to the Cassegrain rotator, and finally the electronics boxes are fitted.

Early work

The only change from the system described in Emerson et al. (2004) was that a *Z* filter was added in the camera, as the Raytheon Vision Systems IR detectors were measured to have a quantum efficiency (QE) that was still good even at a wavelength as short as *Z* (0.88 μm) — where QE ~ 70 %.

Commissioning generally went smoothly, with no major problems requiring redesign or re-manufacture, although most tasks tended to take rather longer than anticipated. It was heartening that there were no fundamental problems, but frustrating that many individually small problems each took time to solve. Here we focus on some points that arose, but the emphasis here on problems that were solved should not obscure the fact that VISTA now works very well, as the images from the press release in December 2009 (ESO Press Release eso0949) and the image of part of the Orion Nebula, on the front cover, demonstrate.

Credit: S. Beard

Figure 2. A view of VISTA's camera on the telescope with all the electronics boxes mounted (with their back covers off in this image). The open lifting hatch can be seen on the right, with the yellow crane above. The white circle at the top serves both as a Moon screen, and as a screen for taking linearity sequences and instrument health monitoring frames.

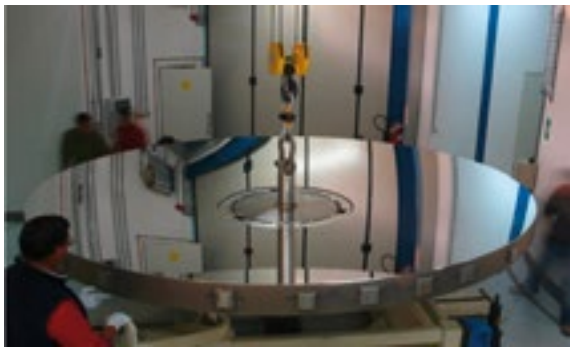

Figure 3. M1 after coating in protected silver in the VISTA coating plant.

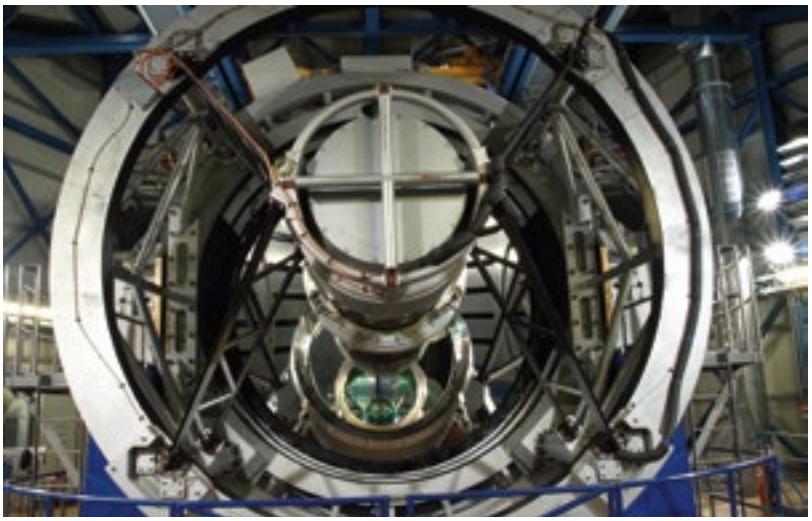

Credit: J. Emerson

Figure 4. The VISTA telescope shown from the front at low elevation.

To start with, construction went smoothly, and the enclosure was ready for the telescope structure, which was installed during 2006. In early 2007, we had a run with dummy masses in place of the mirrors, and a small 20-cm telescope mounted on the Cassegrain rotator, looking up through a hole in the top-end structure (designed for this reason). This run was useful to debug the telescope software, build a preliminary pointing model, and showed that the basic tracking and slewing performance were good.

Shortly afterwards, the secondary mirror (M2) arrived and was successfully coated in protected silver. VISTA's camera was flown to Chile in January 2007 and checked out for performance on site, using a small "spot projector" mounted in front of the window. There had been no damage in transport, and the process of mounting the camera onto the telescope was subsequently tried out successfully (see Figure 1). Figure 2 shows the back view of VISTA, with the camera and its electronics boxes mounted on the Cassegrain rotator.

Primary mirror (M1) polishing

So far so good! However the time taken to complete the polishing of M1 then prevented VISTA being delivered on the timescale expected at that time. This 4.1-metre f/1 mirror is the most highly curved large mirror ever polished and this task proved to take much longer than anticipated. The fast mirror means that it is highly aspheric, with departures from the best-fit sphere of around 0.8 mm; this means that small polishing tools were needed, different for different zones on the mirror, which increases the polishing time. This was a known difficulty from early on, but it appears that the timescales were underestimated by the manufacturer. The lateness was especially frustrating as the very first thing the VISTA project did after securing funding was to purchase the M1 blank in 2001 and the shaping of the blank was complete by April 2003, so it was highly regrettable that completion of M1 took so long, and that the manufacturer's polishing time estimates only converged to the actual time so very near to the end. However, the quality of polishing finally achieved was high. To claw back some time, the M1 was not shipped by sea, but instead was flown from Moscow to Antofagasta in an Antonov transport plane, arriving at VISTA during Easter 2008.

The coating plant provided with VISTA then produced a very high quality and stable coating in protected silver (see Figure 3), enhancing VISTA's sensitivity compared to a conventional aluminium coating.

Camera on sky

As soon as the M1 mirror had been coated it was installed in the telescope, and a test camera containing a Shack–Hartmann system was used to set up an initial pointing model and active optics settings. It soon became apparent that the system showed some trefoil (a third order optical aberration). It was suspected that this was associated with the M2 axial definers, and this was confirmed by mounting the M2 and its cell rotated by 180 degrees, which changed the sign of the trefoil. Then, the M2 manufacturers came to Chile, disassembled and inspected the M2 cell. They found nothing wrong, and it was carefully reassembled, in parallel with VISTA's camera being mounted in place of the test camera (see Figure 4). It was expected that the active support forces on M1 would be able to compensate for the effect of the trefoil on M2, and this indeed proved to be the case. It is still unclear how this trefoil arose. Measurements at the factory showed trefoil was not present there, when tested with similar support forces to those when mounted on the telescope. It is not possible to rotate M2 relative to its cell to see if the trefoil is due to the cell or the mirror itself. As the system image quality now comfortably meets its specification of 50 % encircled energy diameter of 0.51 arcseconds, the trefoil has been accepted, though it would be good to understand its origin and then hopefully get rid of it at source, rather than correcting with M1 forces.

The camera first observed the sky on 23 June 2008 with the auxiliary CCDs (for autoguiding and wavefront sensing), and with the IR detectors on 24 June. The first images were recognisable with the expected setup parameters, and the image quality was improved over the

subsequent nights with various adjustments to the many M1 and M2 positions and forces. The pointing and tracking was good. Figure 4 shows VISTA from the front with all components present and working. No mechanical adjustments were needed to the camera, a tribute to the engineering done by the camera team led by the Science and Technology Facilities Council (STFC) run Rutherford Appleton Laboratory.

The camera background was checked and the non-linearity of the detectors measured robustly. At this stage, image data was not being archived by ESO, so it was written to 250 GB USB disks which were taken back to the UK in hand baggage for analysis in the UK. There were occasional problems with the IRACE number-cruncher workstations overheating causing data outage; once traced, this was simple to solve.

Active optics

Over the following months the active optics corrections for achieving the best image quality were all generated for various azimuths, altitudes and temperatures, and the autoguiding and wavefront sensing software was stress-tested and made more robust. This was quite a lengthy process, since there are numerous correction terms, and the many Zernike polynomials and mirror modes are measured in detector coordinates, but require de-rotating into telescope coordinates to apply corrections to M2 position and M1 forces; thus, getting all the signs and phases right was quite time-consuming. Also, there were some complications: we found a small astigmatism co-rotating with the camera, possibly due to a thermal gradient; this was fixed in software by adding an M1 active force pattern that co-rotates with the camera.

Focus gradients across the very large detector plane were also complicated, and we eventually decomposed these into three problems: one was a subtle software error (dependent on radial position of the wavefront sensor stars), another was a real focus gradient “fixed to the telescope”, and thirdly a smaller focus gradient “fixed to the camera”. The gradient “fixed to the telescope” was quite large, and required a 1.3-mm lateral movement of M1 to align it to the Cassegrain axis; this should have been simple, but in practice there was not quite enough clearance in the M1 axial definers, thus requiring removal of the M1 to adjust the three axial definers. There was considerable worry here about whether the calculated sign was correct, and fortunately it was. The small camera focus gradient is still present at the time of writing, but is soon to be eliminated with a new shim between the camera and Cassegrain rotator. The co-planarity of the 16 detectors appears to be excellent, so once M1 and the camera are one-off aligned to the Cassegrain rotator axis, the active optics system automatically keeps M2 collimated, giving good images across the entire field.

Filter wheel

At first, changing the filters was very reliable, but by October 2008 it was noticed that the 1.37-metre diameter filter wheel (the only moving part inside the cold camera) occasionally failed to reach its demand position. Many experiments were done looking at the software and electronics, but the intermittent problem gradually became more and more frequent. By February 2009 there was nothing for it but to take the camera off, warm it up, open up the cryostat and look at the parts. Surprisingly it was found that a jacking screw (used for assembly and disassembly) had worked loose and had unscrewed itself enough to foul the filter wheel, scraping off a ring of paint and some metal swarf. There were flakes of paint all over the filters themselves, explaining why the flat fields had been becoming unexpectedly variable. The filter trays were removed and the filters cleaned, the debris was cleaned out of the rest of the camera, and the offending jacking screw removed. No damage to the filters or detectors resulted, and the motor drive also proved resilient. The opportunity was taken to change the order of the filters in the wheel to a more efficient one for the selected ESO Public Surveys, and to fill the one remaining empty filter tray with two paired half-sets of narrowband filters at 975 and 985 nm which were available. After the camera was pumped and cooled down again, VISTA was back on sky in March 2009. The filter wheel has worked well ever since.

Unfortunately soon after this, one of the three closed-cycle coolers on the camera had a major breakdown; the required spare parts turned out to be very similar, but not quite identical, to those held in the Paranal stores; hence getting these parts from Europe caused another minor delay.

Azimuth and M2 support oscillations

An annoying problem was that, under certain reproducible conditions (where the azimuth axis was moving very slowly), the azimuth drive servo loop went into oscillation, exciting an 11.6-Hz resonance in the telescope structure and turning the images into “sticks”. This was fixed by installing an electronic notch filter in the servo, after which there were no more azimuth oscillations.

Another problem was intermittent small (~ 1/2 arcsecond) ~ 2 Hz oscillations of the hexapod which controls the position of the secondary mirror, which was small enough to go unnoticed until the focus gradients were sorted out. This was affecting one-third to half of the data taken, and making it very hard to demonstrate the intrinsic image quality of the system. After considerable analysis and experimentation, in August 2009 new servo parameters were identified and these oscillations ceased. After this, it was possible to reliably achieve the required image quality of the final system, and to demonstrate that the 50 % encircled energy distribution was comfortably within the 0.51-arcsecond specification.

The future

The above is only a selection of (perhaps) interesting points, and a fuller description of commissioning will be presented at the 2010 SPIE meeting in San Diego. Much software-related work was also done, both to improve the system, and to ensure that the observing overheads were minimised.

VISTA is now working very well, producing images with the depth and quality

Credit: ESO/J. Emerson/VISTA. Acknowledgement: CASU

Figure 5. Orion Nebula (M 42 and M 43) composite image in *ZJKs* filters is shown. See ESO Press Release eso1006 for more details.

expected, with minor improvements being worked on to further enhance its reliability. The VISTA *ZJKs* 1 × 1.5 degree image of the Orion Nebula in Figure 5, of which the front cover image is a only a small part, indicates how impressive its wide-field views are.

Acknowledgements

The VISTA Project Office at STFC's UK Astronomy Technology Centre managed the integration and commissioning of VISTA and skillfully coordinated the work of all those individuals and organisations involved. The Cambridge Astronomical Survey Unit (CASU), part of the UK's VISTA Data Flow System, provided invaluable assistance in assessing the image data acquired during commissioning.

References

Arnaboldi, M. et al. 2007, The Messenger, 127, 28
Emerson, J. et al. 2004, The Messenger, 117, 27
Emerson, J. et al. 2006, The Messenger, 126, 41

VISTA Science Verification — The Galactic and Extragalactic Mini-surveys

Magda Arnaboldi[1]
Monika Petr-Gotzens[1]
Marina Rejkuba[1]
Mark Neeser[1]
Thomas Szeifert[1]
Valentin D. Ivanov[1]
Wolfgang Hummel[1]
Michael Hilker[1]
Nadine Neumayer[1]
Palle Møller[1]
Kim Nilsson[1]
Bram Venemans[1]
Evanthia Hatziminaoglou[1]
Gaitee Hussain[1]
Thomas Stanke[1]
Paula Teixeira[1]
Suzanne Ramsay[1]
Jörg Retzlaff[1]
Remco Slijkhuis[1]
Fernando Comerón[1]
Jorge Melnick[1]
Martino Romaniello[1]
Jim Emerson[2]
Will Sutherland[2]
Mike Irwin[3]
Jim Lewis[3]
Simon Hodgkin[3]
Eduardo Gonzales-Solares[3]

[1] ESO
[2] VISTA Consortium, Queen Mary University of London, United Kingdom
[3] Cambridge Astronomical Surveys Unit (CASU), University of Cambridge, United Kingdom

The Visible and Infrared Survey Telescope for Astronomy (VISTA) will be mostly dedicated to the execution of ESO public surveys, requiring large amounts of service observing time. VISTA Science Verification (SV) thus differs from that usually implemented for other VLT instruments. VISTA SV consisted of two self-contained mini-surveys: a Galactic mini-survey in the region around the Orion Belt stars; and a deep extragalactic mini-survey of the nearby spiral galaxy NGC 253. ESO astronomers used these mini-surveys as benchmarks to optimise the survey operation procedures, minimise overheads, and experience the full end-to-end process of survey data acquisition. The raw data and associated calibrations from both mini-surveys were released in December 2009, and the reduced images and catalogues will soon be available, enabling the first exciting science with VISTA.

Introduction

In the Commissioning–Science Verification–Paranalisation cycle of VLT instruments, Science Verification is typically executed five to two months prior to the start of operations of a given VLT instrument. In the case of VISTA and its camera VIRCAM (Emerson et al., 2004), its start of operation is equivalent to the start of operation of an entire new telescope, a new instrument and a new schema for operations (Sciops 2.0). For ESO service mode operations, the execution of the VISTA public surveys represents a challenge, since they require the definition of several thousands of observing blocks (OBs) that need to be managed, scheduled and executed in the most efficient way. The service mode operations for public surveys use a new version of the Phase 2 Proposal Preparation tool (P2PP) and a new Observing Tool (OT); see Arnaboldi et al. (2008). The creation of OBs for public surveys also requires a new tool called SADT (Survey Area Definition Tool) for the definition of the survey geometry, e.g., filled field positions (or tiles) at a given position on the sky or large areas of several degrees, and the sequence of "pawprint" offsets required for the homogeneous coverage of the VISTA camera focal plane (the 16 detectors in the VIRCAM focal plane are non-contiguous, see Figure 4 of Emerson et al., 2004), and for finding the necessary guide and active optics stars for each pawprint. In addition, VISTA has a different dataflow and quality control (QC) with respect to the other VLT instruments. Finally VISTA and its camera VIRCAM are expected to produce an order of magnitude more data than all the other VLT instruments combined.

The VISTA SV was therefore a fundamental part of the procedure for verification of the end-to-end system for the VISTA telescope + VIRCAM camera + Quality Control + Archive operations. While the individual components could be tested through previous verification and commissioning activities, VISTA SV has enabled ESO to carry out the full test of the integrated system, tools and interfaces across departments, in a "survey-like" operation mode for the first time, and proves that ESO has a robust system in place.

The VISTA SV projects — the Galactic and extragalactic mini-surveys

SV consists of the execution of two self-contained mini-surveys, one Galactic and one extragalactic, which were defined by teams of astronomers from ESO and the community. The execution of two mini-surveys in a single time allocation of two weeks allowed ESO to optimise the survey operations procedures, experience the full end-to-end process of survey data, and fulfill the goals of the science verification policy by providing the community with a complete and scientifically exciting set of new data.

The VISTA SV Galactic and extragalactic science cases are briefly described.

The Galactic survey project — Orion

Participants:
– ESO: Fernando Comerón, Gaitee Hussain, Monika Petr-Gotzens, Suzanne Ramsay, Thomas Stanke, Paula Teixeira
– External: Juan M. Alcalá, Cesar Briceño, Mark McCaughrean, Joana Oliveira, Loredana Spezzi, Elaine Winston, Maria Rosa Zapatero Osorio, Hans Zinnecker
– QMUL/VISTA/CASU: Jim Emerson, Will Sutherland, Mike Irwin, Jim Lewis, Simon Hodgkin, Eduardo Gonzalez-Solares

The Orion star-forming region had been identified as an ideal VISTA SV target to study several aspects of star formation, early stellar evolution, and the interplay between OB stars and their immediate environment. In particular, an area of approximately 30 square degrees in the region of the Orion Belt, roughly centred at RA = 05h 32m, DEC = – 00° 18′, was chosen for a deep VISTA survey making use of all VISTA broadband filters (*Z, Y, J, H, Ks*). Orion is the closest giant molecular cloud at an average distance of ~ 400 pc, and has been actively

forming stars within at least the last 10 Myr (e.g., Bally, 2008), which is about the timescale on which giant planets are thought to be formed. The VISTA–Orion survey area includes a number of stellar groups of different ages, among which are: very young (~ 1 Myr old) stellar clusters, sometimes still embedded in the molecular cloud material (NGC 2024, NGC 2023, NGC 2068 and NGC 2071, see Figure 1); the intermediate-age cluster σ Ori (age ~ 3 Myr); parts of the older stellar OB associations Ori OB1b (~ 5 Myr) and Ori OB1a (~ 10 Myr); as well as the recently identified stellar group of almost 200 pre-main sequence (PMS) stars around the B-star 25 Ori (~ 10 Myr).

One of the main goals of the Galactic VISTA SV project is to detect the young stellar and substellar populations present in the survey area, to a depth that goes significantly beyond current limits, and hence to investigate the substellar initial mass function (IMF) down to 10–20 M_{Jup}. This study will probe environmental effects and possible non-universality on the very low-mass end of the IMF. With targeted survey sensitivity limits of Z = 22.7 mag, Y = 21.0 mag, J = 20.2 mag, H = 19.2 mag and Ks = 18.4 mag, objects with masses as low as 12 M_{Jup} and as old as 10 Myr can be uncovered. At somewhat younger ages, e.g., 5 Myr, a 10 M_{Jup} object is expected to show a brightness of J = 19.4 mag and Ks = 18.0 mag at the distance of Orion (according to the DUSTY evolutionary models of Chabrier et al., 2000). The use of all VISTA *ZYJHKs* filters allows an optimal photometric selection of candidate pre-main sequence Orion members. Complementary data, for example from Spitzer and X-ray surveys, also provide helpful additional indications for the youth of individual candidate PMS objects. Since variability has been recognised to be another indicator of youth, a small subset of the survey has also been designed to study photometric variability on timescales of days in the field of the stellar aggregate around 25 Ori.

Additional goals of the survey include:

– A comprehensive spectral energy distribution analysis to search for optically thick discs and a further analysis of their evolution over a timescale of 1–10 Myr, the range of ages of the populations present in the VISTA–Orion survey. Understanding the evolution of accretion discs can provide strong constraints on theories of planet formation, and measuring the lowest mass at which young objects harbour circumstellar discs is crucial for determining whether planets can form around low-mass brown dwarfs.
– Detection of scattered light emission from the discs/envelopes of protostars detected by Spitzer observations in the Orion Cloud B. A wavelength coverage from the Z- to Ks-band of such structures is very useful for models of circumstellar envelopes, as they provide a direct estimate of the outflow cavity opening angles and orientations.
– Photometric variability of very low-mass stars and brown dwarfs.

Figure 1. This image shows a roughly 16 × 16 arcminute area of a VISTA tile taken on the Orion cloud B, observing the cluster NGC 2071. The centre of NGC 2071 shows up in scattered light (blue reflection nebulosity). Star formation activity is seen in the immediate surroundings of the cluster. The image is a colour-composite made from observations using the VISTA Z (blue), J (green), and Ks (red) filters. The image is tilted at position angle 15 degrees from north.

Observing strategy for the Orion survey

The survey consisted of observing 20 contiguous tiles covering a total area of ~ 30 square degrees, and with each tile being tilted by a position angle of 15 degrees. Each tile has a size of approximately 1 by 1.5 degrees and defines a fully covered area stacked from six VISTA pawprint positions. Furthermore, the tiles overlap by 60 arcseconds in the X-direction (i.e. along the shorter side of the tile) and by 100 arcseconds in the Y-direction. The creation of observation blocks for the survey area was facilitated

by the mandatory use of SADT, which has been specifically developed for the preparation of extensive survey observations, and by using a newly designed P2PP.

In detail, the following strategy and respective OBs were adopted:

1) Deep imaging at *Z*, *Y*, *H*, *J*, *Ks* for each tile was accomplished by creating two OBs (per tile) that were concatenated, i.e. enforcing their execution in immediate consecutive order. The first OB defined *KsJZ* imaging with typical total exposure times per pixel in the stacked final tile of 96 s (*Ks*), 128 s (*J*), 900 s (*Z*) and two jitters per pawprint position, except for *Z*-band observations that use three jitters. The second OB defined *HYYZ* imaging with typical total exposure times per pixel of 96 s (*H*), 240 s (*Y*), 48 s (*Y*), 48 s (*Z*). Short exposures for *Y*- and *Z*-band with shorter DITs (Detector Integration Times) were performed in the second OB in order to have non-saturated images for the moderately bright objects. The OB execution in concatenation took approximately 2 hours and was motivated by the fact that young low-mass objects are known to be possibly variable on timescales of several hours to days. Hence, an almost simultaneous observation of a tile in all VISTA broadband filters can obtain the true shape of the spectral energy distribution of the sources. Since most regions in the Orion survey area do not show a strong nebulous background and little crowding, the sky was estimated from the science exposures of the tile itself. Tile 4, however, contains NGC 2024, which has extended nebulosity. Therefore, for this tile the sky subtraction strategy was to use the concatenated observations of Tile 4 with an offset sky field, east of NGC 2024, and with the Tile 8 observations to the north of Tile 4.
2) Shallower, repeated imaging of Tile 19, centred on the stellar group of 25 Ori were executed in order to search for variability of sources. An observation at *J*- and *H*-band (one short OB with alternating *H* and *J* observations with NDIT × DIT = 3 × 4 sec (*H*) and 2 × 8 sec (*J*) was executed at least once per night. But typically, two epochs per night were taken with a minimum separation of one hour in time between these two.
3) To improve the sensitivity for observations at *Z*- and *J*-band of Tile 16, which contains the well- studied cluster σ Ori, some additional OBs at *Z*- and *J*-band were prepared. These observations were used as fillers, i.e. were carried out only in case additional time was available, e.g., a few minutes (or tens of minutes) at the end of the observing night when it was not reasonable to start deep observations on a new tile. The settings used for these observations were NDIT × DIT = 3 × 30 sec (*Z*), 8 × 4 sec (*J*), with three jitters per pawprint position.

The extragalactic survey project – NGC 253

Participants:

– ESO: Valentin Ivanov, Emanuela Pompei, Steffen Mieske, Thomas Szeifert (Chile), Magda Arnaboldi, Giuseppine Battaglia, Wolfram Freudling, Eva Hatziminaoglou, Michael Hilker, Harald Kuntschner (Garching), Ingo Misgeld, Palle Møller, Mark Neeser, Nadine Neumayer, Kim Nilsson, Marina Rejkuba, Jörg Retzlaff, Remco Slijkhuis, Bram Venemans, Bodo Ziegler
– External: Enrica Iodice, Laura Greggio
– QMUL/VISTA/CASU: Jim Emerson, William Sutherland, Mike Irwin, Jim Lewis, Simon Hodgkin, Eduardo Gonzalez-Solares

The scientific project of the extragalactic mini-survey investigates the mass assembly history of a spiral galaxy in the context of the cold dark matter (CDM) structure formation scenario. This goal is achieved by using the abundance and properties of galaxy satellites, i.e. their mass function and metallicities, the detection of the brightest stars (supergiants, Asymptotic Giant Branch [AGB] and Red Giant Branch [RGB] stars) in the galaxy halo and in the stellar streams, and the detection of globular clusters and ultra-compact dwarfs in the galaxy outer halo. This information maps the galaxy assembly history, and the underlying galaxy mass distribution for a nearby edge-on spiral galaxy. Observationally, this project requires deep imaging in the *Z*- and *J*- broadbands, plus the NB118 narrowband. The deep narrowband imaging is required to map the opacity of the halo, as well as to probe the star formation rate at a redshift of 0.84 for Hα emitting galaxies.

The target of the extragalactic mini-survey is NGC 253, a barred Sc galaxy, seen nearly edge-on, in the Sculptor group at the distance of 3.94 Mpc (Karachentsev et al., 2003); see the VISTA image in Figure 2. It is one of the best nearby examples of a nuclear starburst galaxy. A wealth of data is available in the ESO archive: narrowband Hα, and (shallower) broadbands from the MPG/ESO 2.2-metre Wide Field Imager (WFI), and imaging and spectra of the nucleus obtained with SOFI and ISAAC. The deep image of Malin & Hadley (1997), reaching 28 mag arcsecond^{-2}, shows the presence of an extended asymmetrical stellar halo plus a southern spur. A very small portion of its stellar halo has been studied for distance determination, and the accurate distance (D = 3.94 Mpc) to the galaxy has been determined by resolving and detecting the RGB tip stars at I = 23.97 ± 0.19 in the outer disc observed with the WFPC2 camera on board the Hubble Space Telescope.

Complementary to the deep *J* and *Z* exposures, shallow *Y*, *J*, *H*, *Ks* images of NGC 253 are also required. The primary goal of a shallow survey is to model the disc and bulge components of NGC 253 and, together with the deep imaging data, to detect any signatures of an extended thick disc component. With the addition of optical data obtained from the WFI, along with a robust bulge plus disc decomposition, one can estimate the mass via luminosity and a colour-based mass-to-light ratio. Both the disc model and the large number of observed wavebands are also used to search for possible substructures in the disc and halo of NGC 253.

A summary of the scientific projects currently underway with the NGC 253 dataset is:

– Morphology of spiral arms and disc;
– Nuclear young massive star clusters and OB associations;
– Streams and satellite galaxy properties;
– Detections of globular clusters, ultra-

Figure 2. A VISTA image of the spiral galaxy NGC 253, located in the Sculptor Group, is shown. This true-colour image consists of co-added VIRCAM tiles in the *J*-band (red), narrowband 1.18 microns (green), and *Z*-band (blue). This 200-Megapixel image tile has a physical dimension of 1.21 × 1.49 degrees, and impressively demonstrates VISTA's field of view (with the detector gaps filled in the tile). The long axis of the camera is aligned at position angle 52 degrees, and north is to the left and east is up. The inset shows a zoom of the north-eastern spiral arm of NGC 253. Complementary to the extremely large field of view attainable with VISTA, this image shows the good image quality achieved during the VISTA SV. Data processing and tile creation courtesy of CASU.

compact dwarfs, dwarfs in the galaxy halo and their physical properties;
– Detection of RGB stars in the NGC 253 halo, their magnitudes, metallicities and spatial distribution;
– High-*z* galaxies and the extinction in NGC 253 halo by counting background galaxies.

Observing strategy

The geometry for the survey consisted of a single tile rotated at position angle 52 degrees so that the major axis of the galaxy was parallel to the shorter side of the tile: the wide VISTA field-of-view and the adopted orientation of the camera allows the survey of about 50 kpc above and below the galaxy disc. With this camera orientation, the disc of NGC 253 is centred on detectors 10 and 11 for pawprints 2, 4 and 6, so that the other three pawprints (1, 3 and 5), and their jittered exposures can be used to create an offset sky image for data processing.

The following observing strategies were adopted: 5.8 hrs in NB118 (NDIT × DIT = 1 × 300 sec), 9.6 hrs in *Z* (NDIT × DIT = 3 × 60 sec) and 24 hrs in *J*-band (NDIT × DIT = 5 × 45 sec) to detect the tip of the RGB stars. We used a sequence of six pawprint exposures nested within a sequence of five jitter offsets. Such a strategy was adopted to ensure the best sky subtraction: the presence of an extended disc covering several detectors would prevent simple sky subtraction using images from different jitter exposures, because the disc is both bright and extended. Having adjacent pawprints made it possible to subtract the sky. This approach had an impact on the data reduction and identified the need for the definition of a sky template.

The shallow observing strategy included short observations in *Y*, *J*, *H* and *Ks* to study the morphology of the disc, the bar and the nuclear regions, and the mapping of the thick disc. Here the implemented strategy tested a possible sky-offset sequence. A concatenation was made with three OBs, the first and the third were centred on the galaxy with the assumption that they would cover two parallel stripes. The second OB was a single pawprint observation of an offset sky. This approach failed because of a mistake in implementation of the SADT definition of some tiles, which was then solved in the official SADT release for the Phase 2 call. The observing strategy was changed on-the-fly and shallow observations with the correct coverage were obtained using the same observing strategy that had proved to work for the deep survey.

The definition of the geometry of the mini-surveys via SADT, and the Phase 2 OBs are available on the VISTA SV web page[1].

VISTA SV — input requests from the PIs

On the basis of the Public Survey Panel's recommendation, the Principal

nvestigators (PIs) of the public surveys were invited by the ESO Director General during the Phase 2 workshop to submit their OBs for targeted observations (up to two hours duration) with observing modes that were not covered by the VISTA SV observing strategies. Details of the VISTA public surveys can be found in Arnaboldi et al. (2007). Public survey PIs Minniti (VVV), Cioni (VMC), Jarvis and Dunlop (VIDEO and UltraVISTA) requested short observations during the VISTA SV for their dedicated tests. More information on the observing strategies and the associated data products are also available on the VISTA SV web pages[1].

VISTA SV — visitor mode observations

Observations were carried out in visitor mode and the observers were Arnaboldi, Hilker, Petr-Gotzens and Rejkuba from 15 October to 3 November 2009. Support astronomers were Szeifert and Ivanov. A complete observing log is available from the VISTA SV web pages[1]. The weather conditions were good for most of the nights with typically clear or photometric atmospheric conditions and seeing ≤ 1.2 arcseconds. Four nights were lost due to weather and technical problems. The galaxy NGC 253 was observed during the first half of the nights at airmasses less than 1.5. Orion was then observable during the second half of the nights, after it had risen above airmass 2.0.

Pawprint-level data products for about 60 % of the observations of the extragalactic mini-survey, and 10 % of the Galactic mini-survey were produced at the Paranal Observatory, in parallel with the observations. The reductions were run on the offline machine with the VIRCAM pipeline version 0.9.6. The reduction blocks were manually adjusted in order to use the latest calibrations available, and include the offset frames for sky subtraction. The OB-level data products consist of stacked jittered images for each pawprint, associated photometric catalogues, confidence maps, as well as offset sky images. These reductions enabled the ESO astronomers involved in the user support and science operations to gain experience with the VIRCAM pipeline and data processing, and to investigate some validity ranges of the different parameters, i.e. de-striping, and the best observational strategy for offset sky observations. At the same time important VIRCAM template parameters and instrument characteristics were measured as described below.

Reductions of SV data beyond the pawprint level — production of tiles, mosaics and band merging of the catalogues — are on-going activities coordinated in ESO Garching by the SV team PIs, Arnaboldi and Petr-Gotzens, and in CASU by Irwin.

VISTA SV — feedback to science operations and user support

The observations carried out during the VISTA SV provided very useful tests on the Phase 2 tools and the science operation in service mode. The results of these tests and the actions taken are briefly described.

The ESO astronomers verified the consistency between the definition of the survey geometry of executed OBs and the acquired frames via the astrometry calibration applied by the VIRCAM pipeline to the OB data products. Important SADT input parameters, e.g., the tile overlaps, tile orientation on the sky and the combination of six pawprints into a tile, were verified with the corresponding data products. The new concepts of the scheduling containers implemented for the first time in the P2PP version for surveys were tested and executed during the VISTA SV. OBs were defined using Time Link, Concatenation, and Group scheduling containers. The implementation at the P2PP level is working well.

The VIRCAM templates allow the use of multiple filters in a single OB. The nesting of different filters, different pawprint sequences and jittering offsets needed to be verified during SV. All available configurations were used and most of them successfully executed. In the case of problems, they were either documented or actions taken to solve them before the Phase 2 call. The overheads for OB execution were measured during the ESO commissioning run in July 2009 and implemented as part of P2PP for the verification of the OBs carried out by the user support astronomers. The overheads were tested during the execution of the SV OBs and further verification is expected during the regular service mode operations, with more robust statistics on a larger number of OBs.

The VIRCAM detectors were tested for persistence, linearity and saturation level. Results based on the observations of bright stars in the Orion survey indicate that only a very low level of persistence is measured. For a star with K = 2.2 mag (HD 36558) a persistence signal of 1.5 σ above the background was detected 1 minute after the saturation occurred. No persistence at all is measurable after 2 minutes. Filters were checked for fringing and none was detected. Linearity and saturation tests were carried out during the VISTA commissioning, and the related information is available from the CASU web page[2].

The intensity of the sky background was monitored during the evening twilight. A long sequence of observations was acquired in J- and Z-band for the NGC 253 mini-survey, and the frame sequence shows a strongly decreasing background as a function of time from the evening twilight for the J-band, and a shallower decrease in the Z-band, see Figure 3.

Feedback to the VISTA Data Flow System

To ensure an early feedback of the VISTA SV results into the Vista Data Flow System (VDFS) , a two-day meeting of the ESO SV team and CASU representatives was organised at ESO on 25–26 November 2009. In the current setup, the VISTA raw data reach CASU one week after they are ingested into the ESO archive; all the data taken with VISTA are processed by CASU, and then transferred to the other VDFS component, the VISTA Science Archive (VSA) at the Wide Field Astronomy Unit (WFAU) in Edinburgh. An important aspect of the operations is that the night logs are very important for the processing of scientific data. Therefore channels for the information to flow both from ESO to VDFS components in the UK and vice versa need to be specifically established, and some areas for improvement were identified.

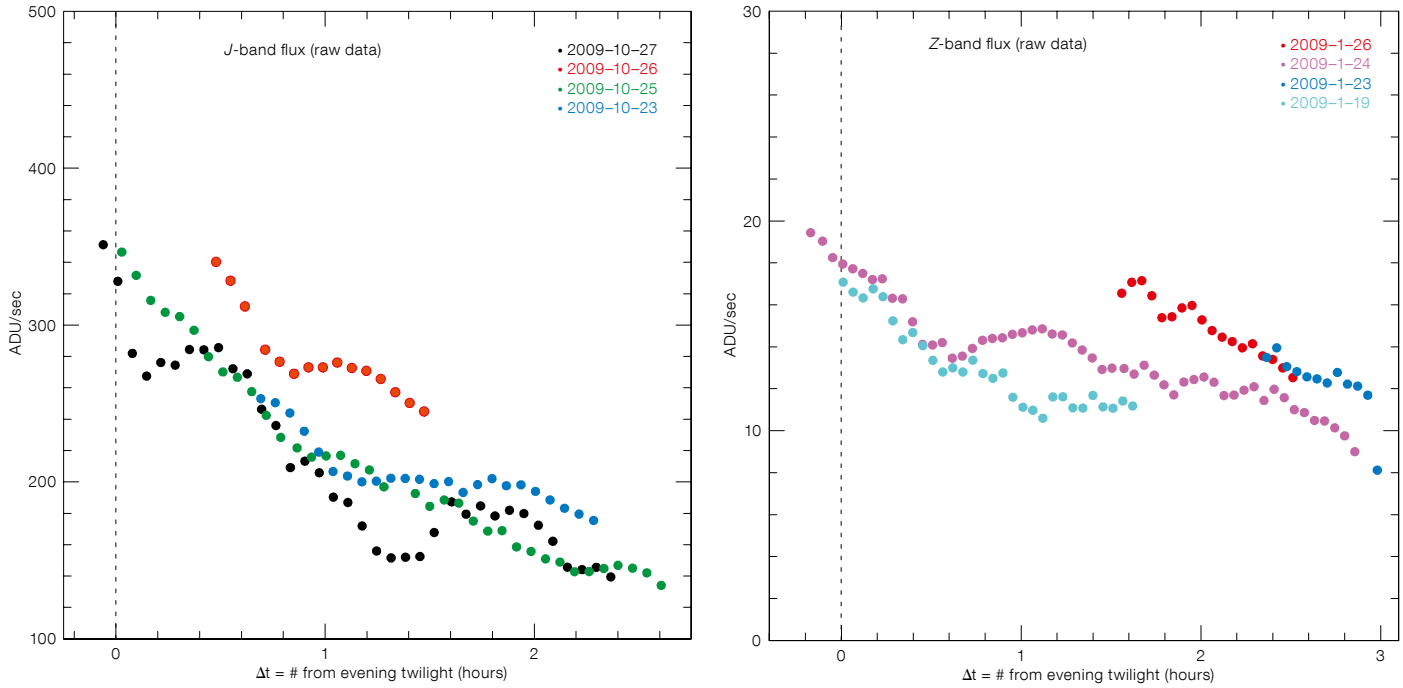

Figure 3. Background flux *vs.* twilight time distance: *J*-band (left panel) shows a rapid decrease in background flux within the first hour from the evening twilight, while the effect is smaller for *Z*-band (right panel). These measurements were made on raw images, but in all cases DIT and NDIT values were the same.

VIRCAM detectors have about 1–10 % deviation from linearity and saturate at about 24 000–37 000 ADU. To ensure the use of VIRCAM detectors in the linearity regime, VISTA users are advised to adopt short integration times, e.g., DIT < 10 s for *H*- and *Ks*-bands. Science operations in Paranal have implemented a careful monitoring of flats in the different bands taken at sunsets, as they can easily be outside the linearity regime.

Both the astrometric and photometric calibration were discussed at length by the ESO and CASU astronomers. The astrometric calibration implemented by the VISTA pipeline seems to work well in the Orion fields, but had some problems in the case of the NGC 253 bright disc. Since it depends on the 2MASS catalogue, when the reference stars are affected by spurious detections because of crowding of bright extended objects in the field, the astrometric calibration computed by the pipeline is not correct. SV data uncovered this problem and allowed more robust quality checks on the 2MASS star catalogue to be established. An updated version of the VISTA pipeline now handles the astrometry correctly. *JHKs* photometry and zero points are computed for each detector by comparison with 2MASS photometry for the same stars. The *Z*- and *J*-bands can be calibrated from the linear relation with 2MASS *J–H* colour, and the independent zero point calibration via standard fields taken during the night.

Publications of VISTA SV data and next steps

The raw data and master calibrations of the two mini-surveys executed during the VISTA SV were published on the dedicated VISTA SV pages[1] and became available worldwide on 21 December 2009. They can be downloaded via the ESO archive web pages; users should be reminded of the large size of these images!

The VISTA SV team is also planning to publish the data products produced by the VDFS pipeline and the advanced data products, e.g., complete mosaicked pawprints into tiles and band-merged catalogues, as soon as these are scientifically validated. Access to these data products via the ESO archive will provide the astronomical community at large with a set of VISTA data ready for scientific exploitation.

References

Arnaboldi, M. et al. 2007, The Messenger, 127, 28
Arnaboldi, M. et al. 2008, The Messenger, 134, 42
Bally, J. 2008, in *Handbook of Star Forming Regions, Volume I: The Northern Sky*, ed. B. Reipurth (San Francisco, ASP Monograph Publications) 4, 459
Chabrier, G. et al. 2000, ApJ, 542, 464
Emerson, J., McPherson, A. & Sutherland, W. 2004, The Messenger, 117, 27
Karachentsev, I. D. et al. 2003, A&A, 404, 93
Malin, D. & Hadley, B. 1997, PASA, 14, 52

Links

[1] VISTA SV webpage: http://www.eso.org/sci/observing/policies/PublicSurveys/VISTA_SV.html
[2] CASU webpage: http://casu.ast.cam.ac.uk/surveys-projects/vista/technical/linearity-sequences

Laser Development for Sodium Laser Guide Stars at ESO

Domenico Bonaccini Calia[1]
Yan Feng[1]
Wolfgang Hackenberg[1]
Ronald Holzlöhner[1]
Luke Taylor[1]
Steffan Lewis[1]

[1] ESO

A breakthrough in the development of sodium laser guide star technology at ESO was made in 2009. The laser research and development programme has led to the implementation of a narrowband Raman fibre laser emitting at the wavelength of the sodium lines at 589 nm with demonstrated power beyond 50 W. Fibre lasers are rugged and reliable, making them promising candidates for use in the next generation of laser guide star systems, such as the Adaptive Optics Facility planned for installation on VLT UT4 in 2013.

Introduction

Laser guide stars (LGS) can be used as reference beacons for adaptive optics (AO) and significantly enlarge the sky coverage of AO on optical telescopes. Sodium LGS are obtained by illuminating the natural layer of atomic sodium in the mesosphere at 80–100 km altitude using a wavelength of 589 nm (the sodium D_2 lines) and causing it to fluoresce. In this way, an artificial "star" can be produced that is a useful alternative to a natural guide star where none exists at that sky location. AO uses the laser guide stars as reference sources to probe atmospheric turbulence and provide feedback to deformable mirrors in order to compensate image blur effects induced by this turbulence. Sodium LGS produce less focus anisoplanatism (cone effect) than Rayleigh LGS and they can probe the entire extent of the atmosphere (Ageorges & Dainty, 2000).

Several large telescopes are equipped with AO and LGS facilities, and future Extremely Large Telescopes will require LGS–AO for some operational modes. ESO installed its first laser guide star on the Very Large Telescope (VLT) Unit Telescope 4 (UT4; Yepun) for the NACO and SINFONI instruments (Bonaccini et al., 2003), and in 2013 the installation of a further four LGS is planned as part of the Adaptive Optics Facility (AOF; Arsenault et al., 2006) project. Future extremely large telescopes such as the European Extremely Large Telescope (E-ELT) will also require multiple laser guide stars (currently 6–8 are envisaged), and it is essential to provide reliable, compact, low-maintenance laser sources at a reasonable cost to meet the needs of these telescopes.

To produce sufficiently bright guide stars, lasers at 589 nm with powers of around 20 W Continuous Wave (CW) and extremely good beam quality are needed. The brightness of the guide star depends, amongst other things, on the detailed atomic physics of the sodium layer. As this has not been well modelled, extensive design simulations of the mesospheric sodium return flux have been undertaken (Milonni et al., 1998; Drummond et al., 2004; Holzlöhner et al., 2010). For the AOF multiple laser guide star facility, this has resulted in specific requirements on the optical characteristics of the laser, as summarised in Table 1.

Firstly, to facilitate efficient optical pumping and achieve small LGS sizes, the emitted laser-beam wavefront error has to be better than 70 nm root mean square (rms), with a goal of 25 nm rms. Secondly, a highly polarised output is needed to produce circular polarisation and perform optical pumping of the mesospheric sodium atoms, which further enhances the resonant backscatter signal. Circular polarisation is obtained by, for example, inserting a quarter-wave plate in the launch telescope system. Finally, re-pumping of the sodium atoms is extremely advantageous (Kibblewhite, 2008) for the LGS return flux and is achieved by emitting two identical laser lines at the centres of the D_{2a} and the D_{2b} sodium lines, with an intensity ratio of 10 : 1. These requirements on the laser and the launch equipment are stringent. For routine operation at astronomical observatories, the laser should also be rugged, turn-key, remotely operated from the control room, and require little maintenance. These laser characteristics have been specified for the AOF, but they are also relevant to the E-ELT baseline requirements. It must be mentioned that special formats of pulsed lasers may become useful in the coming years to reduce or eliminate the effects of spot elongation (Beckers, 1992; Beletic et al., 2005) in large aperture telescopes and to determine the rapidly varying sodium profile precisely, but have not yet been pursued.

Dye lasers provided the first generation of 589-nm lasers to the astronomical community. They were the only possible choice at the time when Keck and ESO decided to build their laser guide star facilities. One model of a 589-nm dye laser was built by the Lawrence Livermore National Laboratory for the Lick and Keck Observatories; a different dye laser model was made for ESO by the Max-Planck-Institut für extraterrestrische Physik in Garching (Rabien et al, 2003), as part of the LGSF project (Bonaccini et al., 2003). Although extremely useful for pioneering LGS–AO techniques and for conducting the first LGS–AO observations, this class of laser has the drawback that it requires high maintenance and preparation time before an observing night, which, at astronomical observatories, creates manpower loads with a considerable footprint on the observatory operation. These considerations make dye lasers possibly undesirable candidates for multiple laser guide star systems. Furthermore, dye lasers are limited to stable gravity vector installations.

When the first conceptual design of the AOF multiple laser guide star facility was conceived at the end of 2005, off-the-

Parameter	Value
Format	CW (continuous wave)
Wavelength	589 nm
Power (laser device/in air)	20 W/16 W
Linewidth	< 5 MHz
Polarisation	Linear, Pol. ratio > 100 : 1
Wavefront error (rms)	< 70 nm (< 25 nm goal)
Sodium D_{2b} re-pumping ratio[1]	12 %

Table 1. Laser optical characteristics specified for the VLT Adaptive Optics Facility.

[1] D_{2b} re-pumping denotes blue-shifting a fraction of the D_{2a} line laser power by 1.71 GHz in order to boost the sodium fluorescence efficiency.

shelf solid-state lasers at 589 nm, with the characteristics listed above, did not exist and ESO therefore launched an internal research and development (R&D) programme to support the goal of achieving second generation laser characteristics: turn-key, compact, solid-state CW lasers at 589 nm to be used routinely, requiring limited maintenance, and sufficiently ruggedised to be mounted next to the laser launch telescopes on the altitude structure of the telescope.

This R&D programme, which reached a successful conclusion at the end of 2009, has resulted in the demonstration of progressively increased laser output power in the last two years, reaching up to 50.9 W CW output at 589 nm and a measured linewidth of 2.3 MHz. During the course of this development, we have capitalised on a significant industry trend towards increasing use of high power fibre lasers in multiple industry segments, while developing a unique and innovative narrowband Raman fibre amplifier technology as a solution to those laser problems that are specific to guide stars and therefore could not readily be solved by recourse to the commercial sector. In the final year of the programme, we have made this technology available to industry and an industrial consortium has been able to independently demonstrate a 20 W class 589-nm laser based on the ESO narrowband Raman amplifier technology.

Courtesy of S. Seip

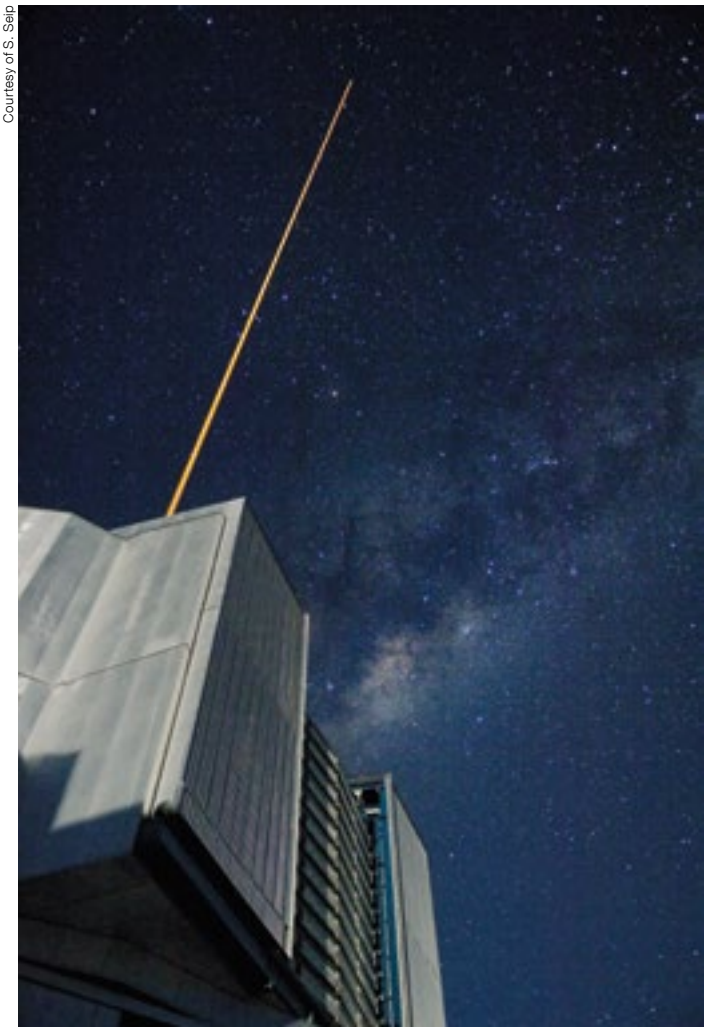

Figure 1. VLT UT4 (Yepun) shown with the LGSF laser beam propagated at Paranal. The Galactic Centre is visible over the dome. The photograph, taken in 2007, is a 5-s exposure during full Moon.

Laser technology background

With the operation and experience of the ESO LGSF, it has become clear that new laser sources had to be developed for the next generation instruments or telescopes, that meet stringent requirements concerning reliability, compactness, and turn-key operation at astronomical sites. When we started the R&D activity, sum-frequency solid-state lasers combining 1064-nm and 1319-nm lasers were being pursued independently by the US Air Force and by the Gemini project together with Coherent Technologies as the industrial partner. In both cases these are solid-state lasers with free-space optics and bulk optical tables full of components that must remain aligned during telescope operation. A broad exploration of the technology readiness levels of different laser technologies was performed at the beginning of the R&D phase, visiting different institutes and several laser companies in Europe and in the US, and studying the vast laser literature.

We decided to explore the technology of lasers at 1178 nm, to be frequency doubled to 589 nm in nonlinear crystals using Second Harmonic Generation (SHG), shown schematically in Figure 2. We studied ytterbium fibre lasers care-

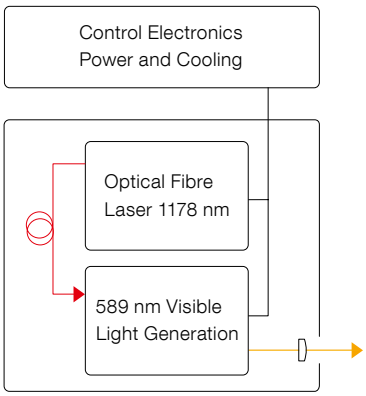

Figure 2. The laser scheme is shown. A fibre laser at 1178 nm feeds a compact second harmonic generation unit based on nonlinear crystals, which converts two photons at 1178 nm into one photon at 589 nm.

fully, but it seemed at that time very unlikely that they can ever lase directly at 1178 nm, while suppressing the amplified spontaneous emission at shorter wavelengths, in particular to 1064 nm. VECSELs (Vertical External Cavity Surface Emitting Laser, also called Optically Pumped Semiconductor Lasers) were considered and discussed with Coherent Inc. in Santa Clara, but their technology readiness was low for our application. We therefore further explored the booming fibre laser technology for the following reasons:

– fibre lasers are alignment-free, being long waveguides with the photons confined to the fibre core;
– their output optical beam quality is diffraction-limited in single mode fibres at the powers of interest to us;
– the heat is distributed along the fibre volume, hence there are no overheating locations in the fibre laser creating strain, lifetime, or beam optical quality issues at the powers of interest to us, contrary to other known solid-state lasers such as VECSELs or waveguide amplifiers;
– there is a robust industrial base for fibre lasers, and they are commercially available (at other wavelengths than 1178 nm) with powers even higher than required;
– fibre lasers can be rack-mounted and located further away from the compact 589-nm SHG unit using the fibre laser output as relay. Thus it is possible to create compact laser heads, where the 589-nm light is produced, that are mounted directly on board the laser launch telescope;
– fibre lasers are simple and contain very few components, hence are generally more reliable and also intrinsically cheaper than other lasers.

Fibre laser technology has made very fast progress in recent years, with Raman fibre lasers used in the telecom industry, and ytterbium lasers used in the material processing and the car industry, among others. This development has led to the availability of in-fibre components such as fibre Bragg gratings (FBG, equivalent to free-space mirrors placed inside the fibre), fibre couplers (equivalent to free-space beam splitters), and wavelength division multiplexers (WDM, equivalent to free-space dichroics). In the broad technological class of fibre lasers, we further narrowed down the technology to Raman fibre lasers, because existing rare-earth doped fibre lasers have low gain at 1178 nm. In contrast to rare-earth doped fibre amplifiers, such as the well-known EDFAs (erbium-doped fibre amplifiers), Raman fibre amplifiers take advantage of a nonlinear conversion process in the fibre which converts “pump energy” from the laser at short wavelengths to the signal wavelength via optical phonons, rather than via atomic transitions. As shown below, however, we had initially to overcome several technological problems.

Broadband Raman fibre amplifiers (RFA) are extensively used in the telecommunications market. Our challenge was to achieve narrowband fibre Raman amplification with powers of about 40 W CW at 1178 nm. As an illustration, the power density in a 5-micron core fibre at 40 W exceeds 2×10^8 W/cm^2, giving rise to nonlinear effects due to the interaction of the electromagnetic radiation with the glass. Today, other laser technologies such as the photonic crystal ytterbium lasers/amplifiers, VECSELs, and bismuth-doped fibre lasers have risen in technology readiness level to become potential laser sources at 1178 nm, both CW or pulsed. Furthermore, new fibre lasers/amplifiers allow novel sum-frequency photon combinations to reach 589 nm, using fibre lasers with rare earth dopants such as thulium or neodymium; however, these developments have yet to be fully demonstrated.

Nonlinear optical effects in optical fibres

Sufficient optical intensities can momentarily modify the optical properties of a medium so that its behaviour depends nonlinearly on light power. This circumstance can be expressed mathematically by expanding the susceptibility χ, which describes the dependence of the optical polarisation of a medium on the electric field, in a Taylor series. The second-order term $\chi^{(2)}$ is responsible for second harmonic generation and sum-frequency generation (SFG) that are used for frequency conversion in materials such as lithium tri-borate (LBO). However, the silica glass, of which optical fibres are made, obeys a structural centre symmetry, implying that $\chi^{(2)}$ vanishes, and thus $\chi^{(3)}$ is the first non-zero nonlinear expansion term ($\chi^{(3)}$ is a complex third-order tensor; Boyd, 2003). In the particle picture, $\chi^{(3)}$ effects describe the interaction of four different photons.

Nonlinear effects due to $\chi^{(3)}$ can be conceptually divided into parametric effects, including the Kerr nonlinearity (index variation of the glass due to high electric fields that can induce self-focusing and self-phase modulation), four-wave mixing (FWM) and non-parametric processes in which light energy is exchanged with the glass, such as stimulated Raman scattering (SRS) and stimulated Brillouin scattering (SBS). While we exploit SRS in Raman amplification, SBS and FWM are unwanted effects. Brief explanations of these effects, important for the LGS development, are presented.

SRS

Stimulated Raman scattering is the nonlinear effect at the core of our RFA technology, producing a frequency shift, in this case of the 1120-nm photons of the pump fibre laser to 1178 nm. SRS is a combination of the Raman inelastic scattering process with stimulated emission, which amplifies the optical signal with low noise and distributed amplification along the fibre. The pump photons undergo inelastic scattering with the glass molecules of the fibre core, exciting vibration states and creating “optical phonons”, which divert part of the photon energy so that the pump photons at 1120 nm are shifted to longer wavelengths, known as the Stokes shift. The extent of the wavelength shift and the efficiency of the Raman process at a given light intensity are related to the material composition and the index profile of the fibre core.

SBS

Stimulated Brillouin scattering limits the output power of the RFA, depending on its emitted linewidth. It arises from the interaction of photons with acoustic phonons generated in the fibre core. In a simplified model of SBS via the electrostrictive effect, a travelling acoustic wave is created that carries forward a periodic variation of refractive index in the fibre core, producing, in effect, a long optical grating that reflects part of the signal back towards the seed laser (see Figure 3). The grating modulation is amplified progressively together with the Raman signal. The onset of SBS with increasing power is very sudden,

and its threshold depends on the fibre length and core material, the fibre acoustic waveguiding properties, the laser wavelength, the optical power and, importantly, the bandwidth of the radiation. Linewidths less than a few tens of MHz lead to low SBS thresholds: a standard RFA at 1178 nm is limited to output powers of only 2–4 W! Valuable experience was gained with mitigation of SBS during the LGSF project, where SBS can occur in the 27.5-metre fibre relay to transfer the Parsec dye-laser beam from the optical bench to the launch telescope, and we developed special photonics crystal fibres to suppress SBS (Hackenberg et al., 1999). In the RFAs described in this article, we employ novel ESO-proprietary SBS suppression techniques that push up the SBS threshold by more than an order of magnitude.

FWM

Four-wave mixing, or self-modulation, is induced by the Kerr effect in the interaction between the photons at different frequencies and the medium. Repeated beating effects between the generated photons at different frequencies create strong line broadening. In optical amplifiers, this effect leads to a mixing of the signal with optical noise and hence broadens the laser line. Counter-propagating the pump laser limits FWM effects in the RFA, and that is the solution adopted. FWM is a phase-sensitive process and can be effectively suppressed by a phase mismatch between the photons at different wavelengths (Boyd, 2003).

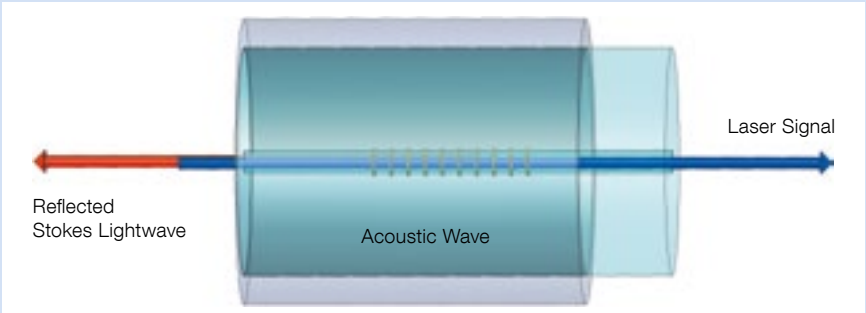

Figure 3. Schematic illustration of the SBS effect is shown. In the fibre core, the forward signal is amplified via SRS. The travelling acoustic wave created by the interaction of the photons with the acoustic phonons creates a periodic refractive index pattern, which extracts energy from the forward signal photons to create phonons, sending back and amplifying a fraction of the lower energy SBS "Stokes" photons, shifted in wavelength to the red. The SBS at high powers can be very effective and send back > 99 % of the forward signal.

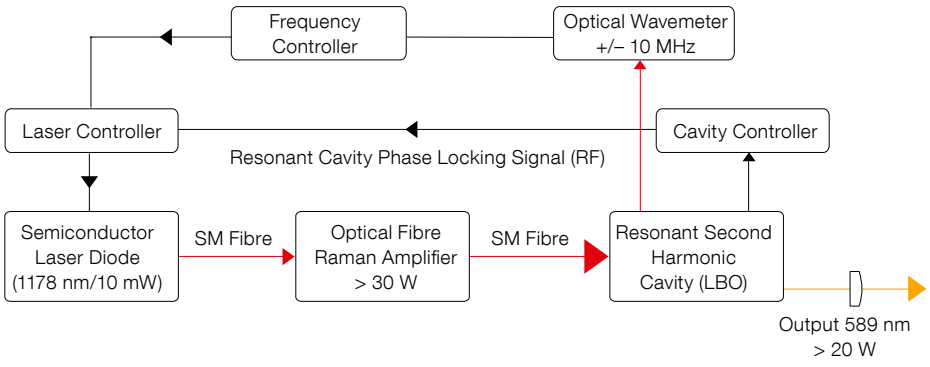

Figure 4. A schematic of the 589-nm fibre laser and its control is shown.

Technical approach

We have pursued 1178-nm narrowband Raman fibre amplifier technology (Bonaccini et al., 2006; Feng et al., 2008). The RFA output radiation is frequency doubled in a commercially available, compact resonant cavity producing a 589-nm beam. Second harmonic generation (SHG), or frequency doubling, is a parametric nonlinear process by which, using suitable nonlinear crystals, two photons are combined into one with twice the energy, or half the wavelength, of each of the fundamental frequency photons. A schematic of the 589-nm laser is shown in Figure 4. All subsystems of the lasers except the RFA are commercially available off-the-shelf. A commercially available 1178-nm seed, frequency stabilised by a wavemeter with an absolute error of less than 10 MHz, feeds, via a single-mode fibre, an 1178-nm high power RFA, whose output is frequency doubled in a compact SHG resonant cavity containing an LBO nonlinear crystal. The 1178-nm narrowband RFA source has been the core of our research.

Nonlinear effects such as Stimulated Brillouin scattering (SBS) and four-wave mixing (FWM) (see insert) were limiting the laser linewidth to tens of GHz for the powers of interest, while we aimed at a few MHz laser linewidth. The invention achieved at ESO, and being patented, uses SBS suppression methods, pushing the SBS threshold power up by an order of magnitude. The FWM is limited by the properties of the fibres and by counter-propagating pump and radiation signals. As a consequence, very little line broadening is observed in the optical amplifier, even at full power.

The high-power fibre components needed for the RFA at 1178 nm had to be progressively developed with the laser industry, such as in-line wavelength division multiplexers, free-space isolators, in-fibre isolators, couplers and high-power 1120-nm polarisation-maintaining (PM) pumps. To minimise the R&D risk, we have furthermore followed two paths in parallel: an in-house development of RFA based on fibres that do not maintain optical polarisation (non-PM); and, in parallel, via contracts with industry, the development of RFA based on PM fibres. Both amplifier

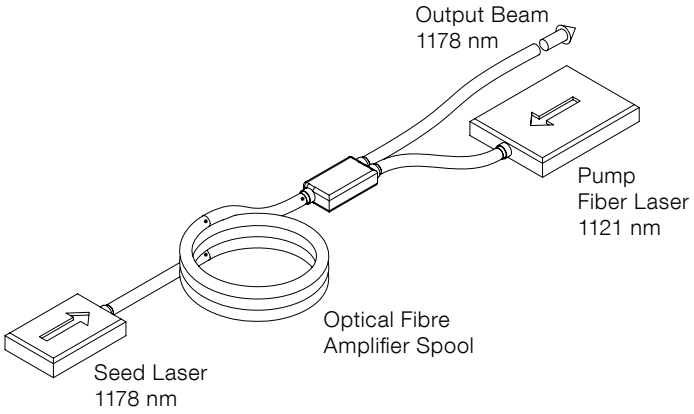

Figure 5. The layout of the Raman fibre amplifier is shown. The output from a high power pump fibre laser at 1121 nm is coupled via a fused glass optical fibre coupler into a fibre spool, where it amplifies the output of a low power seed laser at 1178 nm by the nonlinear optical process of Stimulated Raman Scattering.

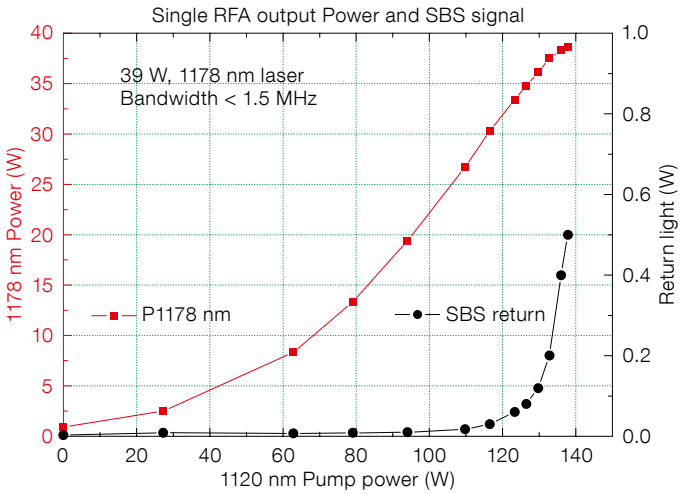

Figure 6. The 1178-nm RFA output power as a function of the pump power at 1120 nm is shown. The maximum value obtained is 39 W. The onset of SBS (black curve, right axis) is seen as return light going back toward the optically isolated seed source. The RFA optical conversion efficiency is 28 % and its wall-plug efficiency 5 %.

technologies have different pros and cons for the RFA and pose different risks. Today we can say that both approaches have been highly successful, meeting and exceeding their goal targets. PM RFA solutions are to be preferred because they are simpler to implement and are thus becoming commercially available.

Besides developing the RFA and integrating them in the laser system at our labs, we have explored the scalability of power, successfully developing coherent beam combination (CBC) schemes. In the following sections we report the results obtained with the single RFA and with coherent beam combination.

Raman amplifier results

We have progressively increased the achieved RFA power once the right methods to overcome SBS were found, following the progressive availability of the necessary fibre components. From 4 W output power at 1178 nm in November 2007, we moved to 39 W in August 2009, maintaining a linewidth below 1.5 MHz and an all-fibre system. In August 2009 we had reached 39 W CW with a single non-PM RFA system developed in-house, together with a novel 150-W fibre laser pump at 1120 nm (Feng et al., 2009); see Figure 6. Using an adaptation of the technology developed at ESO, MPBC Inc. in Canada had produced 44 W with a single PM RFA by the end of 2009. These RFAs give ample margin to reach 20 W at 589 nm — the laser power specification for the AOF with four LGS and the E-ELT LGS system — with adequate linewidth. These results represent both record power and intensity output from a narrowband RFA at spectral power densities well in excess of those normally tolerable in non-SBS-suppressed systems.

The spectral properties of the RFA output are shown in Figure 7, which indicates a very clean spectrum with more than 45 dB emission above amplified spontaneous emission and a linewidth of below 1.5 MHz, measured at 39 W. The 1178-nm laser beam is collimated and mode-matched to a compact resonant cavity (Figure 8). Frequency doubling

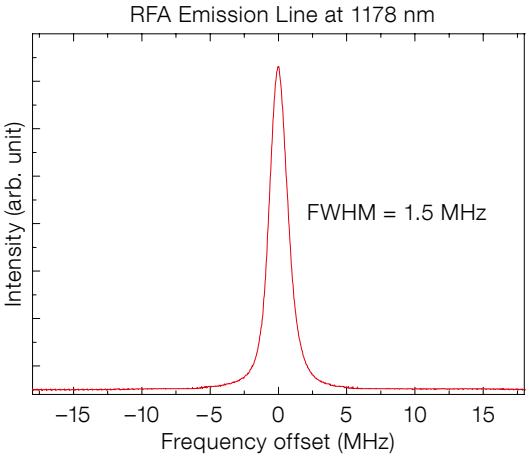

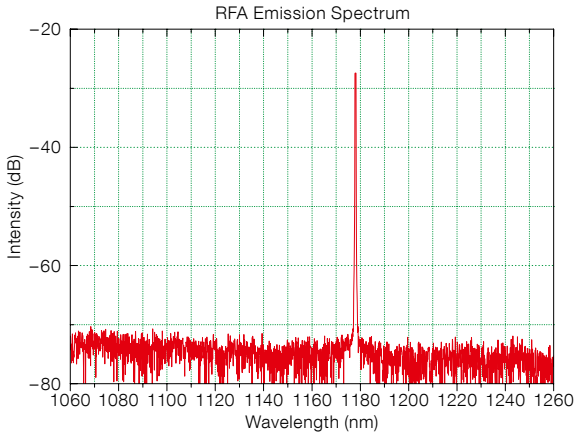

Figure 7. RFA emission linewidth, measured with a scanning Fabry Perot (left, linear plot), and an Ando spectrum analyser (right, log plot) are displayed. The right plot shows that there is a single laser emission line, no residual pump signal at 1120 nm present and no second order SRS Stokes.

is performed by slightly modifying a commercially available SHG unit. The SHG is a very compact bow-tie cavity configuration with a 30-mm long LBO nonlinear crystal (see Figure 10) and a control system based on the Pound–Drever–Hall technique. LBO is well known to be able to handle very high laser powers without lifetime issues. Optical conversion efficiencies up to 86 % have been achieved (Taylor et al., 2009), thanks both to the diffraction-limited beam quality of the single mode RFA (ensuring a good mode-matching capability) and the RFA low intensity/phase noise behaviour. 28 W CW at 589 nm have been obtained (Feng et al., 2009) with a single RFA and SHG in September 2009 (Figure 9 and 10), with excellent beam wavefront quality.

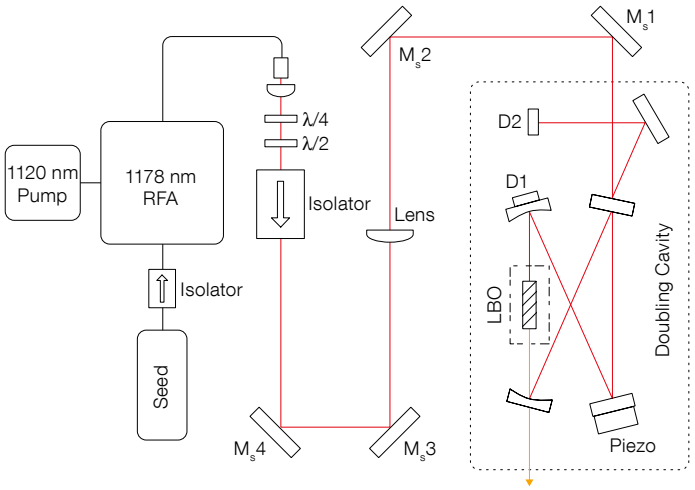

Figure 8. Layout of the RFA and the 589-nm SHG resonant cavity is shown.

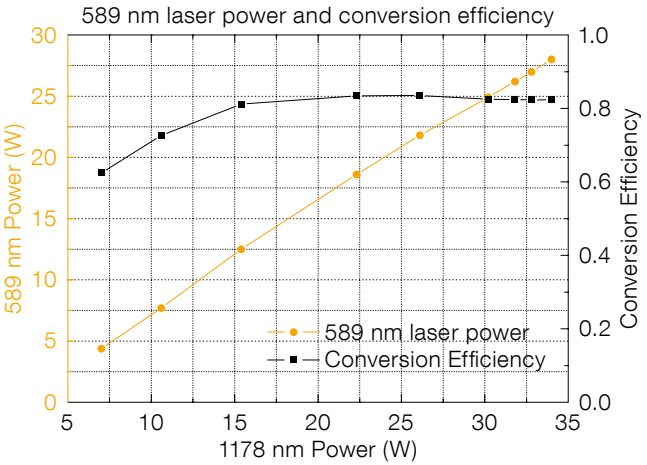

Figure 9. Plots of laser output power at 589 nm (yellow curve, left axis) and SHG efficiency (black curve, right axis) are shown as a function of the 1178-nm power entering the SHG cavity, obtained with the single RFA.

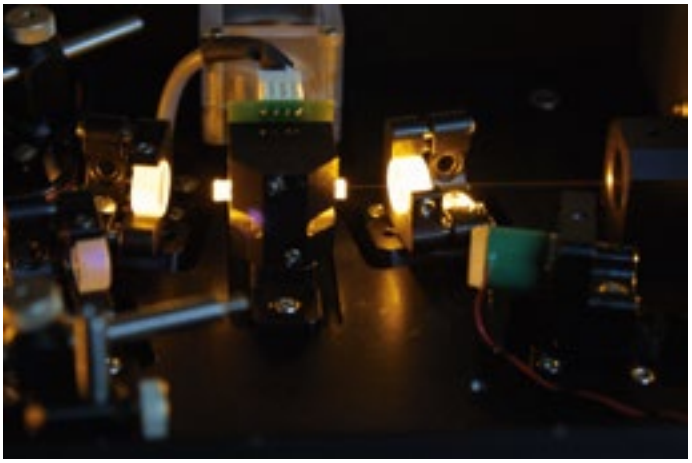

Figure 10. Photograph of the compact bow-tie SHG cavity with the 30-mm LBO crystal mounted in its temperature controlled oven (centre). The 1178-nm laser beam enters from the left side into the crystal; the generated thin yellow beam is visible to the right, exiting the crystal.

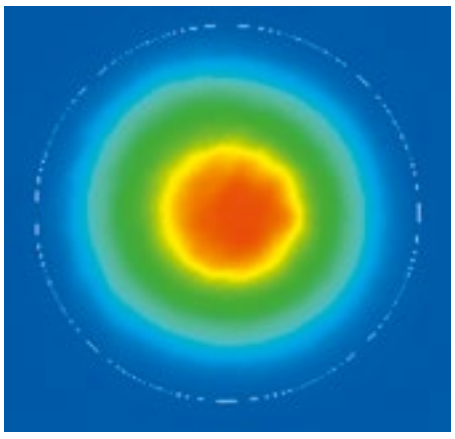

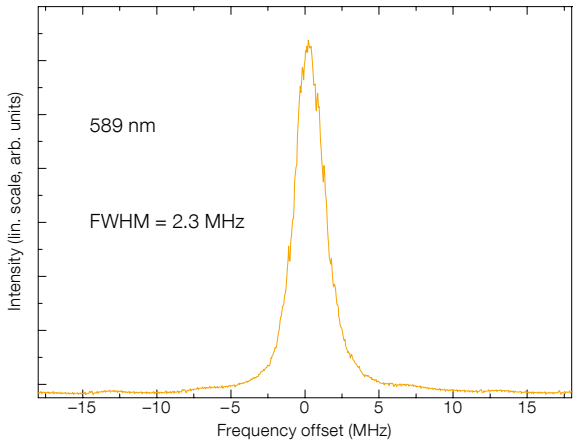

Figure 11. Left: The output laser beam intensity profile taken at 589 nm in high power operation is shown. The wavefront error measured with an interferometer is 11 nm rms. Right: line profile at high power, measured with the optical spectrum analyser.

The output beam quality has been measured at high power using a Phasics SID4 interferometer. The wavefront error measured over the $1/e^2$ diameter was below 0.018 waves, or 11 nm rms (Figure 11), well below the 70 nm rms specification.

Power scaling

During the development there was the risk that a single RFA would not reach sufficient power levels. In order to mitigate this risk, we developed coherent beam combination (CBC) of 1178-nm laser beams. By coherently combining the output beams of different RFAs, the power can be scaled. We have demonstrated that two or more RFAs of equal power can be coherently combined at near-unity combination efficiency, in free space using bulk optics (see Figure 12) via the colinear interference technique, or directly in-fibre without free-space laser beams. We employed a phase control loop acting on a fibre stretcher on one of the RFAs and a 50/50 beam splitter. The loop controls the piston term of the wavefront phase in the fibres at a bandwidth of several tens of kHz. A woofer/tweeter technique was used, cascading two different fibre stretchers, to combine ample phase range to cope with the large phase changes during the laser warm-up with high bandwidth.

CBC has been demonstrated in-house both with bulk optics and, via research contracts with industry, in-fibre (in-line), using 50/50 fibre splitter components (couplers). It has thus been demonstrated for the first time that CBC with narrowband RFAs is possible and indeed extremely efficient. We note that this result is very encouraging and applicable to a wide realm of laser light combination.

We have used CBC with stable output power and efficiencies from 93 % to > 97 % with both PM and non-PM RFAs and with two and three CBC channels. CBC with PM RFA uses in-fibre 50/50 couplers (in-fibre beam splitter). Since the power scaling is done all in-fibre, the setup is extremely compact and there are no optics to align. With two-channel CBC systems we have consistently demonstrated more than 30 W CW at 1178 nm, optically isolated and polarised. In

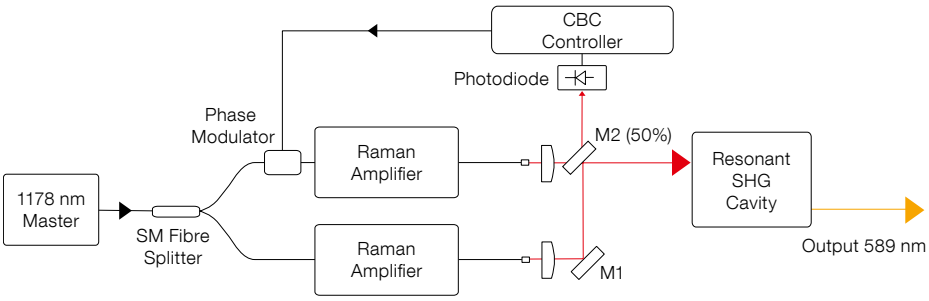

Figure 12. Schematic layout of the power-scaling using free-space coherent beam combination based on non-polarising maintaining RFA is shown. A servo loop controlling the phase of one RFA arm of the CBC allows constructive interference to be kept in the 50/50 splitter M2, in the direction of the SHG cavity.

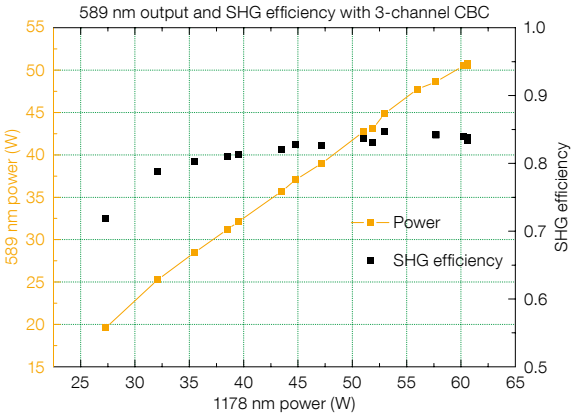

Figure 13. Power-scaling of RFAs using two cascaded coherent beam combinations is shown. In this setup three non-PM RFAs have been combined in sequence via free-space colinear CBC, obtaining, after the optical isolator, power of more than 60 W at 1178 nm, with 93 % CBC efficiency. The CBC output at 1178 nm is used to feed the SHG cavity. The 589 nm power obtained is shown by the yellow curve, related to the left axis. The corresponding SHG conversion efficiency is shown by the black squares, given by the right axis.

August 2009 we demonstrated more than 60 W at 1178 nm, optically isolated and polarised, from a three-arm free-space cascaded CBC system based on non-PM RFAs (see Figure 13). This is the maximum narrowband power at 1178 nm produced so far via CBC.

Thus we have demonstrated that reliable RFA power-scaling is possible and can be efficiently achieved with CBC, even with cascaded CBC systems. The CBC loop controller electronics and the in-fibre phase actuators are commercially available as off-the-shelf components. With the three-way CBC at 1178 nm via SHG, we have reached 50.9 W CW at 589 nm (Taylor et al., 2010), with more than 85 % peak conversion efficiency and a laser linewidth below 2.3 MHz (see Figure 14). We have observed very stable performance of this system.

Outlook

The 589-nm laser research and development programme at ESO has made great progress to support the goal of implementing a second generation of laser technology for multiple laser guide star AO systems. We have designed, built, and demonstrated novel narrowband, CW high-power Raman fibre amplifiers (RFAs) feeding compact 589-nm laser heads, attacking and solving some fairly fundamental laser technology issues. There has been steady progress in terms of laser output power in the past two years for both 1178-nm RFAs and lasers at 589 nm. It has been demonstrated that 589-nm lasers based on a novel RFA, that suppresses stimulated Brillouin scattering, can deliver the required power and spectral formats to meet the needs of the next generation multiple laser guide

Figure 14. 50.9 W CW at 589 nm obtained from the three-way free-space CBC, as shown by the display.

star facility. Moreover, the ESO Laser Systems Department of the ESO Technology Division has achieved a world record in terms of power output of narrowband RFAs, inventing novel techniques to overcome the undesired nonlinear effects in the RFA.

We have further demonstrated laser power scalability via coherent beam combination, using RFAs with PM and non-PM fibre setups, in different configurations. The demonstrations have been done both in-fibre and with colinear beams in free space, obtaining CBC efficiencies up to 97 %. The three-beam, free-space, cascaded CBC produced a laser beam close to 60 W CW at 1178 nm. This laser beam has been mode-matched to the SHG cavity, and we have demonstrated more than 85 % peak conversion efficiency and laser powers up to 50.9 W at 589 nm. This is the highest laser power published so far for narrowband CW fibre lasers at 589 nm. From a laser research perspective, a natural continuation of the team activities would be to investigate the feasibility of the pulsed laser format for "LGS spot-tracking", to cover potential long-term advantages for adaptive optics systems.

In the final year of the programme we have made, and continue to make, these developments available to the laser industry, and an industrial consortium has independently demonstrated a 20 W class 589-nm laser based on narrowband RFA technology. Thanks to the inherent wavelength flexibility of the Raman effect, high-power lasers may also become available at wavelengths inaccessible today, for different applications in astronomy and elsewhere, for example in the life and geophysical sciences. The lasers demonstrate power levels and beam parameters that meet or exceed the AOF requirements and are relevant to the E-ELT baseline laser needs. The research and development programme has given ESO and the astronomical community much more attractive options for the supply and deployment of reliable, compact, next generation lasers for LGS–AO, suited for operation at astronomical observatories.

Acknowledgements

We sincerely acknowledge Guy Monnet, who as Division head very much encouraged and supported the start of the laser development, as well as Roberto Gilmozzi, Martin Cullum and Roberto Tamai, all of whom fostered our continuing work. We also acknowledge the technical contributions to the laser laboratory activities by Ivan Guidolin, Bernard Buzzoni and Jean-Paul Kirchbauer.

References

Ageorges, N. & Dainty, C. 2000, *Laser Guide Star Adaptive Optics for Astronomy, Kluwer*

Agrawal, G. P. 2001, *Non Linear Fibre Optics, Academic Press*

Arsenault, R. et al. 2006, The Messenger, 123, 6

Beckers, J. M. 1992, Appl. Optics, 31, 6592

Beletic, J. W. et al. 2005, Experimental Astronomy, 19, 103

Bonaccini Calia, D. et al. 2003, Proc. SPIE, 4839, 381

Bonaccini Calia, D. et al. 2006, Proc. SPIE, 6272, 627

Boyd, W. R. 2003, *Nonlinear Optics, Academic Press (2nd ed.)*

Drummond, J. et al. 2004, PASP, 116, 278

Feng, Y. et al. 2008, Optics Express, 16, 10927

Feng, Y. et al. 2009, Optics Express, 17, 19021

Feng, Y. et al. 2009, Optics Express, 17, 23678

Hackenberg, W. et al. 1999, The Messenger, 98, 14

Holzlöhner, R. et al. 2010, A&A, 510, A 20

Kibblewhite, E. 2008, Proc. SPIE, 7015, 70150M-1

Milonni, P. W. et al. 1998, JOSA A, 15, 217

Rabien, S. et al. 2003, Proc. SPIE, 4839, 393

Taylor, L. R. et al. 2009, Optics Express, 17, 14687

Taylor, L. R. et al. 2010, Optics Express, accepted

An example of adaptive optics in action is shown, but using natural guide stars. This near-infrared image of the dust-obscured Galactic Bulge globular cluster Terzan 5 was formed from *J* and *K* images obtained with the Multi-conjugate Adaptive Optics Demonstrator (MAD) instrument on the VLT. The field of view is 40 arcseconds. See ESO Press Release eso0945 for more details.

A New Facility Receiver on APEX: The Submillimetre APEX Bolometer Camera, SABOCA

Giorgio Siringo[1]
Ernst Kreysa[2]
Carlos De Breuck[1]
Attila Kovacs[3]
Andreas Lundgren[1]
Frederic Schuller[2]
Thomas Stanke[1]
Axel Weiss[2]
Rolf Guesten[2]
Nikhil Jethava[4]
Torsten May[5]
Karl M. Menten[3]
Hans-Georg Meyer[5]
Michael Starkloff[5]
Viatcheslav Zakosarenko[5]

[1] ESO
[2] Max-Planck Institute for Radio Astronomy, Bonn, Germany
[3] Department of Astronomy, University of Minnesota, Minneapolis, USA
[4] NASA Goddard Space Flight Center, Greenbelt, USA
[5] Institute of Photonic Technology, Jena, Germany

The Submillimetre APEX Bolometer Camera, SABOCA, was successfully commissioned in March 2009 for operation as a facility instrument on the 12-metre APEX telescope, located on Llano de Chajnantor at an altitude of 5100 m. This new camera for the 350-µm atmospheric window uses superconducting bolometers and was built by the Max-Planck Institute for Radio Astronomy in collaboration with the Institute of Photonic Technology. SABOCA complements the existing suite of sub-mm receivers available on APEX, fully exploiting the excellent atmospheric transmission at the site by offering effective mapping of the thermal continuum dust emission at shorter wavelengths.

SABOCA is a bolometric continuum receiver operating in the 350-µm atmospheric window. Its detector array consists of 39 superconducting transition edge sensor (TES) bolometers with SQUID (Superconducting Quantum Interference Device) amplification and time-domain multiplexing. The receiver has been designed and integrated by the bolometer group at the Max-Planck Institute for Radio Astronomy (MPIfR) in collaboration with the Institute of Photonic Technology (IPHT). The MPIfR group has a long track record in the development of bolometers and bolometric cameras for astronomical applications. IPHT is known for building state-of-the-art superconducting devices for over 15 years. The collaboration to build SABOCA merges the technology expertise provided by the two groups.

The instrument development process took several years as it involved a large number of theoretical studies, cycles of manufacture and tests in the laboratory. A prototype system was successfully tested on APEX (the Atacama Pathfinder Experiment; Guesten et al., 2006) during May 2008. Some technical problems were identified and fixed. Thus, commissioning began in September 2008 with an improved version of the receiver. The final version of SABOCA was installed at the beginning of 2009 and commissioning was completed in March 2009.

Motivation

The high altitude and exceptionally dry atmosphere make Chajnantor a unique site for sub-mm astronomy. With its suite of high frequency heterodyne instruments — the Swedish Heterodyne Facility Instrument (SHFI), the Carbon Heterodyne Array of the MPIfR (CHAMP+) and the First Light APEX Sub-millimetre Heterodyne instrument (FLASH), see Guesten et al. (2008) for details — APEX already provides routine observations in atmospheric windows that have so far only seldom been accessible from other sites. Continuum observations are also possible with LABOCA (Siringo et al., 2007; 2009) which is currently the world's largest 870-µm bolometer array. The new 350-µm camera, SABOCA, complements LABOCA and opens up a shorter wavelength atmospheric window, offering, for the first time to the ESO community, a continuum mapping capability well within the sub-mm range.

With its 1.5-arcminute field of view (see Figure 3), SABOCA provides a large-scale sensitivity similar to that of the only other 350-µm bolometer array currently in operation, SHARC-II at the Caltech Sub-mm Observatory (with a field of 2.6 × 1 arcminutes; Dowell et al., 2003). Observations at 350-µm probe warmer dust emission or can constrain dust temperatures and the emissivity index, when combined with measurements at other wavelengths (e.g., LABOCA, 870 µm). For objects at high redshift, SABOCA observes near the peak of the dust emission and can provide important constraints on the total far-infrared luminosity (see for example the article by Swinbank et al., p. 42 in this issue). Finally, the 7.8-arcsecond SABOCA beam size provides 2.5 times better spatial resolution compared to LABOCA, and three times better compared to Herschel/SPIRE (Griffin et al., 2006) at similar wavelengths. The better resolution translates into more accurate size estimates and positions of sub-mm sources, aiding identification of counterparts at other wavelengths. The addition of SABOCA to the range of existing receivers at APEX further demonstrates the commitment of APEX to serve as a "pathfinder" for ALMA. With SABOCA, it gives new access to the highest frequency band (10) of ALMA, in the same way that LABOCA has done in bands 7 and 8.

Figure 1. Picture of a single bolometer used in the actual version of SABOCA. The thermal conductivity depends on the thickness and number of "legs" connecting the central part of the membrane with the outside. Other layouts were produced and even tested but not used finally. All bolometers have cross-dipole absorbing elements.

Instrument description

The bolometers of SABOCA are composite bolometers with superconducting

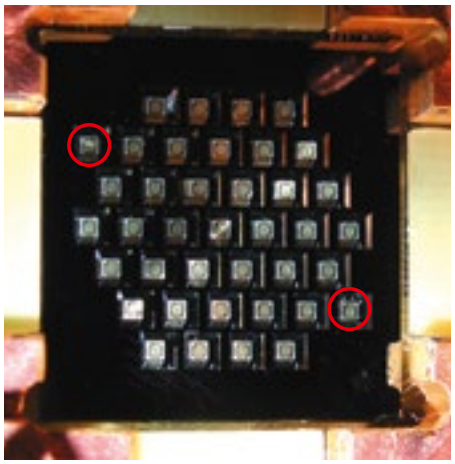

Figure 2. A picture of the bolometer array at the focal plane of SABOCA. One bolometer cell is about 1 mm in size and the full size of the array is about 15 mm. The two red circles show the position of the two blind bolometers.

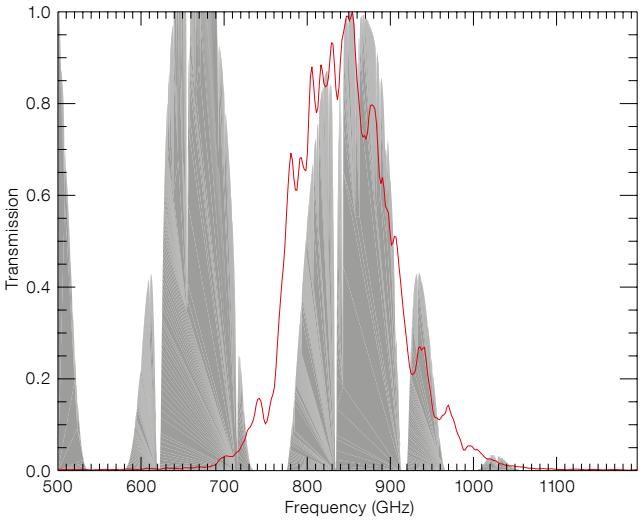

Figure 3. Spectral response of SABOCA (red) compared to the atmospheric transmission (gray). Both curves are normalised to unity.

TES thermistors on structured membranes. The thermistors are bilayers of molybdenum and a gold-palladium alloy deposited on silicon-nitride membranes together with the niobium wiring and the radiation absorbing layer. As part of the manufacture process, the membranes were structured at IPHT in order to control the thermal conductivity. Several layouts have been studied, with different designs of membrane structures, thermistors and absorbing elements. The bolometers selected for SABOCA (see Figure 1) have moderately structured membranes and showed a radiative noise equivalent power (NEP) of 1.6×10^{-16} W/Hz$^{1/2}$ (with 300 K background) during laboratory tests at MPIfR at a transition temperature of 0.45 K.

The array of SABOCA consists of 39 TES composite bolometers. Of these, 37 are arranged in a hexagonal grid consisting of a central channel and three concentric hexagons. Two additional bolometers, identical to the inner 37, but not optically coupled to horns (i.e. "blind" bolometers) were added to the layout, at two diametrically opposite positions, and are used for monitoring purposes. The grid constant of the array is 2.0 mm (see Figure 2).

A monolithic array of conical horn antennas, placed in front of the bolometer wafer, concentrates the radiation onto the bolometers. The 37 conical horns were machined into a single aluminum block in the machine shop at MPIfR. In combination with the tertiary optics, the horn antennas are optimised for coupling to the telescope's main beam at a wavelength of 350 μm.

SABOCA's detectors are designed to work at a temperature of about 300 mK. This temperature is provided by a cryogenic system made of a cryostat using liquid nitrogen and liquid helium, in combination with a closed-cycle helium-3 sorption cooler. After achieving high vacuum insulation, the cryostat is filled with the liquid cryogens. A dry (scroll) pump, installed in the APEX Cassegrain cabin, is used to reduce the vapour pressure on the liquid helium bath in order to lower the boiling point, reaching a temperature of about 1.6 K. This operation requires about one hour. A single stage helium-3 sorption cooler (of the type described by Chanin and Torre, 1984) is then operated to cool the focal plane to about 300 mK. The cryostat needs to be refilled, pumped and recycled every 48 hours. The helium pumping system and the operation of the sorption cooler have been automated and remotely controlled, allowing operation of the telescope during part of the cool-down process (about 2 hours).

The spectral response of SABOCA (Figure 3) is defined by a set of cold filters, installed inside the cryostat, mounted on the liquid nitrogen and liquid helium shields. The passband is centred at 852 GHz (352 μm), about 120 GHz wide, and is formed by an interference filter made of inductive and capacitive meshes embedded in polypropylene. The low frequency edge of the band is defined by the cutoff of a cylindrical waveguide. A freestanding inductive mesh provides shielding against radio frequency interference.

The TES bolometers are read out in a time-domain multiplexing scheme via four independent chains of SQUID amplifiers and multiplexers, providing ten channels each for a total of 40 possible elements. The multiplexers and associated electronics have been designed and manufactured by IPHT. The four SQUID amplifiers are attached to the liquid helium cold plate and operated at the temperature of the pumped liquid helium (~ 1.6 K). The 40 multiplexing SQUIDs are located in four groups of ten at the four sides of the bolometer array. They are operated at the same temperature as the bolometers (~ 300 mK).

SQUIDs are extremely sensitive to magnetic fields. Thus, the level of static (trapped flux) and variable (therefore interfering) magnetic fields in the Cassegrain cabin of APEX are a concern. Several measures were taken to ensure that these fields do not compromise the performance of SABOCA: a) an external shield, made of high magnetic permeability metal (called mu-metal) is wrapped around the lower part of the cryostat; b) the multiplexing SQUIDs have input coils differentially coupled, therefore only sensitive to gradients of the magnetic field; c) the

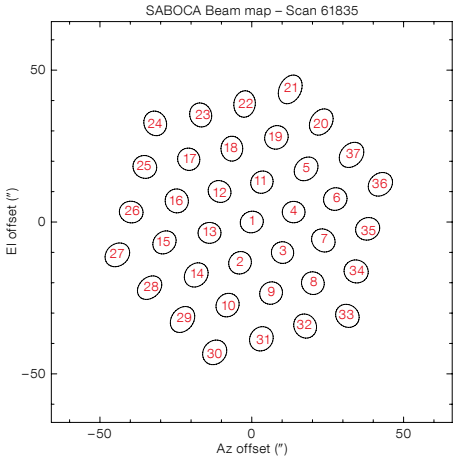

Figure 4. On-sky footprint of SABOCA, derived from one single beam map of Mars. The beam distortions are partially due to atmospheric refraction and fitting accuracy.

array and multiplexers are enclosed in a capsule, on the helium-3 stage, made of an aluminum alloy with a critical temperature of 1.2 K, which becomes superconducting during operation. The horn array, also made of the same material, is part of the capsule; d) the readout SQUIDs are protected by shields made of Cryoperm (a type of mu-metal for low temperature applications); e) only selected non-magnetic materials are employed in the surroundings of the array. The operation of SABOCA at APEX confirmed the reproducibility of the SQUIDs' operation point and therefore the effectiveness of the shielding. The multiplexing frequency is fixed to 2 kHz, which gives 200 samples per second per bolometer.

So as to be fully integrated into the APEX environment, SABOCA is provided with a hardware/software infrastructure similar to that of LABOCA. Front-end software (running on the same front-end computer used by LABOCA) is used to control and monitor the hardware of the system (temperature monitoring, SQUID tuning, helium pumping and recycling, and more). The back-end software (running on the same back-end computer used by LABOCA) is used to collect the bolometer signals from the de-multiplexing electronics and to provide a networked data stream required by the APEX control software. With the use of the same bridge computer as LABOCA, real-time digital signal processing (anti-alias filtering and down-sampling) of the raw data is possible, although not strictly required. All the software modules of SABOCA provide SCPI interfaces (Standard Commands for Programmable Instrumentation), allowing full remote operation of the instrument.

Performance on sky

Characterisation on sky of the final version of SABOCA was completed in February 2009. The array parameters are estimated averaging the results of fully sampled maps (called beam maps) of planets with useful flux and angular size (namely Mars, Uranus and Neptune, see Figure 4). The main beam, determined combining several beam maps, is circular and has a deconvolved full width at half maximum (FWHM) of 7.8 arcseconds, close to the expected value of 7.5 arcseconds. The beam starts to deviate from a Gaussian at a relative intensity of ~ 6 % (–12 dB) where the error pattern of the telescope becomes visible.

The 37 on-sky bolometers of SABOCA all perform better, in terms of detector noise distribution, than the bolometers with semiconducting thermistors (used in LABOCA) and do not show *1/f* noise down to below 30 mHz. The clean quality of the signals is mainly due to the use of the new superconducting TES bolometers, which are practically insensitive to microphonics, and therefore particularly suitable for a noisy environment like the Cassegrain cabin of APEX.

Following the successful example of LABOCA, SABOCA has also been designed to be operated in "fast scanning" mode (Reichertz et al., 2001) without chopping the secondary mirror. The observing modes, therefore, are the same as for LABOCA, but scaled to the different size of the beam and of the array: spiral patterns, a raster of spirals for compact sources and rectangular on-the-fly for large maps of extended sources (for more details see Siringo et al. [2009] or online[1]).

The sensitivity of SABOCA was derived from blank-sky observations after correlated noise removal. The mean receiver sensitivity was found to be 200 mJy $s^{1/2}$. For average observing conditions (i.e. precipitable water vapour [PVW] ~ 0.5 mm and 60-degree source elevation), the receiver sensitivity translates into an on-sky sensitivity of 750 mJy $s^{1/2}$. In terms of mapping speed, that value corresponds to a uniform coverage of a 10 × 10 arcminute sky area down to a residual root mean square (rms) noise of ~ 300 mJy/beam in one hour of observing time (two hours including overheads). The image in Figure 5 for example was made in 1.5 hours of on-source integration. The effective sensitivity, however, strongly depends on the amount of PWV along the line of sight. An observing time calculator is available online[2].

Science with SABOCA

SABOCA is a versatile instrument that can observe a range of objects of great interest in the different fields of today's astrophysics: from our own Solar System to the debris discs around nearby young stars; from molecular clouds and star-forming regions in our Milky Way to cold dust in galaxies at various redshifts and evolutionary stages; all the way to the early epochs of the Universe, constraining the star formation rates in high-redshift starburst galaxies.

Within the first year of operations, a number of important scientific results have already been obtained with SABOCA. One of the most frequent applications of this new bolometer camera has been in follow-up observations of targets already observed with LABOCA. The 2.5 times higher angular resolution of SABOCA can reveal new details in the morphology of sources with compact extended emission. In parallel, its spectral passband centred at 350 µm complements the determination of the characteristic temperatures of sources.

To display the mapping capabilities of SABOCA, in Figure 5 we show a large map of the 350-µm emission from the Orion Molecular Cloud-1 (OMC-1) that, at a distance of 400 parsec, is the closest known star-forming region undergoing massive star formation. The map covers a sky area of more than 10 × 10 arcminutes with an angular resolution of ~ 8 arcseconds and with a uniform residual noise of ~ 100 mJy/beam. It required

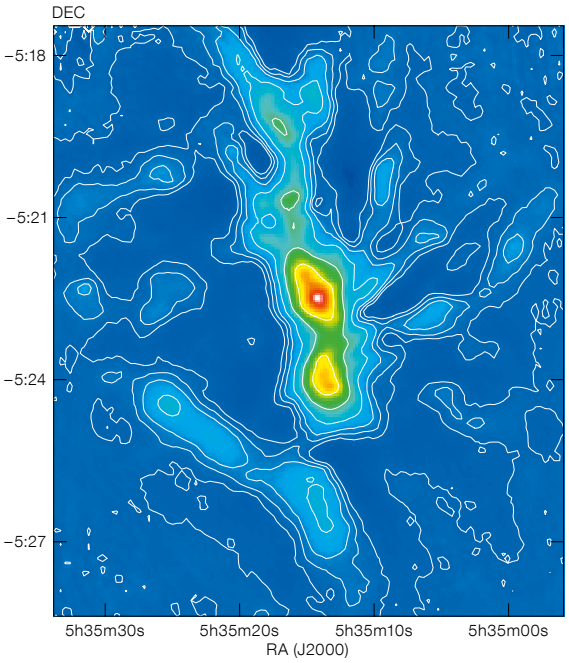

Figure 5. The Orion Molecular Cloud 1 (OMC-1) as seen by SABOCA at 350 µm. Contours show the flux at 0.3 %, 1.0 %, 3.0 %, 10 %, 30 % of the 720 Jy/beam peak at the centre of the map.

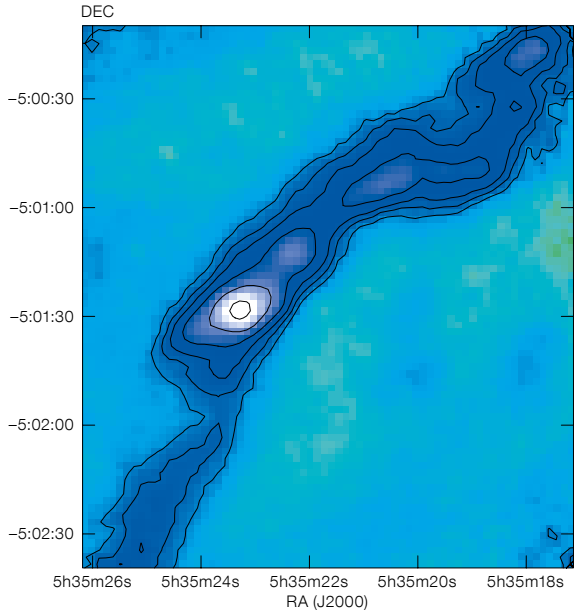

Figure 6. SABOCA map of the OMC-3 molecular cloud at 350 µm. Contours show the flux at 1 %, 5 %, 10 %, 20 %, 40 % of the brightest peak in the map, 60 Jy/beam.

Figure 7. SABOCA map of the "Eyelash", the brightest sub-mm galaxy known to date, at $z = 2.326$. The observed 350-µm flux is 530 ± 60 mJy (colour bar in signal-to-noise units). This map has a diameter of 180 arcseconds.

1.5 hours of on-source integration time under very good sky conditions (PWV ~ 0.1 mm). Figure 6 shows the Orion Molecular Cloud-3 (OMC-3, located about 20 arcminutes north of OMC-1) belonging to the same dense filament of which OMC-1 is the brightest part. It features a chain of very young, deeply embedded low- to intermediate-mass protostars (Chini et al., 1997).

Figure 7 shows SABOCA observations of SMM J2135-0102, also known as the "Eyelash". This object, at $z = 2.326$, is the brightest sub-mm galaxy known to date (see article by Swinbank et al., p. 42). The source shows a 350-µm peak flux of 530 mJy and was detected at a 20 σ level in a total observing time of 2.7 hours (including all overheads). The map was obtained with a sequence of scans in raster spirals observing mode, providing a fully sampled image.

New possibilities for APEX

The successful commissioning of SABOCA on APEX has further significance: it demonstrates that the new superconducting technology (TES bolometers and SQUID amplification and multiplexing) is viable outside of the protected environment of the laboratory. With proper shielding, the devices can be used even in an electromagnetically polluted environment, such as the Cassegrain cabin of APEX. Moreover, our tests at the MPIfR lab have also shown that the superconducting technology is compatible with the use of a pulse tube cooler (a type of closed-cycle cooling machine), thus allowing instruments to be operated without the need for regular replenishment of liquid cryogens. An immediate advantage of a bolometer camera based on superconducting technology and operated on closed-cycle cryogenics is the option of keeping the receiver cold most of the time with minimum maintenance. This would greatly enhance the operability of the system, allowing a more flexible observing schedule and reducing the work load for the ordinary maintenance of the receiver at the telescope.

Acknowledgements

Some of the results published here were observed during ESO Director's Discretionary Time. The authors would like to thank Mark Swinbank for providing SABOCA data from one of his observing projects (see Swinbank et al., p. 42). We acknowledge the APEX staff members for their support during installation and commissioning.

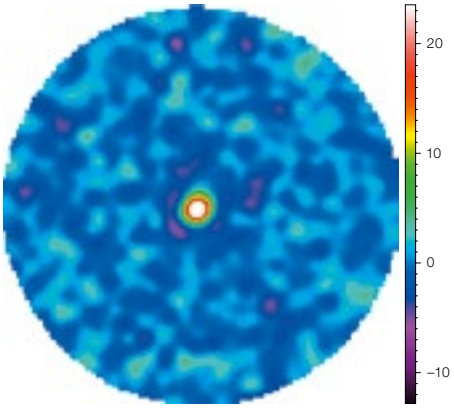

References

Chanin, G. & Torre, J. P. 1984, J. Opt. Soc. Am. A., 1, 412
Chini, R. et al. 1997, ApJL, 474, L135
Dowell, C. D. et al. 2003, Proc. SPIE, 4855, 73D
Griffin, M. et al. 2006, Proc. SPIE, 6265, 7G
Guesten, R. et al. 2006, A&A, 454L, 13
Guesten, R. et al. 2008, Proc. SPIE, 7020
Reichertz, L. A. et al. 2001, A&A, 379, 735
Siringo, G. et al. 2007, The Messenger, 129, 2
Siringo, G. et al. 2009, A&A, 497, 945

Links

[1] Observing with LABOCA: http://www.apex-telescope.org/bolometer/laboca/observing/
[2] SABOCA observing time calculator: http://www.apex-telescope.org/bolometer/saboca/obscalc/

Recent Progress on the KMOS Multi-object Integral Field Spectrometer

Ray Sharples[1]
Ralf Bender[2, 4]
Alex Agudo Berbel[4]
Richard Bennett[3]
Naidu Bezawada[3]
Nicolas Bouché[4]
David Bramall[1]
Mark Casali[6]
Michele Cirasuolo[3]
Paul Clark[1]
Mark Cliffe[3]
Richard Davies[4]
Roger Davies[5]
Niv Drory[4]
Marc Dubbeldam[1]
Alasdair Fairley[3]
Gert Finger[6]
Reinhard Genzel[4]
Reinhold Haefner[2]
Achim Hess[2]
Paul Jeffers[3]
Ian Lewis[5]
David Montgomery[3]
John Murray[3]
Bernard Muschielok[2]
Natascha Förster Schreiber[4]
Jeff Pirard[6]
Suzie Ramsey-Howat[6]
Phil Rees[3]
Josef Richter[2]
David Robertson[1]
Ian Robson[3]
Stephen Rolt[1]
Roberto Saglia[2]
Joerg Schlichter[2]
Matthias Tecza[5]
Stephen Todd[3]
Michael Wegner[2]
Erich Wiezorrek[4]

[1] Department of Physics, University of Durham, United Kingdom
[2] Universitätssternwarte München, Germany
[3] United Kingdom Astronomy Technology Centre, Royal Observatory, Edinburgh, United Kingdom
[4] Max-Planck-Institut für extraterrestrische Physik, Garching, Germany
[5] Sub-Department of Astrophysics, University of Oxford, United Kingdom
[6] ESO

KMOS is a near-infrared multi-object integral field spectrometer that is one of a suite of second generation instruments under construction for the VLT. The instrument is being built by a consortium of UK and German institutes working in partnership with ESO and is now in the manufacture, integration and test phase. In this article we describe recent progress with the design and construction of KMOS and present the first results from the subsystem test and integration.

KMOS is one of a suite of second generation instruments which, along with HAWK-I (Kissler-Patig et al., 2008), X-shooter (Vernet et al., 2009), MUSE (Bacon et al., 2006) and SPHERE (Beuzit et al., 2006), will revolutionise the observing capabilities of the Paranal Observatory in the next decade. KMOS is a unique design of near-infrared multi-object spectrograph that uses deployable integral field units (d-IFUs) to obtain spatially resolved spectra for multiple target objects selected from within an extended field of view. d-IFUs have a significant advantage over multi-slit spectrographs because of the reduced slit contention in crowded fields and their insensitivity to slit losses due to extended galaxy morphology and orientation. KMOS will be mounted onto the Nasmyth platform of the Very Large Telescope (VLT) Unit Telescope 1 (UT1) and will use the Nasmyth acquisition and guidance (A&G) facilities. The top-level scientific requirements are: (i) to support spatially resolved (3D) spectroscopy; (ii) to allow multiplexed spectroscopic observations; (iii) to allow observations across the *IZ*, *YJ*, *H*, and *K* infrared atmospheric windows from 0.8 to 2.5 µm. These requirements have been flowed-down during a series of ever more detailed design reviews to arrive at the final design specification (Table 1). KMOS completed its Final Design Review in April 2008 and is now in the manufacture, integration and test phase. Key milestones are listed Table 2.

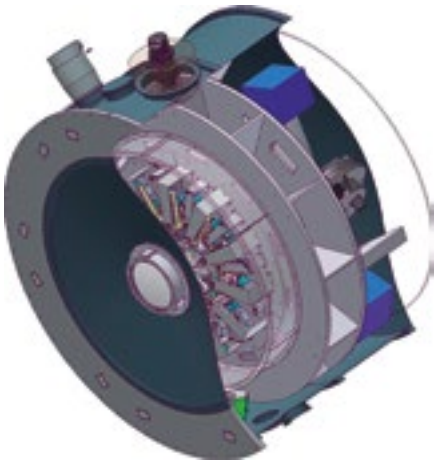

Figure 1. Cutaway drawing of the main KMOS cryostat design showing the entrance window followed by the pickoff arm module layer, the integral field unit module layer and the spectrograph module layer. Each 1/3 sector contains 8 robotic arms, 8 IFUs and 1 spectrograph to allow a sequential approach to assembly, integration and test, and easier maintenance.

The final design employs 24 robotic arms that position fold mirrors at user-specified locations in a 7.2-arcminute diameter field of view (Bennett et al., 2008). Each arm selects a subfield on the sky of 2.8 × 2.8 arcseconds. The size of the

Table 1. Design specifications for the KMOS spectrograph.

Parameter	Final Design
Instrument total throughput (mean)	*IZ* > 20 %, *YJ* > 20 %, *H* > 30 %, *K* > 30 %
Wavelength coverage	0.8 to 2.5 µm
Spectral resolution	R = 3300, 3400, 3800, 3800 (*IZ*, *YJ*, *H*, *K*)
Number of IFUs	24
Extent of each IFU	2.8 × 2.8 arcseconds
Spatial sampling	0.2 × 0.2 arcseconds
Patrol field	7.2-arcminute diameter circle
Close packing of IFUs	> 3 within 1 sq. arcminute
Closest approach of IFUs	Edge-to-edge separation of > 6 arcseconds

Table 2. Key KMOS milestones.

Milestone	Date
Preliminary Design Review Closeout (PDR)	May 2006
Final Design Review Closeout (FDR)	April 2008
Preliminary Acceptance Europe (PAE)	(February 2011)

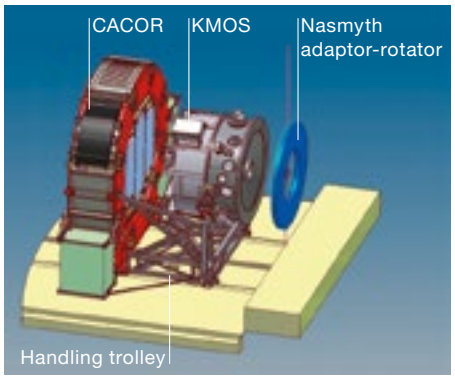

Figure 2 (left). KMOS layout on the Nasmyth platform showing the locations of the main cryostat and the CACOR cable rotator.

Figure 3 (right). The KMOS main cryostat undergoing its first cooldown cycles. The closed-cycle coolers are visible around the base of the cryostat; the remaining ports contain the feedthroughs for some of the 1500 electrical connections into the cryostat. The electronics rack to the right contains all the housekeeping electronics and will eventually be mounted on the Nasmyth platform.

subfields is tailored specifically to the compact sizes of high redshift galaxies, with a spatial sampling (0.2 arcseconds per pixel) designed to sample the excellent infrared seeing at Paranal ($FWHM_{median}$ = 0.52 arcseconds in the *K*-band). The subfields are then anamorphically magnified onto 24 advanced image slicer IFUs that partition each subfield into 14 slices, with 14 spatial pixels along each slice (Dubbeldam et al., 2006). Light from the IFUs is dispersed by three cryogenic grating spectrometers that generate 14 × 14 spectra, each with ~ 1000 Nyquist-sampled spectral resolution elements, for all of the 24 independent subfields (Tecza et al., 2006). The spectrometers each employ a single 2k × 2k Hawaii-2RG HgCdTe detector. The optical layout for the whole system has a threefold symmetry about the Nasmyth optical axis, allowing a staged modular approach to assembly, integration and test (Figure 1).

In the following sections we present the progress on the individual subsystem components within KMOS and note where design changes have been implemented compared to our original concept (Sharples et al., 2005).

Cryostat and CACOR

The KMOS cryostat is the main support structure for the optomechanical components that make up the instrument and mounts directly onto the Nasmyth rotator. It uses three low-vibration Leybold 10MD cryocoolers to maintain an internal optical bench at a temperature below T = 140 K, in order to minimise the thermal background radiation and to keep the detector at a temperature below T = 80 K to minimise dark current and persistence. A major design change after the preliminary design review has been to remove the electronics racks and services from the outside of the cryostat and to mount these on a co-rotating structure (CACOR) located separately on the Nasmyth platform (Figure 2) in order to provide an improved mass margin with respect to the telescope Nasmyth rotator/adaptor limit (3000 kg). The cryostat is a hybrid aluminium–steel vessel with a diameter of 2 metres. Figure 3 shows the cryostat undergoing its first cooldown in September 2009. The performance is now excellent with plenty of cooling power in reserve and a hold-time of more than three months (without pumping).

Pickoff arms

One of the more unusual elements in KMOS is the pickoff module that relays the light from the 24 selected regions distributed within the patrol field to an intermediate focus position at the entrance to the integral field unit module. The robotic pickoff arms are of an (r,θ) design (Figure 4) with pivot points located in a circle around the periphery of the patrol field and are driven in radial and angular motions by two cryogenically prepared stepper motors.

The arms are arranged into two layers on either side of the Nasmyth focal plane to improve the access to target objects in crowded fields, whilst avoiding interference between neighbouring arms. This focal plane is flat and telecentric thanks to a pair of all-silica field lenses, one of which forms the entrance window to the cryostat. The pickoff arm design has been through a number of refinements based on repeatability, flexure and lifetime tests conducted in a relevant environment (i.e. in vacuum at T ~ 140 K). Whilst the positioning of the arms is open-loop via step-counting from datum switches, there is a linear variable differential transformer (LVDT) encoder on each arm that is used to check for successful movement. In addition a hardware collision detection system is also implemented as a third level of protection which can sense if any two arms have come into contact and stop the movement of arms within 10 µm. The absolute positioning accuracy of the arm when cold has been measured using an automated

Figure 4. One of the fully assembled KMOS pickoff arms. The linear motion is a stepper motor drive in the top of the arm, and the angular motion is a stepper drive in the base. The total length of the mechanism is ~ 50 cm.

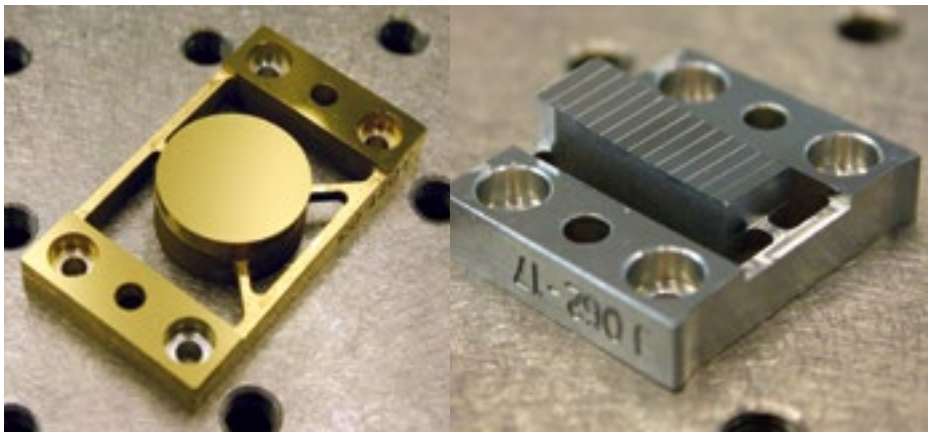

Figure 5. Two of the diamond-machined optical parts from the IFU assembly. On the left is a gold-coated K-mirror (an off-axis parabola) and on the right is an uncoated image slicer array with the 14 slices visible.

laser tracker system and is < 50 µm (0.1 arcseconds).

The pickoff module also contains the instrument calibration unit (tungsten, argon and neon sources) and an order-sorting filter wheel that provides focus compensation between the different bands. The cold-stop for each channel is at the base of the arm, after which an intermediate image is formed by a fixed K-mirror assembly that orientates the pick-off fields so that their edges are parallel on the sky. This enables a sparse matrix configuration for the arms where the KMOS IFUs can be used to map a contiguous region of sky covering 65 × 43 (33 × 16) arcseconds in 16 (9) dither pointings.

Integral field units

The IFU subsystem contains optics that collect the output beams from each of the 24 pickoffs and reimages them with appropriate anamorphic magnification onto the 24 image slicers. The anamorphic magnification is required in order that the spatial sampling pixels ("spaxels") on the sky are square whilst maintaining Nyquist sampling of the spectra on the detector in the spectral dimension. The slices from groups of eight subfields are aligned and reformatted into a single 254-mm long slit at the entrance to the three spectrometers. The optics in a single IFU comprises: two off-axis aspheric re-imaging mirrors; a third re-imaging mirror defined with a more complex geometry using Zernike polynomials; one monolithic slicing mirror array containing 14 slices with spherical surfaces in different orientations; two monolithic pupil mirror arrays containing seven facets, each with spherical surfaces; and one monolithic slit mirror array containing 14 facets with toroidal surface form. All of the micro-optics in the IFUs are produced by diamond-machining using a combination of diamond-turning and raster fly-cutting techniques. This technique allows arrays of multi-faceted components to be manufactured with in-built mounting surfaces, all to sub-micron accuracy. Particular attention was paid to minimising the micro-roughness on the optical surfaces, which was in the range 5–10 nm root mean square (rms) for many components. Detailed metrology measurements are being performed on every element to ensure that the stringent tolerances in form error and alignment for the IFUs have been achieved. Figure 5 shows some examples of the IFU components produced so far.

Spectrographs

The three identical spectrographs each use a single off-axis toroidal mirror to collimate the incoming light, which is then dispersed via a reflection grating and refocused using a six-element transmissive achromatic camera onto a single Hawaii-2RG infrared detector. The gratings are mounted on a five-position wheel which allows optimised gratings to be used for the individual bands together with a single lower resolution grating covering two atmospheric bands (*H*+*K*). Following a decision early in the project to extend the wavelength of operation below 1 µm, where the detector still has excellent quantum efficiency, a series of optimised order-sorting filters have been procured as shown in Table 3. After initial cold performance tests at Oxford University, the first spectrograph has now been integrated into the main cryostat to begin full system tests (Figure 6).

Table 3. Spectrograph bandpasses.

Band	*IZ*	*YJ*	*H*	*K*	*HK*
λ_{start} (nm)	800	1020	1450	1950	1500
λ_{end} (nm)	1080	1345	1850	2500	2380
Spectral resolution	3327	3387	3840	3766	2052

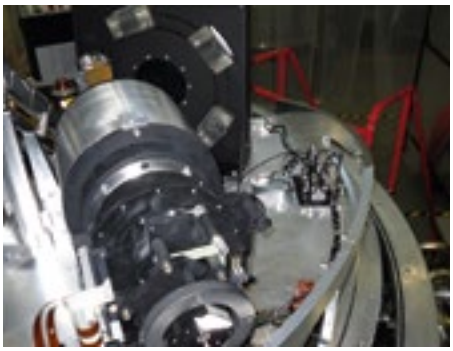

Figure 6. The first KMOS spectrograph mounted on its baseplate. The camera barrel is in the middle distance, with the detector focus mount in the foreground, and the grating turret with dummy gratings at the back.

Control electronics and software

KMOS will be one of the most complex cryogenic instruments at the VLT with almost 60 degrees of freedom in the cryogenic mechanisms alone. Robust efficient software and reliable control electronics will be key to successful long-term operations and are being developed at the Universitäts-Sternwarte (USM) in Munich (Figure 7). In addition to instrument control software and housekeeping diagnostics, KMOS will have an optimised arm allocation tool, known as KARMA, which links directly to the ESO observation preparation software (P2PP). KARMA assigns arms to targets in a prioritised

Figure 7. An advanced prototype of one of the final electronics cabinets controlling four of the KMOS pickoff arms during tests at USM.

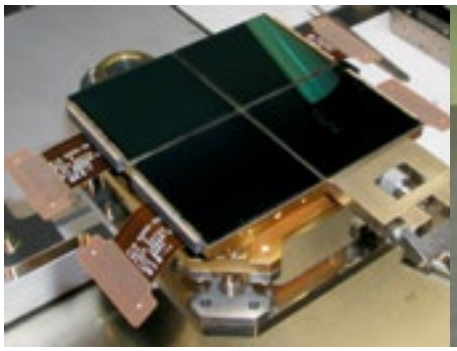

Figure 8. On the left the three KMOS science-grade detectors and one engineering-grade detector are shown mounted on a temporary four-chip mosaic mount for device characterisation at ESO. On the right are two of the three single-detector focus stages.

Figure 9 (below). The top image shows a subsection of the full Hawaii-2RG array containing a 2D argon arc *H*-band spectrum through one channel. In the spatial direction there are 14 separate slitlets (slices) visible. The lower image shows a 1D wavelength slice through this spectrum. The *FWHM* of the lines is ~ 2 pixels. This is one of the first spectra taken with the full KMOS instrument with only initial adjustments for focus/tilt/alignment.

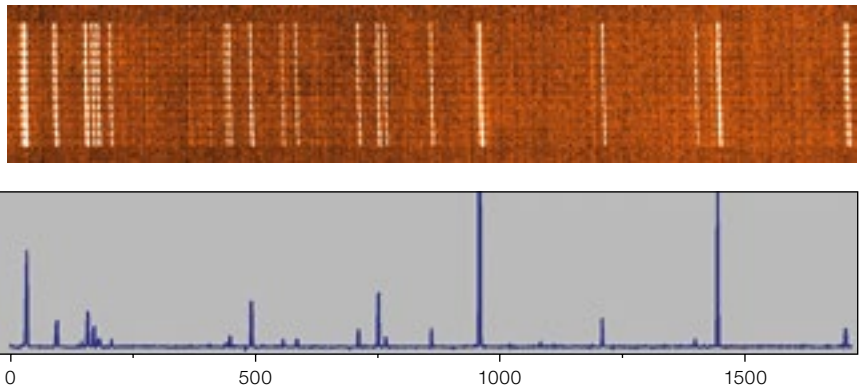

way, whilst ensuring that no invalid arm positions are selected and allows the user to manually reconfigure the list of allocated targets.

Detectors

The KMOS detector system and electronics are being developed at ESO Garching and will use the latest generation of Hawaii-2RG detectors in combination with the new Next Generation Controller (NGC) readout system. The detectors will be fully substrate-removed to give excellent quantum efficiency (> 80 %) across the whole 0.8 to 2.5 µm region and have excellent performance (readout noise < 10 e^- rms on all four detectors for a single double-correlated sample (DCS) readout; dark current at T = 60 K is < 0.001 e^-/sec/pixel). Each detector is adjusted manually for tip-tilt, but is mounted on a remotely operated focus stage (Figure 8).

Data reduction pipeline

A customised data reduction pipeline is being provided for KMOS that will allow the observer to evaluate the data quality after each readout and apply sophisticated algorithms for coadding data cubes and subtraction of the sky background. With over 4000 spectra per integration, automatic data processing and reduction methods will be essential to exploit fully the scientific potential of KMOS. The data reduction pipeline is being developed at the Max-Planck-Institut für extraterrestrische Physik (MPE) and will make use of the considerable experience and heritage available from the VLT SINFONI instrument.

Current status

KMOS is currently undergoing the first stage of a sequential integration process at the UK Astronomy Technology Centre (ATC) in Edinburgh. The first step is to obtain an end-to-end qualification check of the complete cryogenic performance using a part-populated front segment with two complete channels comprising pickoff arms, IFUs, spectrograph and detector system. Figure 9 shows the technical "first light" KMOS spectrum with the instrument cold, obtained using the instrument calibration unit on 20 January 2010. This significant milestone, which tests all the integrated subsystems, marks the first step towards Provisional Acceptance Europe, after which KMOS will be shipped to Paranal to begin telescope commissioning. We look forward to seeing the first exciting science from KMOS in 2011/12.

References

Bacon, R. et al. 2006, The Messenger, 124, 5
Bennett, R. et al. 2008, Proc. SPIE, 7018, 73
Beuzit, J.-L. et al. 2006, The Messenger, 125, 29
Dubbeldam, M. et al. 2006, Proc. SPIE, 6273, 105
Kissler-Patig, M. et al. 2008, The Messenger, 132, 7
Sharples, R. et al. 2005, The Messenger, 122, 2
Tecza, M. et al. 2006, Proc. SPIE, 6269, 141
Vernet, J. et al. 2009, The Messenger, 138, 4

A colour-composite image of the nearby dwarf irregular galaxy NGC 6822, also known as Barnard's Galaxy, taken with the MPG/ESO 2.2-metre telescope and the Wide Field Imager. Four separate images in *B*, *V*, *R* and *Hα* filters were combined and west is to the left, south to the top. This Local Group gas-rich dwarf galaxy at 460 kpc shows several prominent shell HII regions, indicative of high mass star formation (see Press Release eso0938 for more details).

A Slitless Spectroscopic Survey for Hα-emitting Stars in the Magellanic Clouds

Christophe Martayan[1,2]
Dietrich Baade[1]
Juan Fabregat[3]

[1] ESO
[2] GEPI, Observatoire de Paris, France
[3] Observatori Astronòmic, Universitat de València, Spain

The slitless-spectroscopy mode of the Wide Field Imager was used for a comprehensive survey of the Magellanic Clouds to detect stars exhibiting Hα line emission. A total of eight million spectra were recorded. Analysis of 84 open star clusters in the Small Magellanic Cloud confirms that the fraction of extremely rapidly rotating Be stars increases with decreasing metallicity. The very large database also enables other aspects of the complex interplay of early-type stars with stellar evolution, metallicity, mass loss and rapid rotation to be examined.

The Be star phenomenon

Be stars are B-type stars that have been observed to exhibit Hα in emission at least once. They rotate so close to the break-up velocity that some relatively minor extra kick in velocity, for example by non-radial pulsation, magnetic flares, or in an eccentric binary orbit, can make the star lose matter that then forms a circumstellar disc. The Hα line emission resulting from the recombination of the gas, which is ionised by the hot central star, is strongly broadened by the rapid rotation of the disc. The effects of rotation still pose a challenge to stellar evolution models, and mass loss from early-type stars has a strong impact on the chemical and dynamical evolution of their host galaxies. Therefore, Be stars are prominent astrophysical reference laboratories.

The evolutionary phase(s) during which this Be phenomenon occurs, as well as the mechanism(s) over and above rotation that cause the mass loss, are not strongly constrained by observations. Therefore, a broad survey of Be stars in both open clusters and the field is important. The multitude of stellar emission-line objects and the ability to suppress confusion with other classes of objects by means of simple colour–magnitude diagrams provides many more suitable target fields in the Magellanic Clouds than the Galaxy, where distance moduli are extremely difficult to determine. At least as valuable, from a diagnostic point of view, is the lower metallicity ($Z_{SMC} \approx 0.1\ Z_{\odot}$ and $Z_{LMC} \approx 0.4\ Z_{\odot}$), which places such studies into a wider perspective of stellar evolution and rotation.

In fact, Martayan et al. (2006, 2007) and Hunter et al. (2008) have already found that OB and A-type stars rotate faster at low metallicity than at high metallicity. This can be understood as the result of radiatively-driven winds being weaker at lower metallicity and removing less angular momentum. If there are fewer metals, the fraction of the stellar radiation that can be absorbed by them is lower, and the resulting reduced effective radiation pressure leads to weaker winds and mass loss. Since ultra-fast rotation seems to play a dominant role in Be stars, the frequency of Be stars should increase with decreasing metallicity. Some preliminary empirical evidence has already been reported by Maeder et al. (1999). However, this work only rests on a small number of open clusters. A broader survey is desirable to disentangle the partially overlapping effects of rotation and evolution that can lead to wrong conclusions.

Spectro-tiling the Magellanic Clouds with the Wide Field Imager

Even after careful pre-selection of candidate objects, any attempt to obtain fairly complete coverage of the Magellanic Clouds with conventional multi-object spectroscopy techniques is hopeless in view of the large amount of telescope time required. Moreover, the widespread diffuse background emission in the Magellanic Clouds would require slits to be used in order to identify objects with intrinsic line emission, thereby eliminating fibre-fed spectrographs that do not have integral field units, and so much reducing the achievable multiplex.

By contrast, a slitless spectrograph delivers spectra of all sufficiently bright sources and the entire background area so that these problems do not arise (cf. Figure 1). However, in crowded areas spectra will overlap and a narrowband filter may be needed to reduce the length of the spectra. For the same reason, the spectral resolution must be low. If the field of view is large and the objects stand out well above the background flux, then the multiplex of a slitless spectrograph is unrivalled.

At ESO, the grism mode of the Wide Field Imager (WFI; Baade et al., 1999) attached to the 2.2-metre MPG/ESO telescope at La Silla offered such observing opportunities. It could utilise about 75% of the direct imaging field of view of 34 × 33 arcmin^2 so that, with 14 and 20 pointings, a good coverage of the main areas of the Small Magellanic Cloud (SMC) and Large Magellanic Cloud (LMC), respectively, could be achieved (see Figure 2). In the SMC, the mean Hα width for Be stars is about 5 nm (range, 0.5–7 nm) thus corresponding to a nominal resolution of 5.1 nm at Hα (or R = 128), very well matched to the resolving power of 130 with the R50 grism. Since even the Hα lines of Be stars remain just unresolved, the detection sensitivity is maximised. A filter of 7.4-nm bandpass, roughly centred on Hα, was inserted into the beam in order to limit the length of the spectra and, thereby, their crowding.

The observations were carried out on 25 and 26 September 2002. Due to poor weather the second night was only partly useful. The typical exposure times were 600 seconds, thus allowing the detection of main sequence stars up to type F. The seeing was about 1.1 arcseconds. No direct images were taken due to bad weather although this was foreseen. The main disadvantages of the absence of direct images are: the difficulty of obtaining accurate astrometry, so the astrometric calculations had to be based on the centre of the spectra; the absence of corresponding photometry on the same date (to mitigate the variability typical of Be stars), which helps in the classification of the stars.

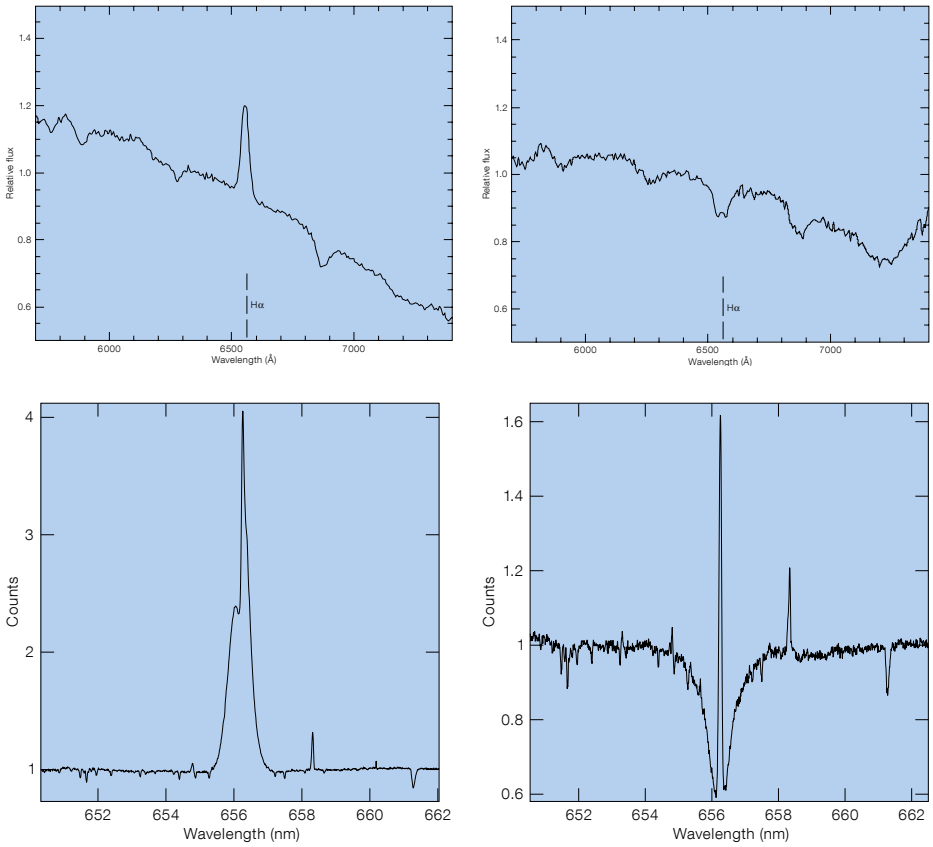

Figure 1. Comparison of the spectra of two Galactic stars (left and right) observed, in Hα, with a slit (lower left) and the FLAMES–GIRAFFE spectrograph (lower right) and with the WFI in slitless mode (left and right upper). The star shown left has a circumstellar disc, while the star at right only happens to lie in an area with diffuse nebular line emission. While the circumstellar emission (left) is found with both instruments, only the slit spectrum (lower right) includes a strong emission line from the large-scale diffuse nebulosity. On account of the lack of spatial resolution across the single fibre, it is not possible to decide whether or not the emission line is intrinsic to the star (lower right). Only the slitless spectrum (upper right) reveals that the line emission is not associated with the object. These two Galactic stars from the open cluster NGC 6611 were observed with a broader WFI filter than the one used for the Magellanic Clouds.

Extraction and analysis of the WFI slitless spectra

In total, the raw data include spectra of about three million sources in the SMC and roughly five million sources in the LMC. Thanks to a special adaption of the SExtractor code (Bertin & Arnouts, 1996) the detection and extraction of the spectra could be performed fully automatically. With the help of an initial astrometric solution, spectral order –1 was identified; subsequently this order alone was used for analysis.

The very difficult (out-of-focus) point spread function (cf. Martayan et al., 2010) rendered various neural network codes unable to find emission-line objects with acceptable failure rates. Therefore, we developed the IDL code Album, which computes a regional average spectrum and subtracts it from each extracted source, satisfying a number of quality criteria (tilt angle of the spectrum, distortion, etc). In the resulting difference spectra, the Hα line emission stands out fairly prominently. Therefore, the difference spectra were arranged in a photo-album-like fashion, making the detection by eye, even of a large number of line emission sources, quite manageable.

For each extracted source, astrometry was performed with the ASTROM package of Wallace & Gray (2003), assigning the source coordinates to the centre of the spectrum. The achieved accuracy of about 0.5–1 arcseconds was sufficient to cross-identify the WFI sources with photometric catalogues such as OGLE. Using additional calibrations, the OGLE photometry was converted into approximate spectral types so that the detected emission-line sources could be classified.

The reliability of the detection process was verified by means of higher resolution FLAMES spectra of 31 emission-line sources in the field of the SMC open cluster NGC 330, of which 28 are classical Be stars, while the other three are of a different nature (planetary nebula, B[e] star and supergiant). Up to a *V* magnitude of 16.5, line emission above 100 nm equivalent width or with a peak intensity higher than twice the ambient continuum level, was successfully detected in the WFI spectra. Thus completeness of the compiled Be-star catalogue begins to fail at a spectral type of B3.

Results

The SMC database includes 84 open clusters. The combined colour–magnitude diagram of the stars classified with the WFI is presented in Figure 3, distinguishing stars with and without Hα line emission. The comparison in Figure 4 of the fraction of emission-line stars per spectral sub-type between the Galaxy (McSwain & Gies, 2005) and the SMC shows a clear overfrequency by up to a factor of five of Be stars at low metallicity. Further analysis suggests that this result can no longer be dominated by evolutionary differences. Therefore, the expectation is confirmed that, because low metallicity stars lose less angular momentum through their radiatively-driven winds, and thus, on average, rotate more rapidly, Be stars are more abundant in

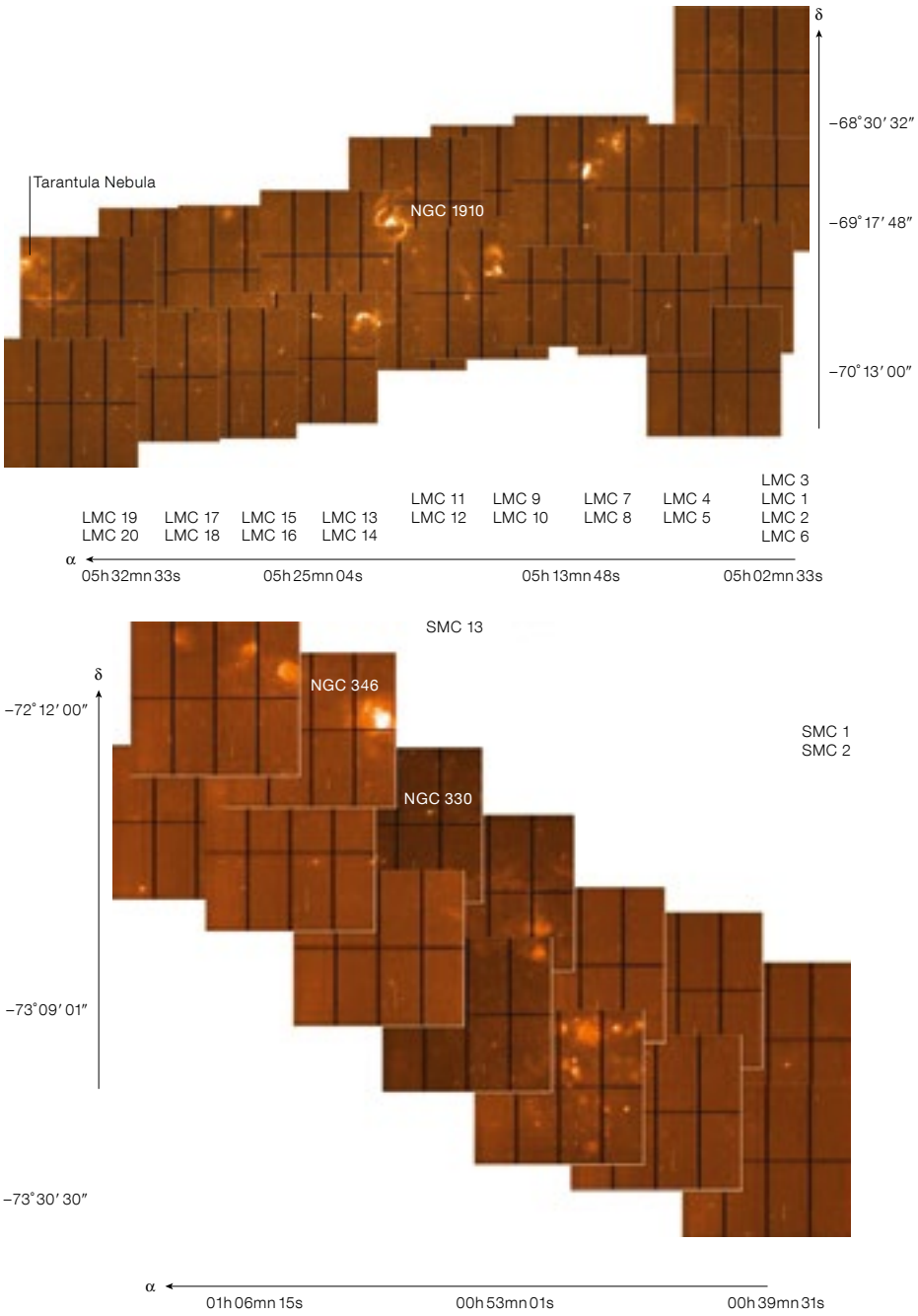

Figure 2. The spatial coverage achieved with the WFI slitless survey of the LMC (top) and SMC (bottom) is shown. Each pointing is named (LMC 1–20 and SMC 1–14) and several SMC clusters are indicated. In the LMC, the nebulosity at the centre hosts the LBV star S Doradus, and the nebulosity at the left is part of the Tarantula Nebula.

the SMC than in the Galaxy. Extrapolated to the extremely low metallicity of first generation stars, this result suggests that, in the early Universe, rapid rotation and the Be phenomenon were probably more common. Such stars may also be related to the predecessors of gamma-ray bursters, which may require very rapid rotation to develop an accretion disc that controls the formation of polar jets.

In both the Galaxy and the SMC, the variation of the fraction of Be stars with spectral type is about the same and, therefore, does not depend on metallicity. From the distribution with cluster age it is apparent that the Be phenomenon is strongest in the latter half of the main sequence phase. Accordingly, some B-type stars acquire Be characteristics only during their main sequence evolution. But others are already formed as Be stars. Probably, the evolution of the fractional critical rotation rate Ω/Ω_c is the key parameter governing these differences. Due to the metallicity dependence of mass loss, the evolution of Ω/Ω_c, too, depends on metallicity. However, this dependency is different for different mass ranges, requiring a large database for its observational analysis.

The WFI slitless Hα survey is not restricted to open clusters. In the 4.5 % of the SMC field area analysed so far, 477 emission-line objects were found. This suggests that the complete survey will identify 4–6 times as many emission-line objects as the previous most complete survey (Meysonnier & Azzopardi, 1993), which was still based on photographic data. As the result, several of the currently less populous classes of emission-line objects will grow to statistically meaningful numbers. Among the young stars, there will also be quite a few Herbig Ae/Be stars.

Inclusion also of the LMC data will extend the parameter space of the Be-star sample towards both intermediate metallicity as well as young stellar ages. This will form an excellent basis for an in-depth spectral analysis of selected targets and areas at higher resolution with FLAMES on the VLT. The results will highlight the metallicity-dependent effect of rapid rotation on the evolution of early-type stars. Most notably, the evolution of Ω/Ω_c should become traceable from observations.

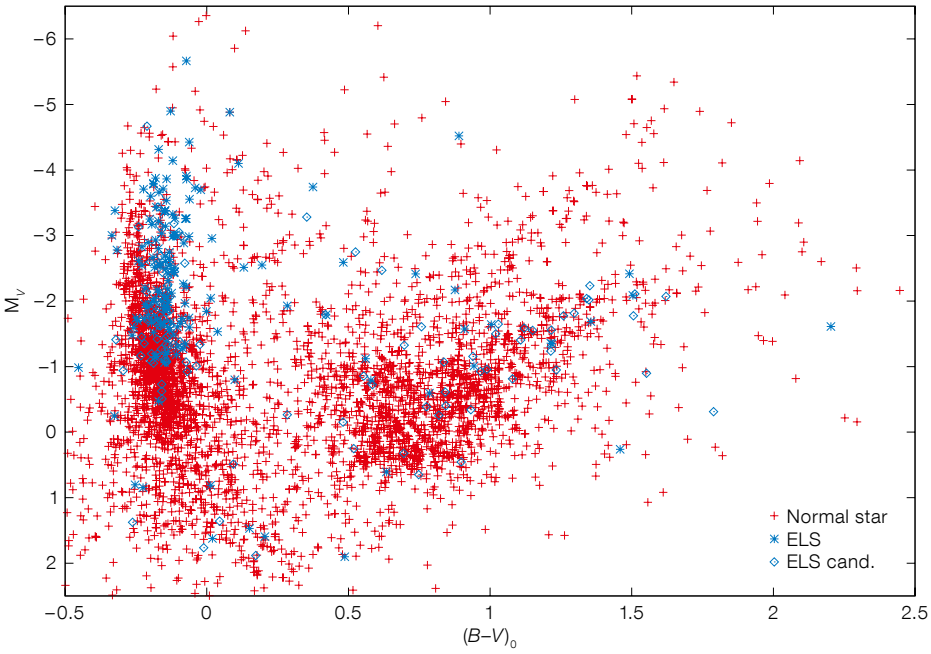

Figure 3. Absolute *V* magnitude versus de-reddened colour $(B–V)_0$ for the full WFI sample of 4437 stars observed in 84 SMC open clusters. Blue asterisks mark emission-line stars, blue diamonds denote candidate emission-line stars, and red plus signs identify normal stars.

Acknowledgement

The authors are grateful to Dr. Emmanuel Bertin for adapting his SExtractor code to the special needs of this project.

References

Baade, D. et al. 1999, The Messenger, 95, 15
Bertin, E. & Arnouts, S. 1996, A&AS, 117, 393
Meyssonnier, N. & Azzopardi, M. 1993, A&AS, 102, 451
Hunter, I. et al. 2008, A&A, 479, 541
Maeder, A., Grebel, E. K. & Mermilliod, J.-C. 1999, A&A, 346, 459
Martayan, C. et al. 2006, A&A, 452, 273
Martayan, C. et al. 2007, A&A, 462, 683
Martayan, C., Baade, D. & Fabregat, J. 2010, A&A, 509, A11
McSwain, M. V. & Gies, D. R. 2005, ApJS, 161, 118
Wallace, P. T. & Gray, N. 2003, ASTROM User Guide

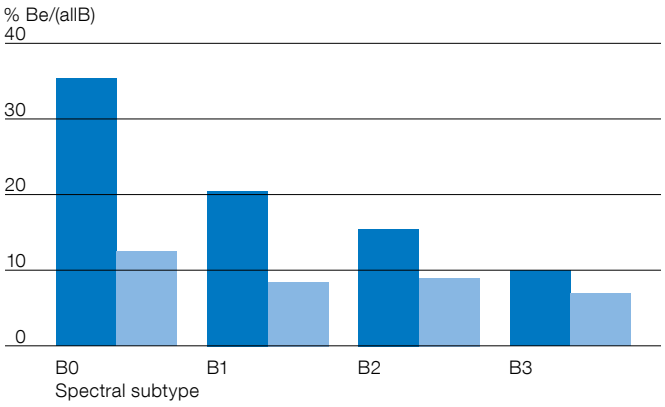

Figure 4. Percentage per spectral subtype of Be stars among all B-type stars. Dark blue left bars are for the SMC (Martayan et al., 2010), and light blue right bars present the Galactic data (McSwain & Gies, 2005). The WFI sample is incomplete for stars with spectral type B3 and later.

CRIRES–POP — A Library of High Resolution Spectra in the Near-infrared

Thomas Lebzelter[1]
Andreas Seifahrt[2,11]
Suzanne Ramsay[3]
Pedro Almeida[3]
Stefano Bagnulo[4]
Thomas Dall[3]
Henrik Hartman[5]
Gaitee Hussain[3]
Hans Ulrich Käufl[3]
Maria-Fernanda Nieva[6]
Norbert Przybilla[7]
Ulf Seemann[2,3]
Alain Smette[3]
Stefan Uttenthaler[8]
Glenn Wahlgren[9,10]
Burkhard Wolff[3]

[1] Department of Astronomy, University of Vienna, Austria
[2] University of Göttingen, Germany
[3] ESO
[4] Armagh Observatory, United Kingdom
[5] Lund Observatory, Sweden
[6] Max-Planck-Institut für Astrophysik, Garching, Germany
[7] Dr. Remeis Observatory, Bamberg, Germany
[8] Institute for Astronomy, Katholieke Universiteit Leuven, Belgium
[9] Catholic University of America, Washington, USA
[10] NASA Goddard Space Flight Center, Greenbelt, USA
[11] University of California, Davis, USA

New instrumental capabilities and the wealth of astrophysical information extractable from the near-infrared wavelength region have led to a growing interest in the field of high resolution spectroscopy at 1–5 µm. A detailed knowledge of the resident spectral features is necessary to fully utilise the diagnostic power of this region of the spectrum. We report on our ongoing project of obtaining a high resolution, high signal-to-noise library of near-infrared spectra between 1 and 5 µm using the CRIRES spectrograph at the VLT. The library will be made public.

After the long domination of astrophysical observations by the visual spectral range, the past years have very clearly shown that the near- and mid-infrared (NIR and MIR) range will play a leading role in many prime areas of astronomical research for the coming decades. This part of the spectrum opens up a universe of "cool" phenomena, such as discs, planets or the extended atmospheres of evolved stars.

In order to understand the contents of the NIR spectral range better, high resolution spectroscopy is mandatory. Considerable progress has been achieved over the past twenty years concerning the sensitivity and size of infrared detectors, allowing efficient spectrographs for the near-infrared to be built for current astronomical use. However, to utilise this part of the spectrum fully, detailed knowledge of the range of spectral features is necessary. This requirement has not yet been reached: line lists, especially for the various molecules, are inaccurate and/or incomplete; many weak lines have not been identified or studied; and the widespread telluric absorption features are a source of confusion. The potential for important discoveries in spectra taken with ESO's CRyogenic Infra-Red Echelle Spectrograph (CRIRES) will not be realised until the spectral features can be identified and line data are made available.

A public library of high resolution NIR spectra of stars of various types throughout the Hertzsprung–Russell diagram (HRD) is needed to meet this challenge. Such a library would not only provide a database from which to select the wavelength range best-suited to a specific scientific question, but it would also be used to compare observations with a reference star, for example in order to measure abundance anomalies or to detect indicators of faint companions. Full coverage spectra of stars of different effective temperature and surface gravity will allow testing of not only atmospheric models with an unprecedented accuracy, but also the atomic and molecular line data used in these models, and determine where improvements are required.

Earlier work, such as the atlas of the solar spectrum (Wallace et al., 1996) or for the K giant Arcturus (Hinkle et al., 1995) illustrated the value of a stellar reference spectrum at high spectral resolution and high signal-to-noise (S/N). However, an inventory of complete NIR stellar spectra at such a resolution across the HRD is not yet available.

Against the background of this unsatisfactory situation, we have formed a team with research interests spread all across the HRD and with the common intention of optimising the usability of the NIR range for high spectral resolution studies, mainly focused on deriving element abundances in stellar atmospheres. As a consequence, we proposed to obtain high resolution spectra of the complete NIR wavelength range for a sample of bright stars of various luminosity, temperature, and chemical composition using CRIRES at the VLT (currently mounted on Unit Telescope 1, UT1). The CRIRES instrument is one of the current workhorses in the area of high resolution NIR spectroscopy[1]. A detailed description of this spectrograph can be found in Käufl et al. (2004).

Our proposal comes as a filler programme for UT1, as the brightness of the stars and the flexibility of the wavelength settings allow us to use almost any weather conditions. Our proposal was granted observing time both in semesters P84 and P85 to begin the collection of a CRIRES spectral library, which, in succession to the UVES Paranal Observatory Project (UVES–POP[2]), was named CRIRES–POP. A continuation of the programme in forthcoming semesters will be proposed.

Target selection

As a starting point for the target selection, we use the UVES–POP library (Bagnulo et al, 2003). Thus, a considerable fraction of the NIR spectra of the stars in our library will have continuous high resolution extension towards the visual and blue range. A further criterion for target selection is a low rotation velocity, to provide sharp-lined spectra. For stars at the extremes of the HRD, the UVES–POP targets are either too bright (at the cool end) or too faint (at the hot end) to be observed with CRIRES. Alternative targets were chosen in these cases. Whereas the UVES–POP library contains spectra of about 400 different stars, the CRIRES–POP will be significantly smaller. The CRIRES spectrograph can obtain

only a comparably small part of the spectrum at each observation, thus a large number of wavelength settings is needed for a complete scan of the NIR range, even when omitting a few settings due to heavy telluric absorption.

Our aim is to obtain CRIRES spectra of 30 bright field stars, each of them composed from almost all of the 200 grating settings. With this number of targets, we cover a sufficient range of stellar parameters across the HRD for a reasonable investment of telescope time. Roughly five targets are foreseen for each semester. Proposed targets for P84 and P85 and their location in the spectral-type *vs.* luminosity plane are shown in Figure 1.

	O	B	A	F	G	K	M	S/C
I								
II			e Vel		HD 109379			X TrA (C)
III						HD 83240	YY Psc	NZ Gem (S)
IV				LHS 1515				
V		τ Sco					Barnard's star	
Deviating abundance pattern			HD 118022					

Figure 1. Spectral classification of the CRIRES–POP targets in the first two observing periods (P84 and P85). The final library will consist of 25–30 stars.

Science goals

The CRIRES–POP science goals are at least as diverse as the fields of interest of the team members. At the cool end of the target list, a major goal is to identify line transitions of the molecules forming in the atmospheres. Depending on the prevailing chemistry of the target, either line transitions of oxygen-bearing molecules (e.g., H_2O or SiO) or of carbon-bearing molecules (CN-, CH-, C_2-components) can be identified. Objects enriched in *s*-process elements (S-type stars) offer a unique opportunity to identify lines of these interesting elements, but also of iron-peak elements whose line lists are far from complete in the NIR. We expect that new diagnostic features for studying the chemical and physical properties of stellar atmospheres will be identified in this way. Both the study and identification of molecular and atomic lines requires collaboration with laboratory spectroscopists, who are among the members of our team. The CRIRES–POP library and the lines identified in the spectra will be important when setting priorities for the laboratory work.

Nearby M dwarfs have recently come into focus for precise radial velocity studies to search for the lowest mass planets. Their intrinsic faintness and variability in the optical makes them ideal candidates for search campaigns in the NIR. The first successful studies have just been launched (e.g., Bean et al., 2009), but the choice of the optimal wavelength region for these studies is still ongoing (e.g., Reiners et al., 2009) and no empirical high resolution atlas for M dwarfs at 1–5 µm exists to help evaluate other spectral features beyond the well known CO overtone spectrum at 2.3 µm. The CRIRES–POP programme will address this question and thus deliver an important input for the study of extrasolar planets.

A broad range of science goals related to understanding stars is directly met by the CRIRES–POP programme. However, stellar photospheric features can also be a source of systematic error, for example when seeking to detect a faint companion or gas emission line from a circumstellar disc. For example, Ramsay Howat & Greaves (2007) found that removal of the spectrum of the stellar continuum of the M3.25 star ECHAJ0843.3-1705 increased the accuracy of the detection of the signal from molecular hydrogen (v = 1–0 S(1)) at 2.122 µm by 10 %, with a corresponding effect on the estimated mass of gas in the disc. Therefore, it is also our intention to provide a library of template stars that may be used to calibrate, and remove, continuum features from stellar photospheres that may mask faint spectral features which are the subject of a science programme.

Hotter stars can also be used both as telluric standards and to address scientific questions. Most prominently, NIR spectroscopy at high resolution will allow us to study the early phases of hot stars when they are still enshrouded by the gas and dust of their parental clouds.

The CRIRES–POP data will play a crucial role in testing and improving model atmosphere techniques across the HRD. Quantitative analyses of NIR spectra can involve a non-trivial extension of classical work in the optical, in particular for the hotter stars. The challenge is to model non-local thermodynamic equilibrium effects in the correct way. Surprisingly, even in the simplest case of hydrogen, the atomic data were, until recently, shown to be of insufficient quality to achieve consistency from the optical and NIR analyses (Przybilla & Butler, 2004). CRIRES–POP data will guide the work on refining the modelling to facilitate unbiased stellar parameter and element abundance determinations at high accuracy in the NIR domain.

Data reduction and release

The CRIRES–POP library of high S/N 1–5 µm spectra will allow for improvements in the general extraction and calibration of CRIRES spectra, and will foster intensive interaction with the CRIRES pipeline developers at ESO. Key interest comes from a strong improvement in the removal of telluric lines, as it opens up

the study of weak features, such as from circumstellar material or rare elements and isotopes. In our approach, we will not use individual observations of telluric reference stars, but instead use one of the CRIRES–POP spectra of an early-type star to produce an accurate model of the atmospheric spectrum. This in turn will then be the basis for the removal of telluric lines from the CRIRES–POP data (cf. Seifahrt et al., 2010; Smette et al., 2010).

All raw data obtained for this programme become immediately public in the ESO archive. At the time of writing, complete spectra from 1 to 5 μm exist for two stars, namely the M giant YY Psc and the F8 subgiant LHS 1515 (see Figure 1). Two parts of the spectrum of YY Psc are shown in Figures 2 and 3, illustrating both the high quality of the spectra and the good results achieved for fitting the telluric spectrum with our model.

As soon as the full wavelength coverage for a star is complete and a brief quality check has been done by our team, the raw data become — in a more user-friendly way — available also on our project website[3]. Once available, all reduced spectra will be placed there as well. All spectra will be reduced in the same consistent way to ensure easy comparability between stars with different stellar parameters. Usage of these data will be made freely available, but we ask that researchers make reference to this *Messenger* paper or our forthcoming paper in a refereed journal (Lebzelter et al., in preparation).

Conclusions

We believe that our high quality NIR spectral library will be an extremely useful tool, e.g., for proposal planning and evaluation. In fact, these spectra will be of considerable interest for a wide variety of scientific investigations not only by the proposers, but by many others in the astronomical and laboratory astrophysics communities. CRIRES–POP will be well suited to the testing of atmospheric models, and for a revision and extension of atomic and molecular line lists, as well as for discovering weak features imposed on the spectral background of a bright star (e.g., for discovering companions or discs).

The CRIRES–POP spectra will be used in conjunction with the UVES–POP spectra and available UV spectra from satellite observatories (HST, IUE) in order to provide wavelength coverage from the far ultraviolet to the NIR. The extent of these data will trigger new ideas by allowing the entire spectrum to be considered. In the absence of high resolution ultraviolet spectra in the post-HST/STIS era, it may be necessary to create infrared diagnostics to replace those at ultraviolet wavelengths. With the focus of major forthcoming astronomical facilities, such as the James Webb Space Telescope or the Extremely Large Telescope projects, on the NIR, we expect that the CRIRES–POP library will find wide use throughout stellar astrophysics.

Further details on CRIRES-POP can be found on the project website[3].

Acknowledgements

The CRIRES–POP team wishes to thank the night astronomers and telescope operators at UT1 (Antu) for their support. Thomas Lebzelter acknowledges funding by the Austrian Science Fund FWF under project number P20046-N12. Henrik Hartman acknowledges support from the Swedish Research Council (VR). Stefan Uttenthaler acknowledges support from the Fund for Scientific Research of Flanders (FWO) under grant number G.0470.07.

References

Bagnulo, S. et al. 2003, The Messenger, 114, 10
Bean, J. L. et al. 2009, ApJ, accepted, arXiv:0911.3148
Hinkle, K. H., Wallace, L. & Livingston, W. 1995, *Infrared Atlas of the Arcturus spectrum 0.9-5.3 μm*, ASP, San Francisco
Käufl, H. U. et al. 2004, SPIE, 5492, 1218
Przybilla, N. & Butler, K. 2004, ApJ, 610, L61
Ramsay Howat, S. & Greaves, J. S. 2007, MNRAS, 379, 1658
Reiners, A. et al. 2009, A&A, accepted, arXiv:0909.0002
Seifahrt, A. et al. 2010, submitted to A&A
Smette, A., Sana, H. & Horst, H. 2010, in preparation
Wallace, L. et al. 1996, ApJS, 106, 165

Links

[1] The CRIRES instrument: http://www.eso.org/sci/facilities/ paranal/instruments/crires/
[2] UVES–POP page at ESO: http://www.eso.org/sci/observing/tools/uvespop/
[3] CRIRES–POP: http://www.univie.ac.at/cririespop/

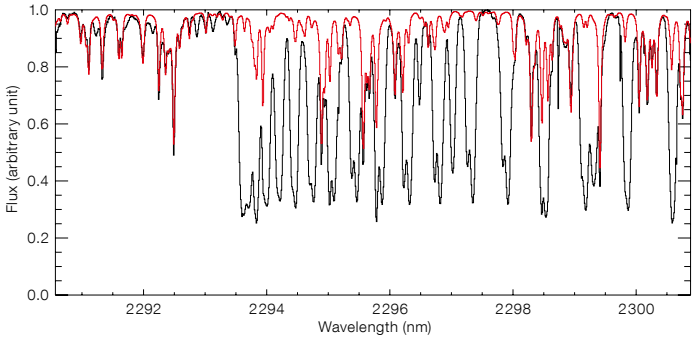

Figure 2. CRIRES spectrum of the M3 giant star YY Psc (black line) taken at the reference wavelength 2308.7 nm, showing the prominent 2–0 band head of CO. The red line shows the telluric model spectrum with lines mainly caused by water vapour and methane fitted to the observed spectrum.

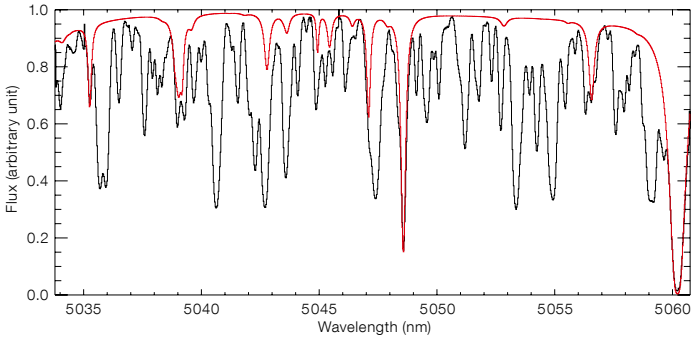

Figure 3. CRIRES spectrum (black line) of YY Psc taken at the reference wavelength 5114.0 nm. The spectrum is dominated by lines of CO and includes interesting low excitation lines of $^{13}C^{16}O$ and $^{12}C^{18}O$. The red line shows the telluric model spectrum with lines caused by water vapour fitted to the observed spectrum.

SINFONI on the Nucleus of Centaurus A

Nadine Neumayer[1]
Michele Cappellari[2]
Paul van der Werf[3]
Juha Reunanen[4]
Hans-Walter Rix[5]
Tim de Zeeuw[1,3]
Richard Davies[6]

[1] ESO
[2] University of Oxford, United Kingdom
[3] Sterrewacht Leiden, the Netherlands
[4] Turku University, Finland
[5] Max-Planck-Institut für Astronomie, Heidelberg, Germany
[6] Max-Planck-Institut für extraterrestrische Physik, Garching, Germany

The prominent radio galaxy Centaurus A is the closest active galaxy and a prime opportunity to study the central supermassive black hole and its influence on the environment in great detail. We used the near-infrared integral field spectrograph SINFONI to measure Centaurus A's black hole mass from both stellar and gas kinematics. This study shows how the advance in observing techniques and instrumentation drive the field of black hole mass measurements, and concludes that adaptive optics assisted integral field spectroscopy is the key to identifying the effects of the active galactic nucleus on the surrounding ionised gas. The best-fit black hole mass is $M_{BH} = 4.5\,^{+1.7}_{-1.0} \times 10^7\,M_\odot$ (from H_2 kinematics) and $M_{BH} = 5.5 \pm 3.0 \times 10^7\,M_\odot$ (from stellar kinematics; both with 3σ errors). This is one of the cleanest gas versus star comparisons of a black hole mass determination, and brings Centaurus A into agreement with the relation of black hole mass versus galaxy stellar velocity dispersion.

During the last few years it has been realised that most, if not all, nearby luminous galaxies host a supermassive black hole in their nucleus, with masses in the range of one million to ten billion solar masses. The black hole mass (M_{BH}) is tightly related to the mass or luminosity of the host stellar spheroid, or bulge, and with the velocity dispersion σ (called the M_{BH}–σ relation) of the stars therein. These correlations have an amazingly low scatter, perhaps surprisingly low, since the black hole and the bulge probe very different scales. These facts indicate that the formation of a massive black hole is an essential ingredient in the process of galaxy formation.

Centaurus A — a special case?

At a distance of less than 4 Mpc NGC 5128 (Centaurus A, hereafter Cen A) is the closest giant elliptical galaxy, the closest active galaxy and the closest recent merger. Cen A hosts an active galactic nucleus revealed by the presence of a powerful radio and X-ray jet. Although this is one of the nearest supermassive black holes, its mass was long under debate (see Neumayer, 2010, for a review). Recent stellar dynamical measurements and modelling by Silge et al. (2005) result in a black hole mass of 2.4×10^8 solar masses, in agreement with the gas dynamical study of Marconi et al. (2001), who found 2×10^8 solar masses (although with a large error bar, depending mainly on the unconstrained inclination angle of the modelled gas disc).

This measurement of the black hole mass placed Cen A almost an order of magnitude above the M_{BH}–σ relation, and made it one of the largest outliers to this relation. The question was whether this is an intrinsic property of Cen A or whether the ground-based seeing-limited observations were not sharp enough to resolve the "sphere of influence" of Cen A's black hole. This is the radius where the black hole dominates the gravitational potential, and, according to the mass predicted from the M_{BH}–σ relation, would be 0.3 arcseconds — not resolved by seeing-limited observations.

Adaptive optics to the rescue

In 2003 we embarked on a comprehensive study of the nucleus of Cen A using the near-infrared imager and spectrograph NAOS–CONICA (NACO) at the VLT. Guiding on the dust-enshrouded nucleus with the unique infrared wavefront sensor that NACO possesses, we obtained images and long-slit spectra at or close to the diffraction limit of the VLT. This study showed that adaptive optics actually works and is applicable to active galactic nuclei (AGN; Häring-Neumayer et al., 2006). It resulted in a black hole mass about a factor of three lower than previous measurements. However, with only four slit positions we were not able to constrain fully the inclination angle of the modelled gas disc.

An ideal combination

With the arrival of SINFONI at the VLT, the study of black holes in galaxy centres made a big leap forward. SINFONI provides integral field spectroscopy at adaptive optics (AO) resolution (Eisenhauer et al., 2003; Bonnet et al., 2004). An ideal combination for studying galaxy centres in great detail! We obtained high signal-to-noise 3D spectra in *J*-, *H*- and *K*-bands (see Figure 1) with two different spatial scales: (i) 0.250 × 0.125 arcseconds (250-milliarcsecond scale) with a field of view of 8 × 8 arcseconds, and (ii) 0.10 × 0.05 arcseconds (100-milliarcsecond scale) with a field of view of 3.2 × 3.2 arcseconds. These spectra show a wealth of gas emission and stellar ab-sorption lines, and enabled us to extract the morphology and kinematics for dif-ferent gas species (Figure 2) as well as the stars, simultaneously. The 100-milliarcsecond data have a spatial resolution of 0.12 arcseconds (full width at half maximum, FWHM) and comfortably re-solve the sphere of influence of the putative black hole.

The SINFONI data reveal vividly how the flux distribution and kinematics in the gas change when going from high to low excitation states. When comparing the velocity fields of [Si VI], [Fe II], and H_2 (middle panels in Figure 2), one notices that the velocity field of [Si VI] consists of two major components: rotational motion around the nucleus (marked with a cross) and translational motion along the jet direction (P.A. = 51°). The non-rotational motion along the jet is less severe, but still remarkable in [Fe II]. The situation is different for molecular hydrogen: the kinematics of H_2 is completely dominated by rotational motion. The molecular gas seems to be well settled in a rotating disc around the black hole without suffering major distortions by the jet. For this reason, we focus on H_2 as the dynamical tracer for the central mass concentration.

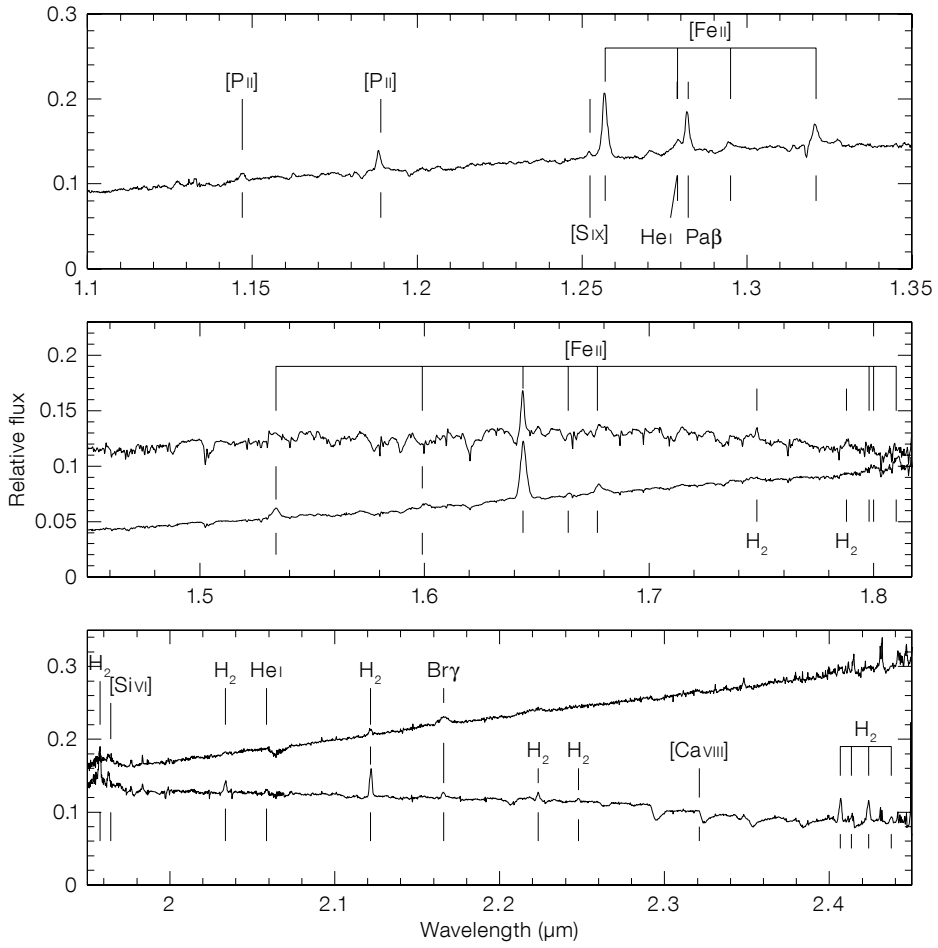

Figure 1. SINFONI spectra in *J*-, *H*- and *K*-band (from top to bottom) of the central 3 × 3 arcsecond circumnuclear region of Cen A. For *H*- and *K*-bands the spectrum is extracted in two different regions, one including the central source (lower line in *H*-, upper line in *K*-band) and one excluding it, i.e. showing the stellar contribution (upper line in *H*-band, lower line in *K*-band).

The SINFONI maps constrain the geometry of the gas disc much better than the few long-slits have done before. The disc is not flat, but appears warped, as indicated by the twist in the line-of-nodes. It connects well with the warped molecular gas disc at larger radii (Quillen et al., 2010). Moreover, the gas disc is consistent with an orthogonal jet-disc picture, and its orientation matches well with a dust disc identified from MIDI observations (Meisenheimer et al., 2007).

In addition to the gas kinematics we have also extracted stellar kinematics from the high signal-to-noise SINFONI *K*-band data. The near-infrared *K*-band spectral region is dominated by the strong stellar absorption feature of the 2.30-μm (2-0) ^{12}CO band head. At this wavelength, the galaxy spectrum is dominated by the light from cool and evolved giant stars. As a library of stellar templates, we used a set of eleven dwarf and giant stars (luminosity class II–V) of late spectral types (K–M), observed with the same instrumental setup as for the Cen A observations. As there is no evidence for a sudden change in the stellar population in the nucleus of Cen A, we assume that the stellar template is fixed and model the non-thermal continuum via additive polynomials, plus we include in the fit the additive contribution of a scaled version of the nuclear non-thermal spectrum (Figure 3). This approach allows us to reliably extract σ in the high resolution 100 milliarcseconds as observations down to a radius of 0.2 arcseconds, before the photon noise of the nucleus eliminates all stellar information from the spectra. For the kinematic extraction the emission from the highly ionised species of [Ca VIII] at 2.32 μm and an H_2 line at 2.35 μm was excluded from the fits (see Figure 3).

The nuclear stellar rotation (Figure 4) is counter-rotating (by about 180°) with respect to the regular H_2 nuclear gas rotation (Figure 2). The stars rotate with a maximum velocity of 25 km/s and are thus much slower than the gas, which reaches a maximum velocity of 130 km/s at $R \approx 0.5$ arcseconds. This indicates that the recent gas acquisition was not able to produce a significant fraction of stars near the nucleus. This is consistent with the lack of evidence for any change in the nuclear stellar population of Cen A.

Modelling the black hole mass: from gas kinematics…

In order to explain the H_2 gas motions seen in the centre of Cen A we construct a kinematic model, where we assume that the gas moves in a thin disc solely under the gravitational influence of the surrounding stars and the expected central black hole. The stellar potential is derived from a composition of NACO, NICMOS, and 2MASS *K*-band images of Cen A. Under the assumptions of spherical symmetry and combined with a dynamically-derived stellar mass-to-light ratio, this gives a three-dimensional mass model, setting the stellar velocity contribution to the dynamical model. Since the observed velocity dispersion of the H_2 gas at the nucleus of Cen A exceeds the mean rotation by more than a factor of two, we need to account for the velocity dispersion in the dynamical model.

We model the kinematics via a tilted-ring model, where the inclination angle and position angle of the gas disc are a function of radius. The orbits of the gas at each radius remain circular, but neighbouring orbits are not necessarily in the same plane. The gas disc geometry changes from coplanar to warped. We calculate a grid of possible models for varying disc inclination and central black hole mass to obtain the set of values

that best match the observed data (Figure 4). The best-fitting black hole mass in our tilted-ring model to the H_2 kinematics is $M_{BH} = 4.5\ ^{+1.7}_{-1.0} \times 10^7\ M_\odot$ for a median disc inclination of 34° ± 4° (error bars are given at the 3σ level).

…and stellar kinematics

For the stellar dynamical modelling, the integral field, high spatial resolution SINFONI observations are essential to tightly constrain the black hole mass

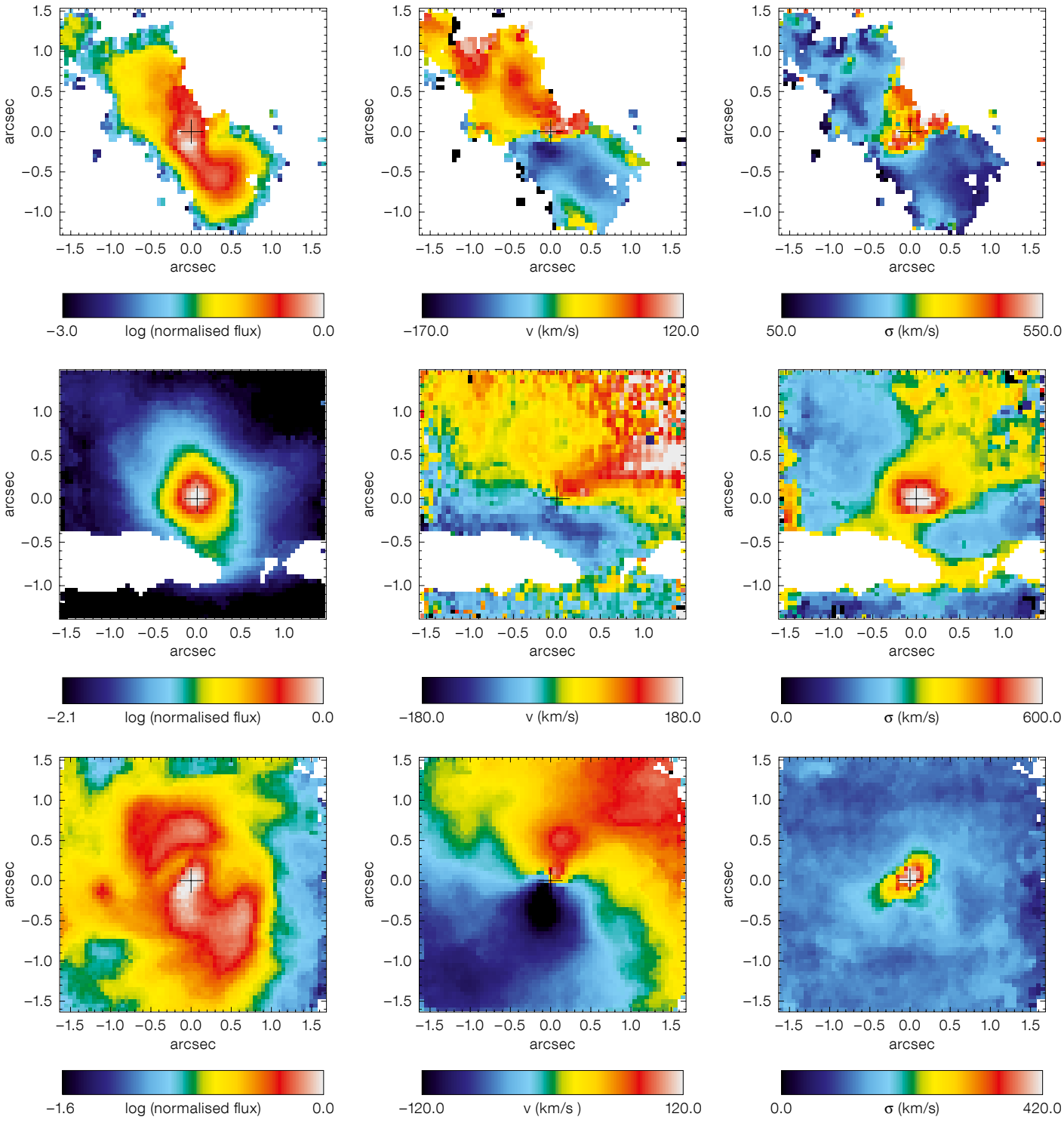

Figure 2. Flux, velocity, and velocity dispersion maps (left to right) of the [SiVI], [FeII], and molecular hydrogen line emission (top, middle, and bottom, respectively). Note the different morphology and kinematics of the ionised gas ([SiVI] and [FeII]) *vs.* the molecular gas.

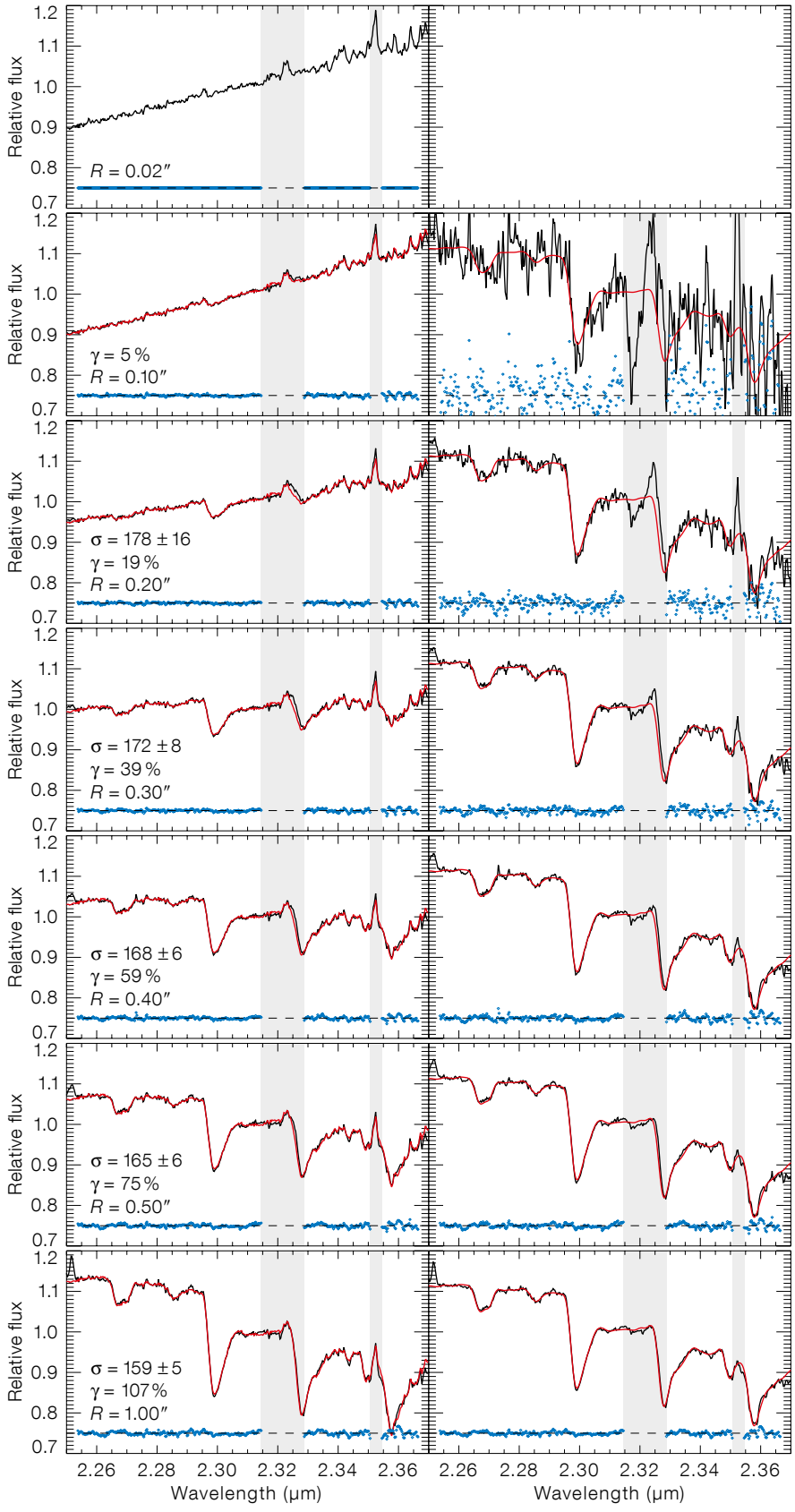

and stellar orbital distribution. However, they are not sufficient as they sample only a small fraction of the half-light radius of Cen A (R_e = 83 arcseconds in the *K*-band). For this reason we complemented our data by the *K*-band kinematics obtained with the Gemini Near Infrared Spectrograph at Gemini South by Silge et al. (2005), which are in very good agreement with the SINFONI data outside the central 2 arcseconds. The stellar kinematics are fit by axisymmetric three-integral orbit-superposition models (Figure 5) to determine the best-fitting values for the black hole mass M_{BH} = 5.5 ± 3.0 × 10^7 (3σ errors) and mass-to-light ratio M/L_K = (0.65 ± 0.15) in solar units. This black hole mass value is in very good agreement with the determination from the kinematics of molecular hydrogen. This provides one of the cleanest gas versus star comparisons for a black hole mass determination, due to the use of integral field data for both dynamical tracers and due to a very well-resolved black hole sphere of influence. Moreover, it brings Cen A into agreement with the M_{BH}–σ relation (Figure 6).

Lessons learned

The development of the black hole mass measurement in Cen A over the past eight years reflects the advance in observing techniques, especially in the near-infrared. High spatial resolution observations are crucial to determine the influence of the central black hole on the gas and stellar kinematics. Adaptive optics actually works! With the advent of near-infrared adaptive optics assisted spectrographs, such as NACO at the VLT,

Figure 3. Radial variation in the spectrum of Cen A in the 100-milliarcsecond SINFONI observations. Left-hand column: different panels show the observed spectra (black solid line) obtained by co-adding the spectra of the spaxels contained within circular annuli of radius *R* and one pixel width (0.05 arcseconds). The best-fitting model (red solid line) consists of the stellar template plus a fourth degree additive polynomial, plus a scaled copy of the non-thermal nuclear spectrum (top panel). The residuals are shown at the bottom of each panel with the blue dots. Right-hand column: the convolved optimal template (red solid line) is compared to the observed spectrum after subtraction of the nuclear spectrum and polynomial contributions (black solid line). The blue dots show the residuals.

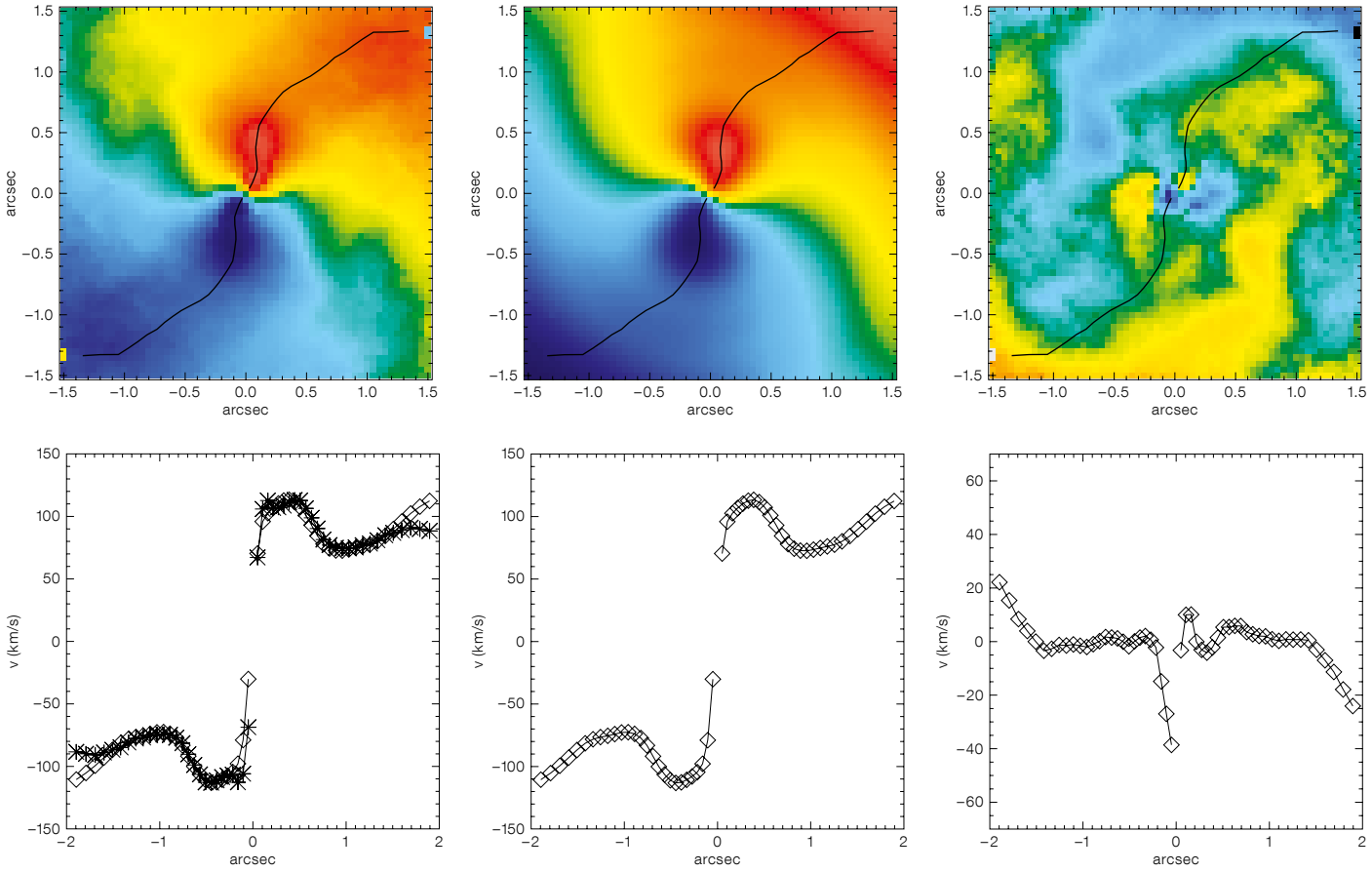

Figure 4. Symmetrised velocity map (upper left) in comparison to the model (upper middle; M_{BH} = 4.5 + 1.7 × 10^7 $M_\odot$, median disc inclination 34°). The residual (data-model) is shown in the upper right panel. The velocity curves in the bottom panels are extracted along the line-of-nodes (overplotted on the velocity maps), and therefore represent the peak velocity curves; the three panels show the observed and model points, the model points only and the residuals. The diamonds correspond to the model velocity curve while the asterisks correspond to the data. The agreement is very good along the line of nodes. The mismatch in data and model for radii beyond r ~ 1.7 arcseconds is likely due to the fact that the inclination angle of the modelled gas disc is not well represented in the outermost parts. This has no impact on the derived black hole mass (taken from Neumayer et al., 2007).

even dust-enshrouded galaxy nuclei became accessible at a spatial resolution of 0.1 arcseconds. This becomes even more powerful when combined with integral field spectroscopy, as in SINFONI. Mapping the gas and the stars in 3D allows the morphology and kinematics of different gas species, plus the stars, to be compared directly and simultaneously. Having this powerful tool in hand, the influence of the inner jet on the kinematics of the ionised gas in Cen A could be revealed, and, moreover, molecular hydrogen could be identified as the ideal gas tracer for the central gravitational potential. The physical state of the gas is therefore very important when using it as a tracer for the dynamical models. The decrease of the value of the black hole mass from Marconi et al. (2001) to Neumayer et al. (2007) was due to the increase in spatial resolution, plus the fact that the kinematic tracer changed from ionised gas to molecular hydrogen.

The presence of an AGN can definitely influence the kinematics of the gas, while the stellar kinematics should be unchanged by this. However, the extraction of the stellar kinematics from the spectral absorption features becomes increasingly difficult in the close vicinity of the AGN, as the AGN continuum dilutes the stellar absorption lines. This is the main difference in the analysis of Silge et al. (2005) and Cappellari et al. (2009). While Silge et al. (2005) first subtract the AGN contribution and then fit the stellar line-of-sight-velocity distribution, Cappellari et al. (2009) include the fit of the AGN continuum in the extraction of the stellar kinematics. This is a very interesting lesson that we learned from Cen A, and we should be cautious when extracting kinematics from other, more distant objects. We also learned that high signal-to-noise data are crucial to extract the stellar kinematics reliably down to small radii. Cen A is indeed the closest AGN and at the same time it is very complex. Every leap in instrumentation development is likely to reveal more complex substructures. This warrants our continuous attention, in order to reveal intrinsic properties in the data and understand shortcomings in the models that aim to predict the observations.

Acknowledgements

Nadine Neumayer acknowledges support from the DFG Cluster of Excellence, Origin and Structure of the Universe. Michele Cappellari acknowledges support from an STFC Advanced Fellowship (PP/D005574/1).

References

Cappellari, M. et al. 2009, MNRAS, 394, 660
Bonnet, H. et al. 2003, SPIE, 4839, 329
Eisenhauer, F. et al. 2003, The Messenger, 113, 17
Häring, N. & Rix, H.-W. 2004, ApJ, 604, L89
Häring-Neumayer, N. et al. 2006, ApJ, 643, 226
Marconi, A. et al. 2001, ApJ, 549, 915
Meisenheimer, K. et al. 2007, A&A, 471, 453
Neumayer, N. et al. 2007, ApJ, 671, 1329
Neumayer, N. 2010, to appear in PASA special CenA issue, arXiv:1002.0965
Quillen, A. C. et al. 2010, to appear in PASA special CenA issue, arXiv:0912.0632
Silge, J. D. et al. 2005, AJ, 130, 406
Tremaine, S. et al. 2002, ApJ, 574, 740

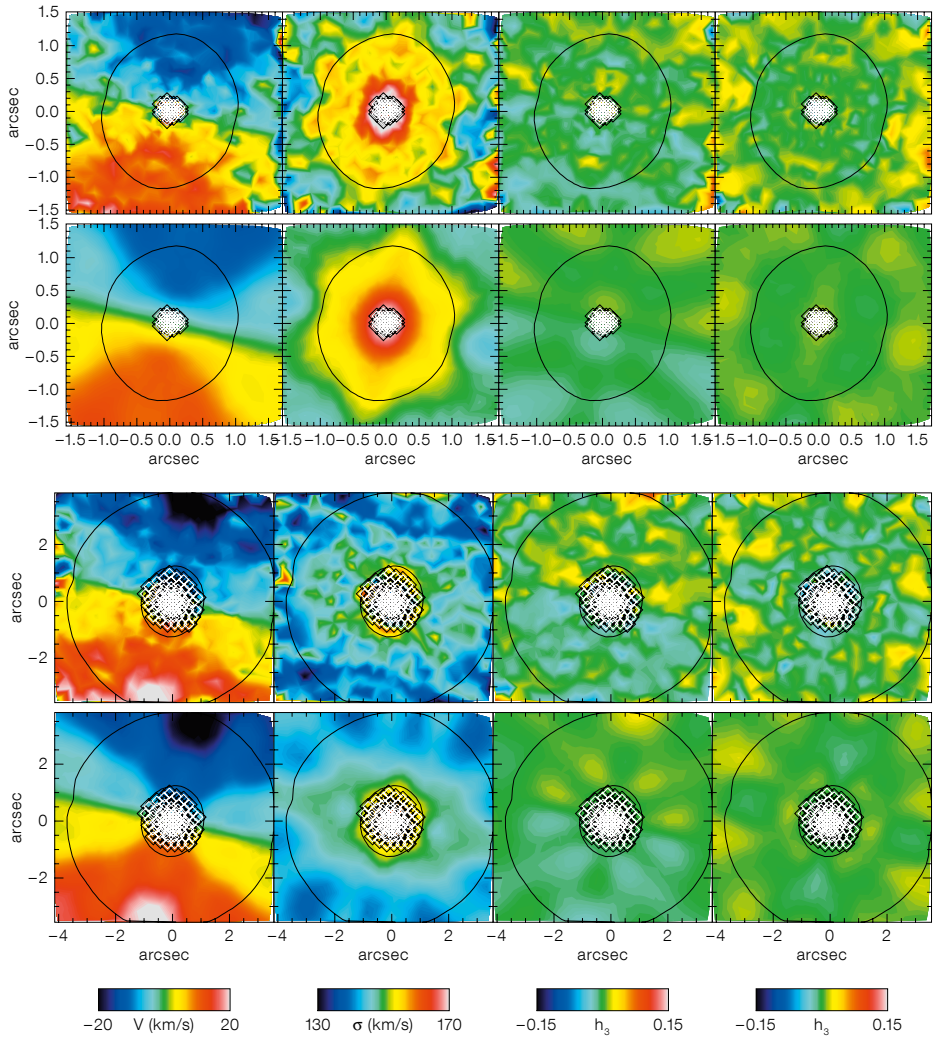

Figure 5 (left). Data-model comparison for the best-fitting three-integral model. Top two panels: the top row shows the bisymmetrised and linearly interpolated 100-milliarcsecond SINFONI data. The second row shows the best-fitting dynamical model predictions. The central bins that were excluded from the fit are shown with the white diamonds. Bottom two panels: same as in the top two panels, for the 250-milliarcsecond SINFONI kinematics. For each quantity, the colour scale is the same in the two instrumental configurations.

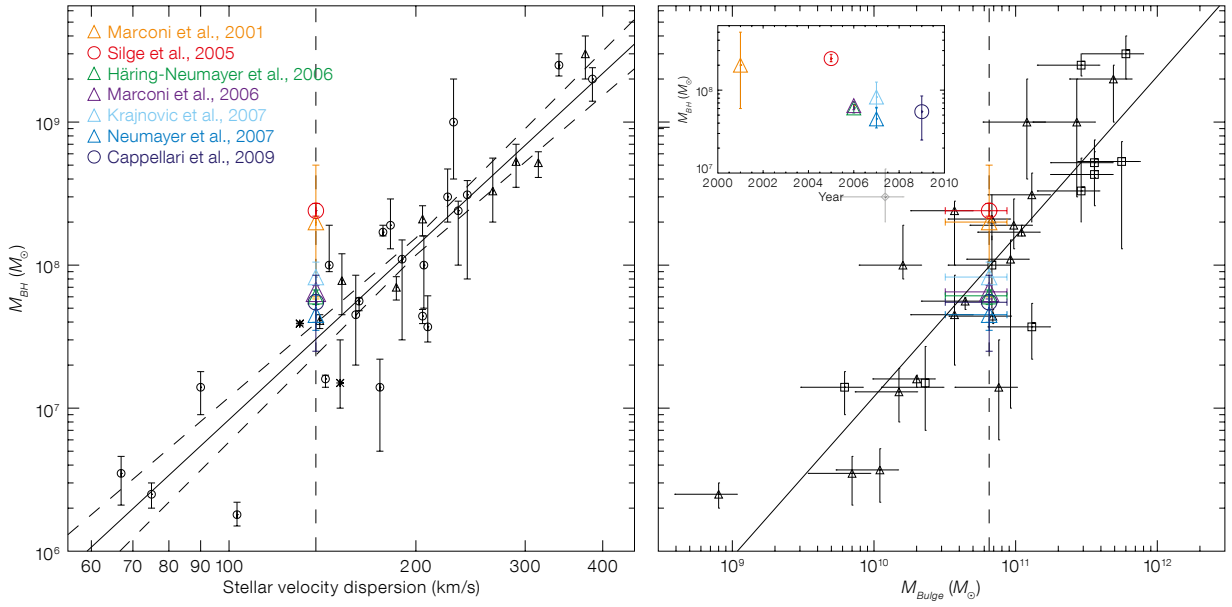

Figure 6 (below). Cen A's black hole mass measurements are plotted on the two black hole mass–galaxy scaling relations. The left panel shows the M_{BH}–σ relation reproduced after Tremaine et al. (2002). The right panel shows the the M_{BH}–M_{Bulge} relation as presented in Häring & Rix (2004) with Cen A values over-plotted. The plot symbols are indicated in the upper left corner. Their time sequence is plotted in the upper left corner of the right panel. In the left panel (and for Cen A measurements) triangles refer to gas kinematical measurements, while circles refer to dynamical models using stellar kinematics.

The Properties of Star-forming Regions within a Galaxy at Redshift 2

Mark Swinbank[1]
Alastair Edge[1]
Johan Richard[1]
Ian Smail[1]
Carlos De Breuck[2]
Andreas Lundgren[2]
Giorgio Siringo[2]
Axel Weiss[3]
Andrew Harris[4]
Andrew Baker[5]
Steve Longmore[6]
Rob Ivison[7]

[1] Institute for Computational Cosmology, Department of Physics, University of Durham, United Kingdom
[2] ESO
[3] Max-Planck-Institut für Radioastronomie, Bonn, Germany
[4] Department of Astronomy, University of Maryland, College Park, USA
[5] Department of Physics and Astronomy, Rutgers University, Piscataway, USA
[6] Harvard-Smithsonian Center for Astrophysics, Cambridge, USA
[7] United Kingdom Astronomy Technology Centre, Edinburgh, Scotland

The discovery and subsequent follow-up of one of the brightest sub-mm galaxies discovered so far is presented. First identified with the LABOCA instrument on APEX in May 2009, this galaxy lies at $z = 2.32$ and its brightness of 106 mJy at 870 μm is due to the gravitational magnification caused by a massive intervening galaxy cluster. Follow-up observations with APEX SABOCA have been used to constrain the far-infrared spectral energy distribution and hence measure the star formation rate, and Swedish Heterodyne Facility Instrument observations help constrain the excitation of the cold molecular gas. Furthermore, high resolution follow-up with the sub-mm array resolves the star-forming regions on scales of just 100 parsecs. These results allow study of galaxy formation and evolution at a level of detail never before possible and provide a glimpse of the exciting possibilities for future studies of galaxies at these early times, particularly with ALMA.

Massive galaxies in the early Universe have been shown to be forming stars at surprisingly high rates. The most prominent examples are sub-millimetre galaxies (SMGs) whose star formation rates can exceed 1000 $M_{\odot}$ year^{-1} (Chapman et al., 2003; Coppin et al., 2008). With this intense star formation rate, a massive galaxy (comparable to the stellar mass of a local elliptical galaxy) can be built in just 100 million years (Tacconi et al., 2008). As such, the sub-mm galaxy population may represent the formation epoch of today's massive elliptical galaxies (Lilly et al., 1999; Smail et al., 1997).

This is, however, a theoretically provocative conclusion as it is at odds with theoretical models. Indeed, sophisticated galaxy formation models have had to alter their prescriptions for starbursts radically, invoking exotic physics such as strong variations in the stellar initial mass function in order to account for the SMG population (Baugh et al., 2004). Although controversial, there is growing evidence that the increased interstellar medium (ISM) pressure within the warm, dense gas in local ultra-luminous infrared galaxies (ULIRGs) results in an increased Jeans mass (Perez-Torres et al., 2009). In order to test these controversial prescriptions, direct observational constraints on the properties of individual star-forming regions within high redshift galaxies are necessary. Such observations are technologically challenging, requiring the increased collecting area and sensitivity of the next generation telescopes, such as the Extremely Large Telescopes currently being planned and the Atacama Large Millimeter/Submillimeter Array (ALMA) under construction. Moreover, since the most intensely star-forming galaxies are also the most obscured, they are optically faint and difficult to identify and study on sub-kiloparsec (sub-kpc) scales.

Gravitational lensing

The most promising route for investigating the properties of high redshift galaxies on sub-kpc scales is to use massive galaxy clusters as natural lenses. Galaxy clusters magnify the images of distant galaxies that serendipitously lie behind them. This natural magnification causes background galaxies to be strongly amplified and stretched, providing us with the opportunity of studying young and intrinsically faint galaxies with a spatial resolution that cannot be attained via conventional observations. The natural amplification caused by the galaxy cluster has two effects: (i) the image of the background galaxy is magnified at a fixed surface brightness (i.e. the total brightness is increased); and, (ii) the galaxy is not only amplified, but it is also stretched, making it possible to spatially resolve components of the galaxy from the ground.

LABOCA imaging of distant clusters

During recent Atacama Pathfinder Experiment (APEX) 870-μm observations of a massive galaxy cluster (MACS 2135-0102) we serendipitously discovered an extremely bright sub-mm galaxy with an 870-μm flux of 106 mJy (see Figure 1, left). This is three times brighter than any other known high-redshift star-forming galaxy and even brighter than the Cloverleaf and APM08279 quasars. Due to the high significance of the source, we were able to centroid the sub-mm emission to an accuracy of less than 0.5 arcseconds and identify the mid-infrared counterpart with a bright source detected by the Spitzer Space Telescope Infra-Red Array Camera (IRAC) and Multiband Imaging Photometer (MIPS); see Figure 1 right. Due to the brightness, we were able to obtain a redshift measurement for the galaxy of $z = 2.3259$ via the blind detection of CO(1–0) using the Zpectrometer on the Green Bank Telescope (GBT), confirming that the galaxy is high redshift and strongly gravitationally lensed. Indeed, using a detailed mass model of the galaxy cluster we derive an amplification factor of 32.5 ± 4.5. Intrinsically therefore the 870-μm flux is ~ 3 mJy, typical of the sub-mm background, and, on account of the amplification, an ideal target for study. The CO(1–0) emission line flux can also be used to estimate the cold molecular gas mass; after correcting for lensing amplification we derive a gas mass of $2 \times 10^{10}\ M_{\odot}$.

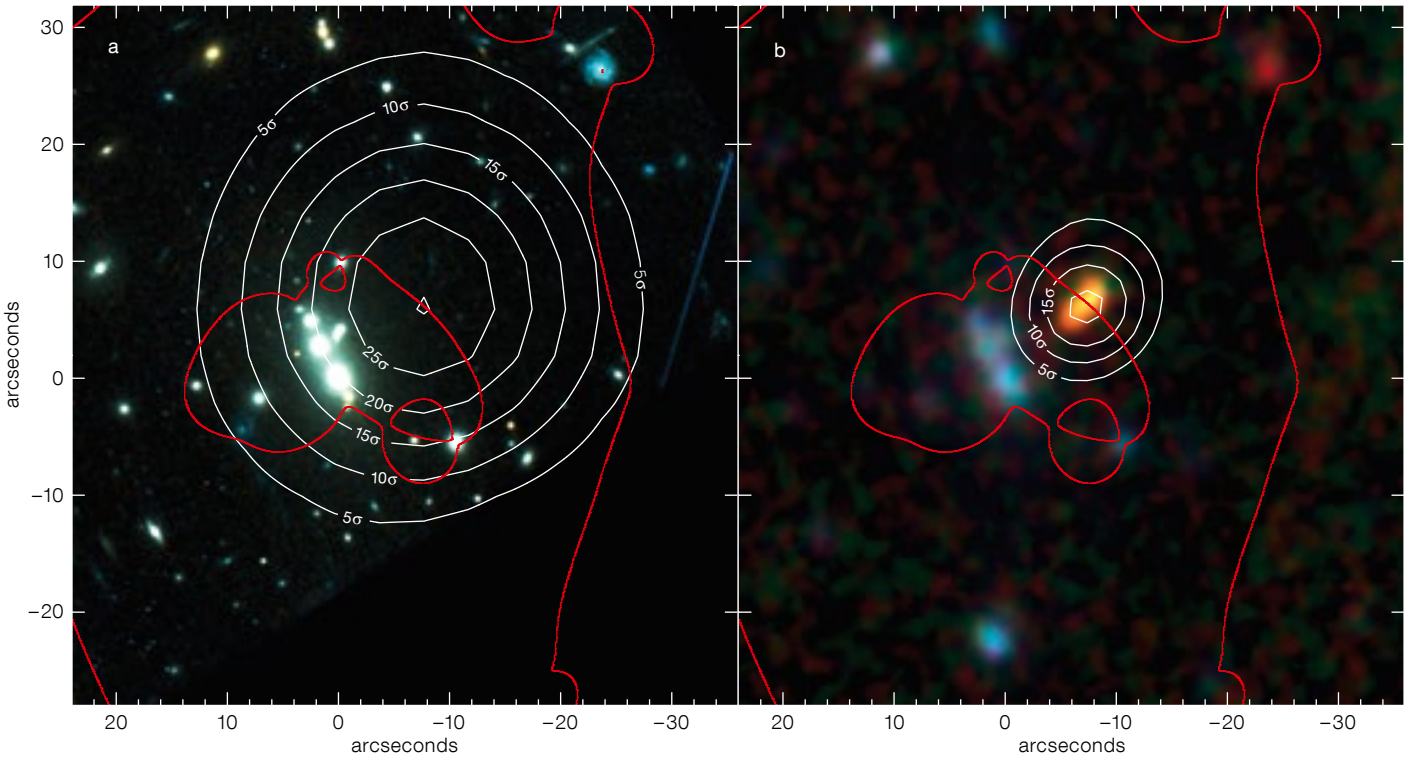

Figure 1. True colour HST *VI*-band image of the massive galaxy cluster MACSJ2135-0102 (z_{cl} = 0.325) is shown (left). The white contours denote the APEX/LABOCA 870-μm contours from the galaxy (contours denote 5, 10, 15, 20, 25, 30σ), identifying an SMG with flux 106 mJy. The solid red lines denote the z = 2.326 radial and tangential critical curves from the best-fit lens model. The true colour IRAC 3.6, 4.5, 8.0-μm image of the cluster core is shown (right). The contours denote the intensity of the 350-μm map and show 5, 10, 15, 20σ. The red lines again show the lens model critical curves.

SABOCA

With confirmation that this is a highly amplified background galaxy, observations at 350 μm using the SABOCA camera (see article by Siringo et al., p. 20) were carried out to parameterise the spectral energy distribution (SED); see Figure 2. With a measured 350-μm flux of 530 mJy we derive an intrinsic far-infrared luminosity of 1.2 × 10^{12} $L_{\odot}$. This suggests a star formation rate of 210 $M_{\odot}$/yr. If this star formation rate has been maintained, then it takes just ~ 120 Myr to build the observed stellar mass of 4 × 10^{10} $M_{\odot}$ and the remaining gas depletion timescale is a further 70 Myr. Together, this suggests that this intense star formation episode may be the first major growth phase of this galaxy.

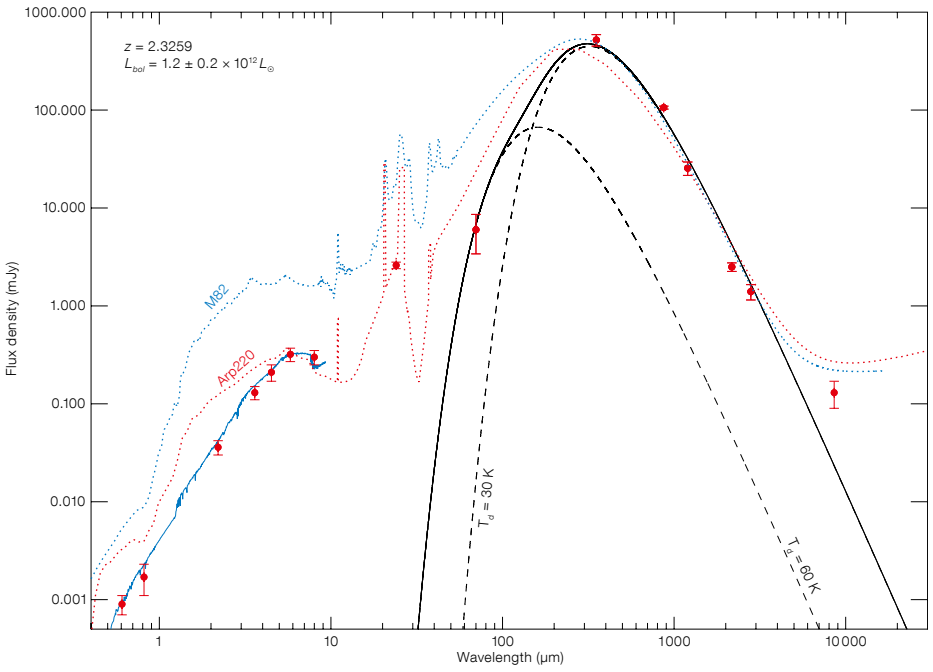

Figure 2. Spectral energy distribution (SED) of the lensed galaxy SMMJ2135-0102 is shown. To test how the SED of the galaxy compares to local starbursts, the SEDs of M82 (blue dashed line) and Arp220 (red dashed line), both arbitrarily scaled to the 1.2 mm flux, are overlaid. The solid black line denotes the best fit modified blackbody to the photometry. Accounting for lensing amplification, the bolometric luminosity of the galaxy is L_{bol} = 1.2 ± 0.2 × 10^{12} $L_{\odot}$ which corresponds to a star formation rate of SFR = 210 ± 50 $M_{\odot}$/yr.

Molecular gas properties

To further constrain the properties of the cold molecular gas, observations of the high-J CO emission (up to $J = 7$) were obtained with a combination of Institut de Radioastronomie Millimétrique Plateau de Bure Interferometer (IRAM PdBI; CO(3–2) up to CO(7–6)) and APEX Swedish Heterodyne Facility Instrument (SHFI) (CO(7–6)). In Figure 3a we show the CO(1–0) and CO(7–6) line profiles obtained with the IRAM Eight MIxer Receiver (EMIR) and APEX/SHFI respectively. All the CO spectra show multiple peaks that we decompose into a "red" component and a "blue" component which are separated by 300 ± 24 km/s. Since the ratio of the high/low-J emission lines reflects the excitation of the molecular gas, we extract and model the CO spectral line energy distribution (SLED) of both "red" and "blue" components using large velocity gradient (LVG) models (e.g., Weiss et al., 2005). Both components are best fit with two excitation models (with temperatures ~ 40 K and densities of approximately 10^3 and 10^4 cm^{-3}; see Figure 3b. The LVG modelling also includes the "equivalent size" of the CO-emitting region as a free parameter, and we are therefore able to estimate the size of each component indirectly. The SLED modelling suggests that both the "red" and "blue" components appear to have a compact core with radius ~ 150 pc surrounded by a more extended, diffuse region with radius ~ 500 pc. Although these equivalent sizes come with some uncertainty, the brightest CO-emitting regions appear similar to those seen locally as starbursts with a dense, active star-forming core surrounded by a diffuse gas disc, perhaps providing the first direct evidence for a diffuse disc in an SMG.

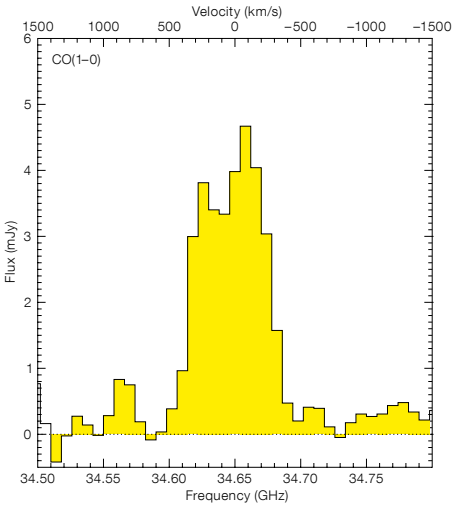

Figure 3a (above). Spectra of the ^{12}CO(1–0) and ^{12}CO(7–6) emission from SMMJ2135-0102 obtained with GBT/Zpec (left) and APEX/SFHI (right). The CO emission shows at least two velocity components separated by 300 km/s.

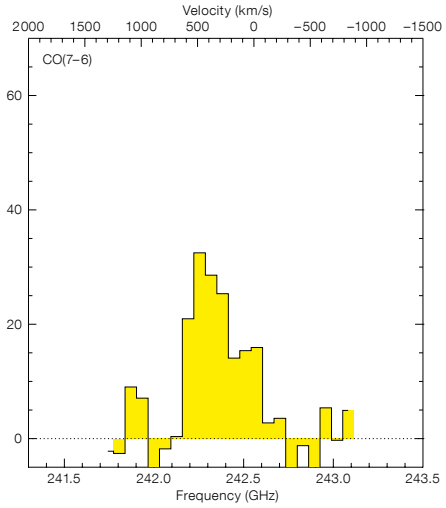

Figure 3b (below). The spectral line energy distributions (SLEDs) for the "blue" and "red" velocity components seen in CO emission.

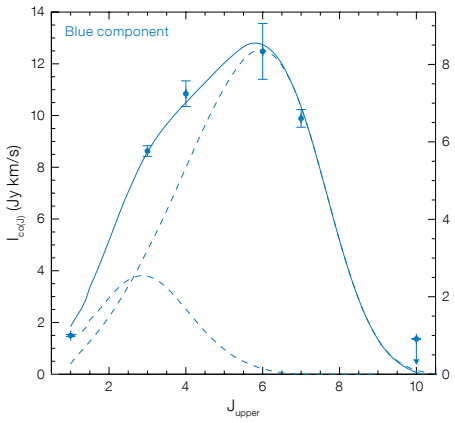

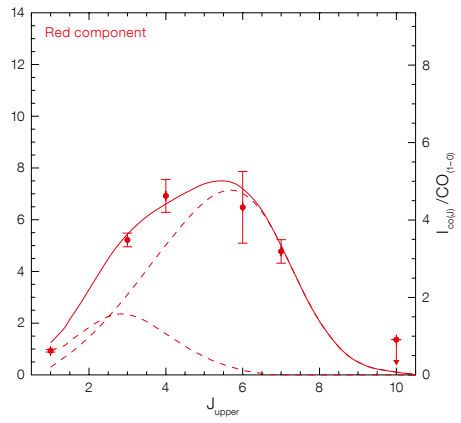

Resolving the star-forming regions

To resolve the sub-mm emission directly, Submillimeter Array (SMA) observations were used to image the galaxy's 870-μm (345 GHz) continuum emission with a 0.2-arcsecond synthesised beam and hence investigate the sub-mm morphology. The map resolves the galaxy into eight discrete components over ~ 4 arcseconds in projection (Figure 4). These components represent two mirror images of the galaxy each comprising four separate emission regions. Reconstructing the source-plane image using the lensing model, the galaxy comprises four bright star-forming regions in the source plane (indicated as A, B, C and D in Figure 4), that are separated by 1.5 kpc in projection. At the most highly amplified position, the source-plane resolution reaches ~ 90 pc which is comparable to the characteristic size of giant molecular clouds in the Milky Way (Scoville et al., 1989).

We compare the sizes and luminosities of the star-forming regions within SMMJ2135-0102 to giant molecular clouds (GMCs) in the local Universe (Scoville et al., 1989; Snell et al., 2002; Caldwell et al., 1996) in Figure 5. Within typical GMCs, constant energy density leads to a correlation between size and 260-μm luminosity, such that luminosity is proportional to radius cubed. However, within the dense cores of GMCs and young HII regions, massive stars dominate the emission and produce luminosity densities a factor ~ 100 times higher than in typical GMCs (Hill et al., 2005) and shown by the upper dashed line in Figure 5. The star-forming regions within SMMJ2135-0102 are ~ 100 pc across, which is 100 times larger than dense GMC cores, but as Figure 5 shows their luminosities are approximately 100 times higher than expected for typical star-forming regions. Indeed, the luminosity densities of the star-forming regions within SMMJ2135-0102 are comparable

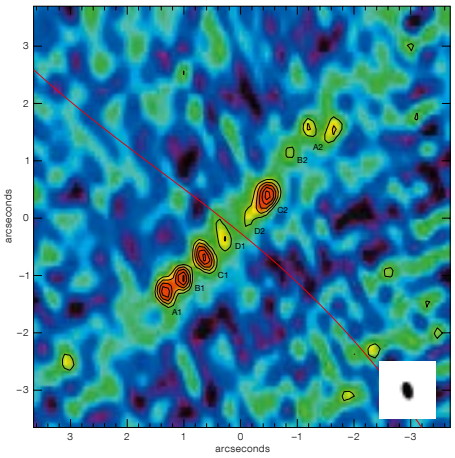

Figure 4a. The SMA map of SMMJ2135-0102 showing the image-plane morphology of the lensed galaxy at 870 μm. The galaxy comprises eight individual components, separated by up to 4 arcseconds in projection. The z = 2.326 radial critical curve (red line) is overlaid. The beam size is shown (lower right).

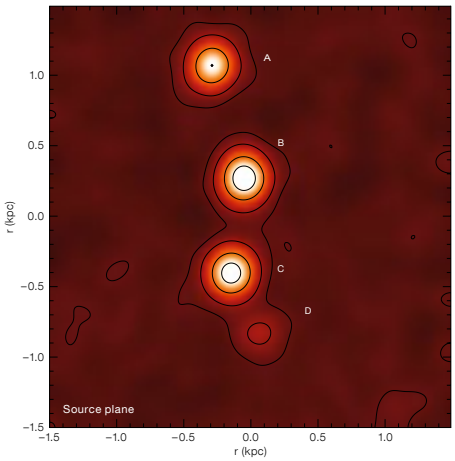

Figure 4b. The spatial distribution of the four components in the image plane from the lens model are shown. Each of the components (A, B, C and D), which are mirrored about the lensing critical curve, are identified.

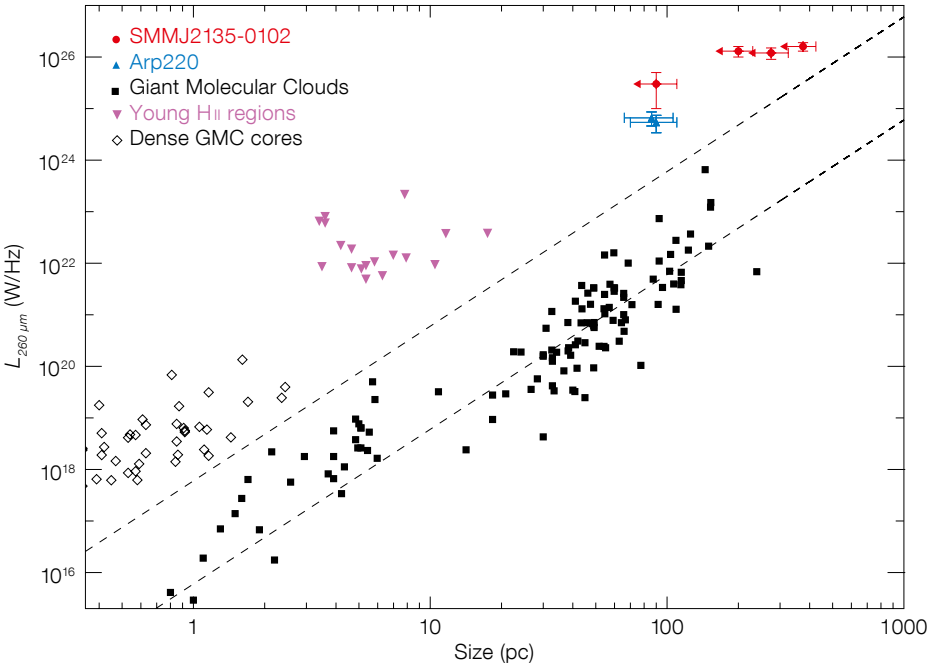

Figure 5. Correlation between size and luminosity for star-forming regions in SMMJ2135-0102 compared to those in the Milky Way and local galaxies. Black squares denote the size and 260-μm luminosities of giant molecular clouds in the Milky Way and the local group. The lower dashed line shows a fit to this relation (with slope fixed at $L_{260\,\mu} \propto r^3$; i.e. constant energy density). The solid red points denote the sizes and luminosities of the star-forming regions in SMMJ2135-0102. The sizes and luminosities of dense cores of galactic GMCs in Henize 2-10 and M82 are plotted (open diamonds) as well as the two dominant star-forming regions within the local ultra-luminous infrared galaxy Arp220 (blue triangles).

to dense GMC cores, but with luminosities 10^7 times larger. Thus, it is likely that each of the star-forming regions in SMMJ2135-0102 comprises ~ 10^7 dense GMC cores.

The luminosity (and therefore star formation) density of the star-forming regions within SMMJ2135-0102 are also similar to those found in the highest density regions of the local starburst galaxy Arp220 (shown by blue triangles in Figure 5), although they are scaled up by a factor 10 in both size and luminosity (Sakamoto et al. 2008). Thus, the energetics of the star-forming regions within SMMJ2135-0102 are unlike anything found in the present-day Universe, yet the relations between size and luminosity are similar to local, dense GMC cores, suggesting that the underlying physics of the star-forming processes is similar. Overall, these results suggest that the recipes developed to understand star-forming processes in the Milky Way and local galaxies can be used to model the star formation processes in these high-redshift galaxies.

Outlook

Overall, these results provide unique insight into the physics of star formation within a galaxy at z ~ 2 on scales that would otherwise only be achieved with the increased light grasp and resolution of the next generation of facilities, such as ALMA. Indeed, due to the lensing effect we are able to provide an effective glimpse of two of the three science drivers for ALMA: to provide images at an angular resolution of 0.1 arcsecond of the dust continuum from distant galaxies; detect spectral CO emission in star-forming galaxies out z = 3 and measure their redshifts; albeit only for a single object. Thus, due to the fortuitous discovery with LABOCA and subsequent APEX/SHFI, SMA and GBT/Zpectrometer follow-up of this galaxy, we are able to provide unique insights into the key science that will be routine once ALMA reaches full science operations.

References

Baugh, C. M. et al. 2004, MNRAS, 69, 3101
Caldwell, D. A. et al. 1996, ApJ, 472, 611
Chapman, S. C. et al. 2005, ApJ, 622, 772
Coppin, K. E. K. et al. 2008, MNRAS, 384, 1597
Hill, T. et al. 2005, MNRAS, 363, 405
Lilly, S. et al. 1999, ApJ, 518, 641
Livanou, E. et al. 2006, A&A, 451, 431
Perez-Torres, M. A. et al. 2009, A&A, 507, L17
Sakamoto, N. et al. 2008, ApJ, 684, 957
Scoville, N. et al. 1989, ApJ, 339, 149
Smail, I. et al. 1997, ApJL, 490, 5
Snell, R. L. et al. 2002, ApJ, 578, 229
Swinbank, A. M. et al. 2010, Nature (in press)
Tacconi, L. et al. 2008, ApJ, 680, 246
Weiss, A. et al. 2005, A&A, 440, 45

Further images in Press Release eso1012.

Credit: IAU/IYA2009/L. Pullen

The closing ceremony of the International Year of Astronomy took place in the Aula Magna of the University of Padova where Galileo Galilei taught. See article by Mignone et al., p. 62.

Report on the Joint ESO/MPE/MPA/LMU Workshop

From Circumstellar Disks to Planetary Systems

held at MPE, Garching, Germany, 3–6 November 2009

Leonardo Testi[1]
Ewine van Dishoeck[2,3]

[1] ESO
[2] Leiden Observatory, Leiden University, the Netherlands
[3] Max-Planck-Institut für extraterrestrische Physik, Garching, Germany

A summary of the joint ESO/MPE/MPA/LMU workshop "From Circumstellar Disks to Planetary Systems" is presented. The meeting reviewed the status of our observational and theoretical understanding of protoplanetary disks, from the formation phase through their evolution to planet formation and debris disks.

The study of circumstellar disks and the formation of planetary systems has experienced enormous progress in recent years. Thanks to wide field imaging surveys with the Spitzer Space Telescope and ground-based near-infrared and submillimetre telescopes, unbiased samples of thousands of young stellar objects with disk luminosities down to 0.01 $L_{\odot}$ (the brown dwarf regime) have been identified in the nearest molecular clouds within ~ 1 kiloparsec. Photometry from optical to millimetre wavelengths provides spectral energy distributions whereas mid-infrared and submillimetre spectroscopy probes the gas and the solid state content. The ESO Very Large Telescope (VLT) and its interferometer (VLTI) in the optical/infrared, combined with millimetre and radio interferometers at longer wavelengths, are providing a wealth of high angular resolution observations to study disk structure and evolution. New and exciting developments range from evidence for grain growth and settling (the first steps in planet formation) as the disks evolve, to the development of gaps and holes in a new set of transitional disks, and to the direct detection of (proto-)planets around pre-main sequence stars. New facilities with enormous potential are lining up and are expected to start producing a wealth of new data: the Herschel Space Observatory and the Atacama Large Millimeter/submillimeter Array (ALMA) with the opening of Early Science in 2011. In the more distant future, protoplanetary disks are also a key theme for the James Webb Space Telescope (JWST) and the European Extremely Large Telescope (E-ELT).

The workshop was organised with the goals of reviewing the status of the field and discussing transformational programmes that will be made possible with the upcoming facilities, and especially by the combined use of present and future ESO facilities. To achieve these goals the workshop brought together the communities working with ground-based infrared large telescopes and interferometers, with space observatories and millimetre interferometers, as well as theorists and modellers. The second half of 2009 was chosen for the workshop on account of the perfect timing to: discuss observational programmes to be carried out with ALMA during Early Science; review the survey results from Spitzer and other large field facilities; present the new high angular and spectral resolution results that are coming from the ESO VLT/VLTI; view the first glimpses of the potential of Herschel. Indeed, this workshop distinguished itself from other recent meetings in the field by covering the full span of observational facilities (rather than just one specific instrument or wavelength) and by having a healthy mix of observations and models.

The workshop covered all the phases of the lifetime of disks: from disk formation, the role of disks in the formation and early evolution of stars, disk evolution including planet formation, debris disks and young planetary systems. The high level of attendance (the meeting was substantially oversubscribed) and lively discussions following the talks and at the poster sessions are a testimony to the maturity and the high rate of progress of the field (see Figure 1). The frequent reference in the talks to the prospects of Herschel, ALMA and in the more distant future, JWST and E-ELT observations, reaffirmed the key role of these facilities for the studies of disks and the formation of planetary systems. Most of the 53 talks presented are available on the workshop web pages[1]. Here we briefly summarise only a few of the many new results presented at the conference.

Selected results

The formation and properties of disks during the early stages of star formation, the so-called Class 0 phase, were discussed in the framework of recent Spitzer, Sub-Millimeter Array (SMA) and Institut de Radioastronomie Millimétrique (IRAM) Plateau de Bure interferometer (PdBI) results. The observations clearly show that compact flattened structures are formed in the very early stages of collapsing protostellar envelopes. The exact nature of these compact sources and their theoretical interpretation are still debated, as current observations cannot fully distinguish the "pseudodisk"

Figure 1. Workshop participants photographed outside the MPE seminar room.

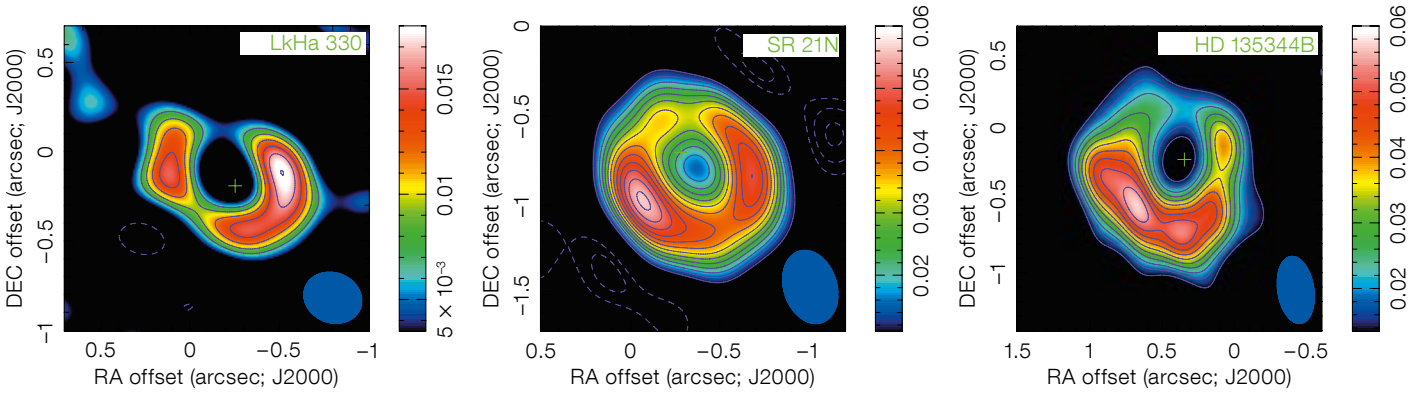

Figure 2. High angular resolution submillimetre continuum images of three transitional disks obtained at the SMA (Brown et al., 2009). The high angular resolution images reveal an inner region of the disk where the dust column density is much lower than in classical disks, possibly a result of disk evolution, which could be caused by photoevaporation, viscous evolution or clearing by young protoplanets.

predicted by models of collapsing magnetised clouds from the classical flat accretion disks. Key tests of the different models will soon be made possible by observing the kinematics of these compact structures using ALMA to detect and image rare molecular species.

The discussion of the statistics, diversity, chemical and physical properties of disks around pre-main sequence stars occupied a large fraction of the meeting. The power of Spitzer as a survey telescope was demonstrated by the results presented for several star-forming regions. It is now well established that disks with similar properties surround young stellar objects with masses ranging from brown dwarfs to a few solar masses, and even more massive stars are found to be associated with disks, albeit with different properties and lifetimes. Much work is being invested in the characterisation of the non-classical disks in an attempt to understand their nature and possible relationship with disk evolution. As an example, the possible role of photoevaporation or planet formation in shaping transitional disks was discussed (see Figure 2). Inner holes are detected in the dust distribution of several of these disks, but in many cases the interpretation is still ambiguous due to the limited resolution and signal-to-noise ratio of the observations, and the lack of high sensitivity and high angular resolution observations of the gaseous component of the disk. Winds and accretion represent an alternative indirect probe of the inner regions of disks and several new results in these areas were discussed at the meeting.

The evolution of the solid and gaseous components of the disks towards the formation of planets was the other major subject discussed by many theoretical and observational talks (see for example Figure 3). Millimetre-wave continuum observations of disks now show convincing evidence for the presence of large (mm–cm size) grains in the outer regions (radii ~ 100 AU) of protoplanetary disks. These findings challenge the theoretical predictions of dust fragmentation and migration and most likely require some form of trapping of large grains in small areas of the disk; a few possible mechanisms to achieve this trapping were presented. Resolving grain growth properties at millimetre wavelengths across disks is going to produce a major breakthrough in this area and should be within the capabilities of ALMA and the Expanded Very Large Array (EVLA).

The last part of the meeting was dedicated to young (exo-)planetary systems, debris disks and the dynamical interactions between planets and dust in young planetary systems. A handful of direct detections of planetary mass companions to nearby stars were presented (see example in Figure 4) and the interactions between these bodies and the debris disks in these systems were discussed in the framework of dynamical evolution models. The sophistication reached by the dynamical interaction models was discussed in several talks. Indeed, the variety of observed debris disk morphologies could be explained by these models using reasonable values for the mass and orbits of the planetary bodies. In addition, population synthesis models of planetary systems have reached a level of complexity that now allows for a detailed comparison of the properties of exoplanets with the observed distributions.

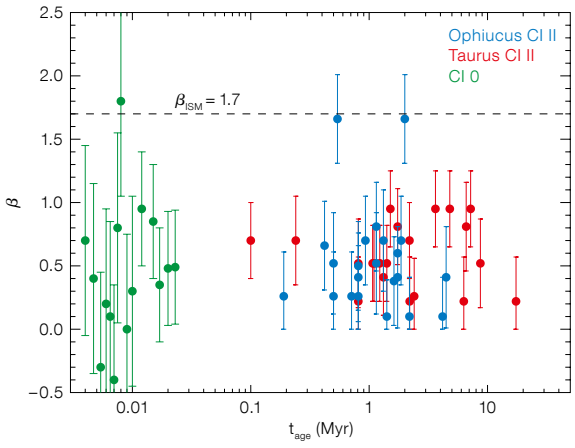

Figure 3. Dust opacity power law index as a function of age for a large sample of disks around isolated pre-main sequence stars in Taurus and Ophiuchus (red and blue points respectively) and for a small sample of young protostars in Perseus and Cepheus (data from Jørgensen et al., 2007; Kwon et al., 2009; and Ricci et al., 2010). The data show that the dust grains seems to have grown at least to millimetre sizes in all but two of the observed systems, suggesting that grain growth may be a fast process in the outer disk and that large grains survive much longer than predicted by models.

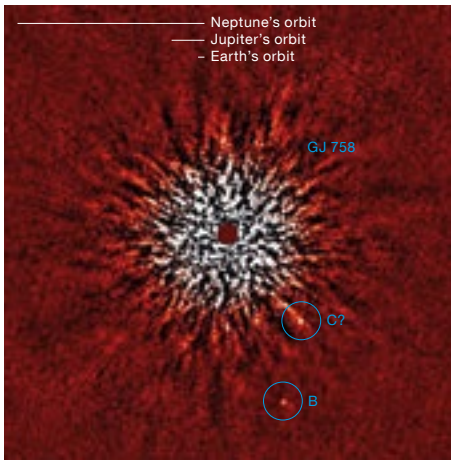

Figure 4 (above). Direct imaging detection of the planets around the G-type star GJ758 announced at the meeting (SUBARU/HiCIAO data, Thalmann et al., 2009).

The success and smooth organisation of this workshop would have not been possible without the help and support of Christina Stoffer and Jasmin Zanker-Smith, as well as the postdocs and students who served with enthusiasm and dedication on the Local Organising Committee (Joanna Brown, Greg Herczeg, Agata Karska, Pamela Klaassen, Luca Ricci, Paula Teixeira — see Figure 5). We also thank all our colleagues at the MPE for their patience and understanding during the invasion of their institute by over 200 conference participants.

References

Brown, J. M. et al. 2009, ApJ, 704, 496
Jørgensen, J. K. et al. 2007, ApJ, 656, 293
Kwon, W. et al. 2009, ApJ, 696, 841
Ricci, L. et al. 2010, A&A, in press, astro-ph: 0912.3356
Thalmann, C. et al. 2009, ApJ, 707, L123

Links

[1] Workshop web page: http://www.eso.org/sci/meetings/disks2009/index.html

Figure 5 (below). Local organisers, from left to right: Joanna Brown, Greg Herczeg, Pamela Klaassen and Paula Teixeira enjoying themselves at the workshop dinner and Luca Ricci and Agata Karska setting up presentations for the speakers during the workshop breaks.

Report on the CAUP and ESO Workshop

Towards other Earths: Perspectives and Limitations in the ELT Era

held in Porto, Portugal, 19–23 October 2009

Nuno Santos[1]
Claudio Melo[2]
Luca Pasquini[2]
Andreas Glindeman[2]

[1] Centro de Astrofísica, Universidade do Porto, Portugal
[2] ESO

A short report on the workshop aimed at exploring the role of the Extremely Large Telescopes in finding and characterising Earth-like planets is presented.

The Centro de Astrofísica da Universidade do Porto hosted an ESO-sponsored conference, which had the main goal of understanding how Extremely Large telescopes (ELTs) will help in finding and characterising other Earth-like planets, as well the challenges that we have to overcome to achieve this goal.

In order to enable the discovery and characterisation of other Earths, a new generation of instruments and telescopes is now being conceived and built by different teams around the world. With the large diameter of their primary mirrors, the new generation of ELTs will play a crucial role in this research and the detection of Earth-mass planets is expected to be within reach.

In parallel, a new generation of instruments for current 8 to 10-metre-class facilities is being planned. The new cut-

The participants at the conference “Towards other Earths” in Porto.

ting-edge suite of instruments include high angular resolution adaptive optics (AO) imagers, micro-arcsecond astrometry with interferometers, and ultra-stable spectrographs at the cm/s precision level. Synergies of these facilities with spaced-based observatories will play a key role in the discovery of Earth-mass planets.

What are the requirements that this instrumentation will have to achieve for us to find other Earths? Do we know how to calibrate the instruments to achieve the required superb level of precision and stability? Equally important are the intrinsic limitations of the parent stars, caused by astrophysical phenomena such as stellar activity, granulation or oscillations. How is it possible to deal with and correct for these effects? What are the ultimate limitations of the different techniques for ground- or space-based facilities?

To address these issues, we proposed to ESO that a specific conference be organised to gather together the community of planetary astronomers and instrumentalists working in the field to: i) review the current status of the search for telluric exoplanets, and present our understanding about their formation; ii) discuss the implications of their main physical properties on the detectability limit with different techniques; and iii) draw a coherent picture of the technical and physical issues that we have to solve to succeed in the fabulous endeavour of finding and characterising other Earths.

The scientific programme of the conference started on Monday morning, following the welcome speeches by the organisers, the director of the Centro de Astrofsica da Universidade do Porto and the vice-rector of Porto University, a representative from ESO, and the president of the Portuguese Fundação para a Ciência e a Tecnologia.

The scientific programme of talks was divided into three sessions. The first was dedicated to the presentation of the current results and status on prospects for Earth-mass/radius planet detection. The second session considered the astrophysical and technical challenges and solutions towards the detection of other Earths, and the third was entitled “Towards the characterisation of exo-Earths”.

In parallel with the talks, an excellent set of posters, often complementing the information given in the talks, was displayed and available for viewing for the whole week.

Session 1: Status and prospects

The first talks were dedicated to the results of different radial velocity surveys. We learned that HARPS is working at full throttle, with the announcement of 32 new planets (including some low-mass ones) from the HARPS guaranteed time observing (GTO) programme. A press conference (associated with an ESO press release, eso0939) was held, making a tremendous impact on the local and international media. According to the HARPS GTO team, it seems that these planets are just the tip of the iceberg, and that many more will be announced over the next couple of years. In one of the HARPS observing programmes, there is evidence that up to 60 % of stars have planets with a mass below 50 times the mass of the Earth.

The derivation of precise radial velocities in the infrared was also a highlight of the first morning. We learned that it is now possible to achieve precisions of the order of a few metres per second with CRIRES, a result that opens up new perspectives for the detection and characterisation of planets around M dwarf stars and more active (younger) stars. Finally, the measurement of the Rossiter–McLaughlin effect during a planetary transit is now providing interesting and unexpected evidence that many short period planets have orbital planes that are misaligned with the stellar equator.

The conference proceeded with a series of talks on the results from transit surveys, both ground- and space-based. The way that these are providing crucial information about planetary interiors was also discussed. It was interesting to learn that, by coupling asteroseismology measurements with transit photometry, we can derive significantly more precise values for the planetary radius. Finally, we learned that in some particular cases the detection of transits from super-Earths is possible using ground-based instrumentation.

The direct imaging of other planets was then the focus of the conference, with some excellent talks describing the most recent results on this topic, and some of the difficulties and advantages of the technique. In particular, we saw that new data confirm some of the previously discovered planets detected in wide orbits, and the discussion is now turning to their formation process.

The first session concluded with a review about the results and prospects for the astrometric and microlensing detection methods. The importance of the astrometric method for the characterisation of exoplanets was outlined, in particular to derive the true masses of radial velocity systems. Finally, the formation and possible composition of other Earths was discussed. Earths and super-Earths should be common, but their composition and evolution is probably dependent on a number of conditions that are hard to predict.

Session 2: Detection challenges

The second session started with a presentation about the ELT instrumentation for Earth-like planet searches and char-

acterisation. We heard that the main purpose of the ELTs will not include the search for planets using astrometry, microlensing or photometric transit techniques (although follow-up using these methods is certainly envisaged). However, a lot is expected from radial velocity and direct imaging, and even the characterisation of their atmospheres is a goal.

Following the Tuesday afternoon social programme, which included a visit to the famous Porto wine cellars and a boat tour on the River Douro, the Wednesday sessions focused on the technical and astrophysical limitations to the detection of other planets using the radial velocity, photometric transit and astrometric techniques. Both the instrumental and astrophysical aspects are providing significant developments. Although stellar intrinsic phenomena and even the existence of multi-planet systems pose some difficulties to the detection of other Earths, a general consensus exists that it will be possible to detect Earth-type planets in the habitable zones of solar-type stars (spectral types G, K and M). Small M dwarfs may be particularly good targets for transit searches, but new generations of stable spectrographs will also allow the discovery of "exo-Earths" orbiting K and M dwarfs.

Most of Thursday was dedicated to discussion of the challenges and progress achieved towards the direct detection of Earth-like planets with ELTs. We learned that although it will be a difficult task, a number of promising extreme AO instruments are being planned that will allow direct images of planets orbiting other solar-type stars to be made.

Session 3: Exo-Earth characterisation

The final session began late on Thursday, opening the window on an impressive number of results showing how the direct detection and characterisation of exo-atmospheres is a fast-growing field. It is already possible to identify molecules in exoplanet atmospheres, to detect day and night temperature gradients, and to find evidence for atmospheric escape and variability. The advent of the ELTs will certainly open the way to new exciting science in this field, and may even allow the detection of biosignatures in the atmospheres of exo-Earths. The difficulty of modelling the atmospheres of exo-Earths was presented; however it was suggested that in this field observations will lead the theoretical findings.

Overall, the exceptional quality of the talks contributed to make this a great conference, where many different ideas were presented and discussed. We would thus like to deeply thank the scientific organising committee, the local organising committee and all the participants for making this a memorable event.

All the talks will be available (both in video and in pdf format) on the website[1] of the conference and a DVD will be sent to all the participants.

Links

[1] http://www.astro.up.pt/toe2009

Report on the ESO Workshop

Galaxy Clusters in the Early Universe

held at the Gran Hotel Pucón, Chile, 9–12 November 2009

Chris Lidman[1,2]
Michael West[1]

[1] ESO
[2] Anglo Australian Observatory, Epping, Australia

A workshop bringing together theoreticians and observational astronomers from different wavebands to discuss the current knowledge of galaxy clusters is briefly summarised.

Galaxy clusters are the most massive bound structures in the Universe. The most massive examples contain thousands of galaxies and are about a thousand times more massive than our own Milky Way. Since clusters can be detected from a time when the Universe was only a few billion years old all the way to present day, they serve as unique laboratories for studying environmental influences on galaxy formation and evolution. If we look back far enough we should be able to see clusters, and the galaxies within them, forming. Moreover, the number density of galaxy clusters is sensitive to cosmological parameters, such as the amount of matter in the Universe, the equation of state of the mysterious dark energy and the primordial power spectrum of density fluctuations.

For these reasons, the search for distant galaxy clusters is currently a very active field, with the number of known distant clusters or proto-clusters increasing rapidly. The detection of distant clusters of galaxies is challenging because methods that have traditionally worked well — such as the detection of the X-ray emission from the hot intracluster gas or optical imaging to detect clusters as enhancements in the projected galaxy

Participants at the workshop with the smoking Volcán Villarrica in the background.

distribution — become much less efficient as one goes to greater distances. Nevertheless, a variety of techniques, including optical, infrared and X-ray surveys, as well as surveys based on the Sunyaev-Zel'dovich effect, have identified a growing number of clusters in the early Universe. Alternative methods, such as the use of powerful radio galaxies and quasars as beacons for locating high-redshift clusters, are also providing promising new ways to identify and study the most distant galaxy clusters.

With this motivation, ESO organised a workshop in the resort town of Pucón in Southern Chile with the goal of bringing together theoreticians and observational astronomers working at different wavelengths to summarise the current state of knowledge of galaxy clusters.

The conference was held over four days in the Gran Hotel Pucón, which is situated on the shore of the beautiful Lake Villarrica. A fifth day was kept free for participants to explore the region and to participate in some of the adventurous activities that are on offer in this part of Chile. Quite a few of the participants climbed Volcán Villarrica, an active volcano that dominates the Pucón skyline. The volcano can be seen behind the participants in the conference photo.

About 100 participants attended the workshop. Over the four days of the conference, there were about 60 talks, of which eight were invited reviews, and twenty posters. The presentations covered a broad range of cluster studies, from the theorist's view of galaxy evolution in galaxy clusters to detailed observations of individual clusters. Particularly impressive to the authors of this report, were the size and quality of the multi-wavelength datasets that were presented during the workshop. These datasets represent the result of many years of dedicated work and many hours of telescope time. Also presented were a few record-breaking high-redshift clusters. We look forward to learning more about these clusters at one of the cluster conferences being held during 2010.

In view of the rapid progress that has been made in this field and the number of cluster conferences that will be held during 2010, the proceedings will only be made available from the conference website[1]. By the time this *Messenger* report appears, all the presentations and some of the first papers will be available.

Acknowledgements

The workshop would not have been possible without the guidance of the scientific organising committee, the dedicated, efficient and friendly support of Daniel Asmus, María Eugenia Gómez, Paulina Jirón, Ricardo Salinas, and Jean Siefken, and of course the participants, who travelled such a long way to attend.

Links

[1] http://www.eso.org/sci/meetings/GCEU2009/

ALMA Achieves Closure Phase with Three Antennas on Chajnantor

Leonardo Testi[1]

[1] ESO

It is an exciting time for the Atacama Large Millimeter/submillimeter Array (ALMA). Following the shift of the focus of the testing activities from the ALMA Test Facility in Socorro, New Mexico (see *The Messenger*, 135, 61) to Chile at the end of 2008, the project has seen truly remarkable progress. Following conditional acceptance of the first antenna at the beginning of 2009, first fringes with two antennas were achieved at the Operations Support Facility (OSF at 2900 m altitude) after a few months (see *The Messenger*, 137, 17). Later in the year, three antennas were transported to the Array Operations Site (AOS, at 5000 m), where fringes were achieved with two antennas at submillimetre wavelengths. Finally, towards the end of the year three antennas were linked together and stable fringes and closure phase was achieved by the ALMA Assembly Integration and Verification (AIV) team (see ESO Press Release eso1001).

Following the successful checks on the three antenna interferometers and the deployment of the latest version of the ALMA software system, on 22 January 2010, the ALMA project has officially entered the Commissioning and Science Verification (CSV) phase. The goal for 2010 is to deliver the hardware, software

Figure 1 (above). The three ALMA antennas on Chajnantor working as an interferometer. The APEX telescope is also visible in the background.

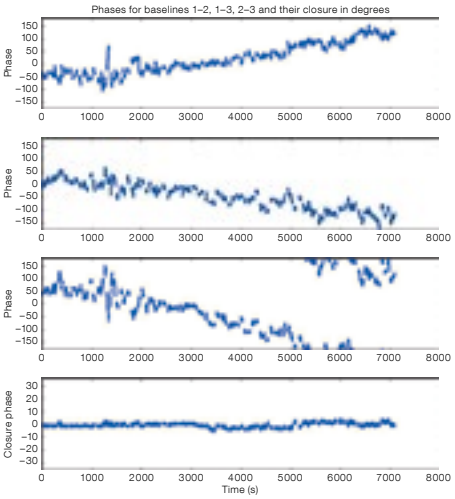

Figure 2 (right). Test of closure phase with three antennas at AOS. The upper three panels show the phase as measured on each of the three baselines and the bottom panel shows the closure phase.

and perform the necessary tests to allow a release of the first call for proposals for Early Science observations with ALMA.

This progress has been made possible by the many people intent on keeping to the schedule for the hardware and software deliveries for the closure phase and the start of CSV activities, as well as by the tireless efforts of the ALMA AIV and CSV teams led by Joe McMullin and Richard Hills.

Report on the Workshop

Data Needs for ALMA

From Data Cubes to Science: Ancillary Data and Advanced Tools for ALMA

held at the I. Physikalisches Institut, Universität zu Köln, Germany, 5–7 October 2009

Leonardo Testi[1]
Peter Schilke[2]
Crystal Brogan[3]

[1] ESO
[2] I. Physikalisches Institut, Universität zu Köln, Germany
[3] National Radio Astronomy Observatory, Charlottesville, USA

A summary of a workshop bringing together laboratory physicists, chemists and astronomers to discuss the needs and strategies for developing common approaches to data and models for ALMA is presented.

The Atacama Large Millimeter/submillimeter Array (ALMA) will revolutionise many scientific areas by providing an unprecedented quantity and quality of high spatial and spectral resolution (sub)millimetre wavelength spectral line data. These data will allow detailed observational tests of astronomical models of astrochemistry, star and planet formation, galaxy formation and evolution, and many others. The high quality ALMA data will allow much more stringent comparison between observations and models than has been possible with data from current instruments. Nevertheless, to achieve this, the models (e.g., chemical network models, radiative transfer programmes, etc.) need to be of commensurate quality. Additionally, given the expected ALMA data production rates, easy and perhaps innovative ways of comparing and visualising models and data must be available. The models need to have access to fundamental physical data, such as molecular and atomic line frequencies and strengths, collision rates, dust properties, etc. While producing the models themselves is a science activity, adapting them for use with ALMA data, and making them available to a larger community (including testing, documentation, etc.) is not. This latter is especially critical since one of the goals for ALMA is to be easily useable by the wider astronomical community and not to be restricted only to experts in millimetre and radio interferometry.

In order to optimise the science output from ALMA, there is therefore a need to produce and gather ancillary data and make them available to ALMA users, as well as adapting and making available scientific models for use by the ALMA community at large. While some efforts along these lines exist, such as the Cologne Database for Molecular Spectroscopy

(CDMS), the Jet Propulsion Laboratory (JPL) Splatalogue, the Observatoire de Paris ro-vibrational collisional excitation database BASECOL, the Leiden Atomic and Molcular Database (LAMDA), the RATRAN radiative transfer programmes, the ease of use of these tools for both data and models is not at the level desired. In addition there is significant concern in the astronomical community regarding the long-term availability of support for the laboratory and theoretical efforts that have been, and are continuing, to produce the basic physical and chemical data required for astrophysical modelling.

The workshop “Data Needs for ALMA”, organised with the sponsorship of Radionet and the major ALMA partners, ESO, the National Radio Astronomy Observatory (NRAO) and the National Astronomical Observatory of Japan (NOAJ), was dedicated to the discussion of the above topics. The workshop brought together laboratory physicists, chemists, and astronomers as providers of data and models, together with astronomers as customers, to discuss data and modeling needs and strategies for developing common databases both of physical data and models for use with ALMA data. The programme and many of the talks are available[1].

Workshop topics

The workshop opened with a summary of the status of ALMA construction and a summary of the plans for ALMA Early Science and user support software and databases. ALMA will provide software to support the various phases of observing programme preparation, from proposal submission (Phase 1) to Scheduling Block preparation (Phase 2), pipeline and offline data reduction software, which, together with the widespread user support through the ALMA Regional Centres, will allow ALMA users to plan for their observations and produce quality-assured data cubes (“ALMA images”) ready for scientific analysis. The need for advanced analysis tools and catalogues for proper exploitation of ALMA data was clearly demonstrated with Institut de Radioastronomie Millimétrique (IRAM) and SubMillimeter Array (SMA) observations of the molecular cores surrounding forming low- and high-mass stars. With a fraction of the bandwidth and sensitivity of the future ALMA observations, we are already detecting not only a variety of molecular lines that require proper chemical modelling, but a large fraction of emission features from molecular species that are not yet identified (see example in Figure 1).

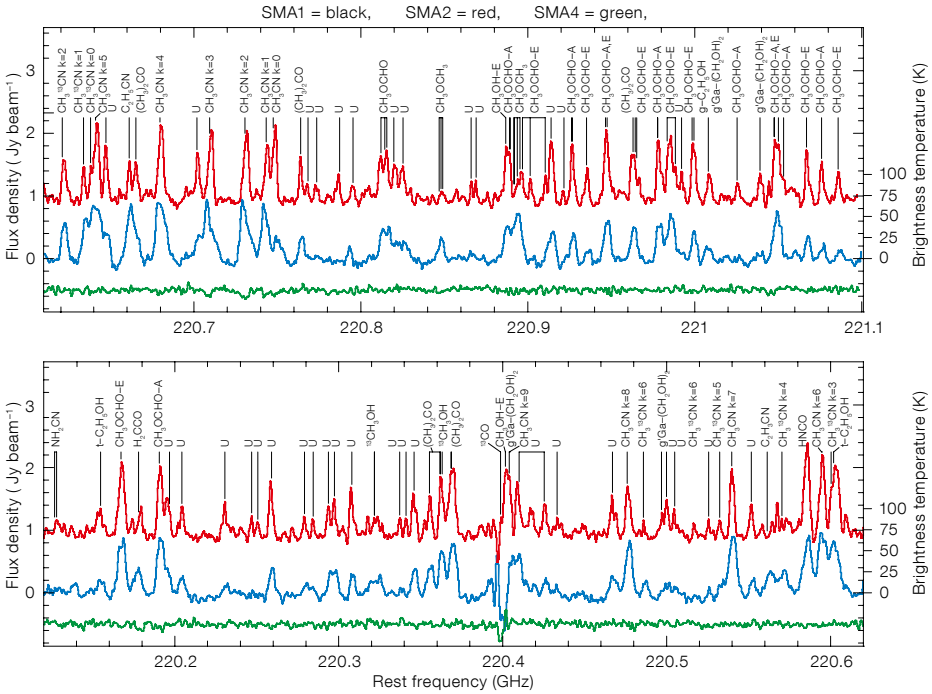

Figure 1. Example of SMA hot core spectra from three massive star-forming cores separated by less than 5000 AU in NGC 6334I, showing the richness of molecular species and the large fraction of unidentified lines (Brogan et al., in preparation).

The need for the development of advanced chemical models, which have to include the treatment of fractionation of different isotopic species, for at least the most common atoms and molecules, was evident from observations of molecules such as CCS, ^{13}CCS and C^{13}CS that were presented at the meeting. These observations show different abundance ratios for the isotopologues than predicted in current chemical models of molecular clouds. In addition, the importance of proper modelling of source structure, and its impact on the chemical structure, the radiation transfer, and ultimately the observed spectrum of the observed sources, was emphasised in several talks.

A number of areas were identified as requiring significant additional resources including: laboratory measurements and theoretical calculations of line frequencies; collisional and reaction rates; and numerical codes to integrate these data with proper source modelling and radiation transfer. One of the major problems, which is especially critical for groups performing laboratory measurements or running theoretical computations to provide data for astrophysical modelling, is the recognition of their “service” work and long-term funding for these efforts. It was also recognised that new software interfaces that allow easy access to the different existing databases, while allowing a more efficient use of the observational data, can introduce an additional divide between the catalogue producers and the astronomers, making it even more difficult to provide the proper recognition for the catalogue contributors and providers. As an additional difficulty, most of the physical and chemical experiments and computations required by the astronomers are not always considered as the highest priority for funding in their own field. It was thus recognised that the laboratory and computational work needed for astrophysical purposes

Figure 2. Example of a Splatalogue[2] search for molecular transitions near 220 GHz.

should be at least partially supported as part of astrophysics programmes.

Several possible models to mitigate this problem were discussed, ranging from direct support of these efforts from the observatories, to automatically providing the proper references to be cited whenever data from the original catalogues or calculations are used (similar to the path followed by the particle physics community). Of the various alternatives, the latter seemed to be favoured by the majority of the participants at the workshop. A first step in this direction is already ongoing with the drafting of a Memorandum of Understanding for collaboration between the Köln astrophysical laboratory spectroscopy group, providing the CDMS, and the JPL spectroscopy group, providing the JPL catalogue. At the same time, an effort is ongoing to find general agreement between the catalogue providers and the Splatalogue spectral line database (also functioning as the data provider for a number of additional catalogues) and query tool developed at NRAO. Splatalogue is available[2] and Figure 2 shows an example search. The aim is to provide a common catalogue interface that will be integrated with the ALMA and Expanded Very Large Array (EVLA) observation preparation and data analysis software. A similar path could be followed by the providers of collisional and reaction rates of astrophysical interest.

Proposals

The participants agreed at the workshop that there is a pressing need to acknowledge and support efforts to secure long-term funding for the community of physicists and chemists who are providing the data necessary to perform the scientific analysis of ALMA data. It was decided to write a White Paper that will highlight the importance of this work for the scientific output of the millimetre and submillimetre observatories. Such a White Paper could be used as a reference when asking for support from funding agencies.

The production of more advanced chemical network models, radiation transfer codes and source structure codes are the result of astronomical research; obtaining proper credit or funding for developing these is not expected to be harder than for any other astrophysical research project. The issue in this case is more to make sure that codes are available and properly documented for the potential users to obtain the best out of them. It was thus suggested that the ALMA Regional Centres could set up web pages to collect links to the available codes in a homogeneous way and in a single easily accessible location.

The workshop was regarded as very useful as a forum for discussions between astronomers, physicists and chemists. The needs posed by the new generation of millimetre observatories were identified and actions on how to provide data and models were defined. It was suggested that these workshops should be organised on a regular basis to track the progress and new developments both on the side of the astronomers needs and on the new developments with experiments, computations and catalogues.

Links

[1] Workshop programme: http://www.astro.uni-koeln.de/projects/schilke/DataNeedsForALMA/Program
[2] Splatalogue: http://www.splatalogue.net

The Messenger on the Web

Christopher Erdmann[1]

[1] ESO

As part of a new ESO initiative, under the direction of the ESO Library, all ESO *Messenger* content from 1974 to the present is now fully available on the ESO web. The project involved scanning roughly the first 80 issues of *The Messenger* for which there were no electronic copies available. In some cases, original copies were obtained from retired staff or from the ESO library in Chile. The greater task, however, required the addition, correction and migration of over 3500 records to a database management system. As a result, improved browsing and search functions are now available on the ESO *Messenger* webpage for all issues from the first, in May 1974, to the present.

Behind the scenes, the journal publication process for *The Messenger* is now handled through a new electronic publishing platform called Marathon. Through Marathon, the *Messenger* editor and layout

and graphic artists can now manage the publication workflow and publish the completed *Messenger* issues directly to the web. Metadata for *The Messenger* can now be easily exchanged through Marathon automatically with the Astrophysics Database System (ADS), the primary literature search tool for astronomers worldwide. Thus author and title information are available in ADS for all *Messenger* articles together with access to the full text.

Additional metadata curation is being planned alongside improvements to the underlying systems and interfaces. In the meantime, *The Messenger* issues and articles are available through the current interface[1]. *The Messenger* can also be accessed through the social publishing website Scribd[2] and visibility has increased through Google.

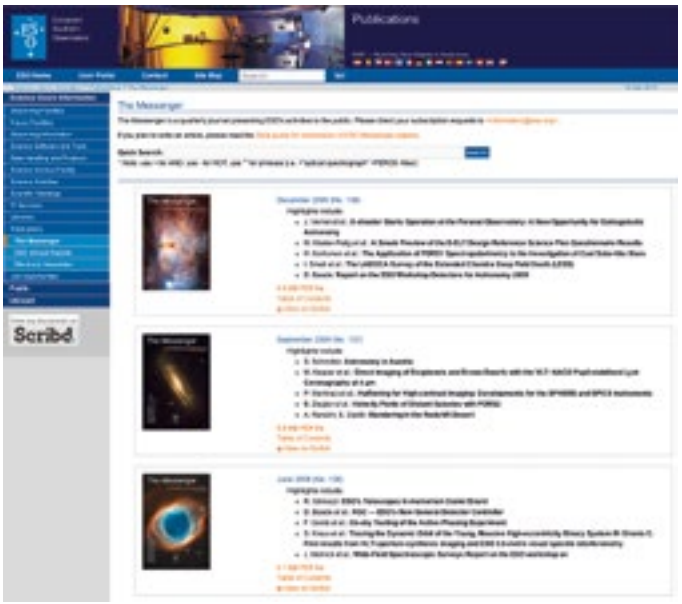

Figure 1. The ESO web page with access to back copies and content of *The Messenger*.

The Messenger digitisation and archiving project is a result of the hard work and support of Marco Schilk of InduPrint, Lee Pullen, Jeremy Walsh, Jutta Boxheimer, Uta Grothkopf, Martin Cullum, and María Eugenia Gómez, under the direction of the author. Future developments will be under the direction of Lars Holm Nielsen, Web & Advanced Projects Coordinator for ePOD.

Links

[1] The Messenger: http://www.eso.org/sci/publications/messenger
[2] Scribd: http://www.scribd.com/

New Staff at ESO

Daniel Bramich

I am a mathematician turned astronomer. I studied maths at Christ's College, Cambridge, from 1997–2000, specialising with my last year in theoretical astrophysics. Not convinced I was ready for a PhD, I spent a year working as a student support astronomer at the Isaac Newton Group (ING) in La Palma, Canary Islands. The time on La Palma sparked my interest in data reduction algorithms and observational techniques, which became an essential part of my work during my PhD, which I carried out under the supervision of Keith Horne in St Andrews. The result of my PhD thesis was a non-result, in that I was looking for a transiting planet and did not find any. However, a null result can be important, and the thrust of my thesis was the calculation of limits on the hot Jupiter planet fraction in the open cluster NGC 7789. Today I am still looking for a transiting planet of my own, and although many have been discovered, they still elude me!

My life seemed to go backwards and forwards between the Canary Islands and the UK, from the sun to the clouds and back again! The last year of my PhD (2004) was spent in Tenerife, and I subsequently carried out short contractual postdocs at St Andrews, Liverpool John Moores University and Cambridge University (2005–2006). By the end of these periods it was clear that my interests and work concentrate on both science and the algorithms and data used to carry out the science, which also suits my strong mathematical background.

Yearning for some more sun, I spent the next three years back on La Palma as a Support Astronomer for the ING, where I expanded my observing experience with the large suite of instruments available at the WHT. My research time was invested in the technique of difference imaging, and I developed a new method for matching the point spread function between two images, with minimal assumptions about the shape of the matching convolution kernel. The method is now starting to prove more robust than the traditional method, and my implementation is now part of an automatic

pipeline in use by at least five large collaborations, searching for planets, variable stars and supernovae.

I arrived at ESO in September 2009 to start work in the Science Data Products (SDP) group in the Data Management and Operations (DMO) department. My presence doubles the size of SDP: I am sure that my supervisor is very pleased about this because he now has someone to whom to delegate! The number "two" seems to feature strongly in this group at other levels, since both its members have twin daughters.

My work at ESO involves verifying the algorithms that are used in the data pipelines for the VLT instruments, and checking that the resulting data products are of sufficient quality to be used for scientific purposes. I am also involved in the testing of ESO pipelines, validating the documentation and providing guidance on the implementation of scientific algorithms. I enjoy working alongside the software engineers who are actually writing the code to do the data processing since it is clear that the results of the collaboration are much better than if either group were to work alone. The software engineers appreciate the insight into the purpose of their software, and the astronomers appreciate a well-written and robust code for data processing. In fact "astronomers" and "good programming technique" are two things you rarely find together!

The other aspect of my work at ESO is my research, which now directly feeds both ways into the operational side of my job, because of my interests in data reduction algorithms. I am confident that as a result I can provide useful expertise to ESO data reduction operations, and that in return I will learn about new areas of data reduction that may help inspire my work into new algorithms.

Elizabeth Humphreys

I seem to keep moving to cold places, so Munich was definitely on the cards when I saw the position of ESO ALMA Regional Centre Astronomer advertised last year. Apart from being British, so obviously very used to bad weather, I've spent the past ten years first as a post-

Daniel Bramich

doctoral fellow at Onsala Observatory, Sweden, followed by a postdoctoral research position and then staff member of the Harvard–Smithsonian Center for Astrophysics, Massachusetts. Both places that have pretty serious winters, so I haven't been phased by all the snow here yet!

I've really liked all of my jobs, and it's been an adventure to live far away for a while, but when I saw an ALMA position that also involved moving closer to home and back to Europe then I couldn't resist. ALMA is literally going to revolutionise all of the research I am planning to do, so I'm really excited to be more involved with the project and see it develop in close up. Literally in close up, as in the autumn I will be going to Chile for six months to work directly with the ALMA commissioning team at Chajnantor.

My research mainly takes advantage of astrophysical masers, which can be used as tools to determine astronomical source conditions, kinematics and magnetic fields. In my PhD at the University of Bristol, UK, this involved studying the mass loss process of evolved stars. I went on to work on the central parsecs of active galactic nuclei, where masers can also be used to obtain high accuracy black hole masses and geometric source distances. This is leading to new avenues of research for me in the realms of the extragalactic distance scale, and determination of the nature of dark energy. I never thought that I'd be researching topics like these when I started out! I'm also interested in the formation process of massive stars, a problem that is in general still far from being understood.

I feel really lucky that I've been able to diversify research topics since being a student, and am now looking forward to the new directions and collaborations that this move to ESO will bring.

Elizabeth Humphreys

Fellows at ESO

Thomas Bensby

Thomas Bensby and family

Having entered a new decade twice within just a few weeks, I realise that time is passing really quickly. It seems that we just came to Chile, and now it's already time to leave. However, considering that the family has grown here in Chile, and that the most recent addition is almost two years old, it must be true. Three years in Chile, but where did the time go?

The short answer: Paranal!

Longer answer (with a prelude): During my PhD, which I finished in 2004 at Lund Observatory in Sweden, I worked on detailed elemental abundance studies of the Galactic thin and thick discs. It was during this time I had my first observing experience with the FEROS and the CES spectrographs on the ESO 1.5-metre and 3.6-metre telescopes on La Silla, and the SOFIN spectrograph on the Nordic Optical Telescope (NOT) telescope on La Palma. Before coming to Chile in 2007 as an ESO Fellow I spent three years as a postdoc at the University of Michigan. Originally I was supposed to do theoretical work on models of chemical evolution, but, as Michigan is a partner in the Magellan consortium, I could not resist applying for observing time. I ended up doing a lot of observing (and less modelling), with the MIKE and the IMACS spectrographs (the latter with multi-slit masks). Naturally, as a consequence of my experience with high resolution spectrographs I have, during my time here at ESO, been a support astronomer on the VLT Kueyen (UT2) telescope with its excellent set of instruments, including the UVES and FLAMES spectrographs. Now with the X-shooter spectrograph installed, UT2 is a Mecca for spectroscopists. I have been fortunate to have been a (small) part of UT2 for a few years, and am really looking forward to coming back as a visiting astronomer.

Outside of Paranal, Chile has offered, given, and also taken a lot. Six months of summer is great, living close to the Andes with spectacular natural environment all around is great, having vineyards everywhere is great, 45 minutes to the ski resort is great, and one hour to the beach is great. Being robbed of all valuables upon arrival at the airport is of course bad. The greatest gift here in Chile has been our third daughter Mira, the only Chilean in the family. Even though the Spanish language has (at least for me) not been easy, our other two daughters Sofia and Alva are, after our "tour de las Americas", trilingual, happily speaking Swedish, English and Spanish. So, after six years "on tour" it is with mixed feelings we go back. Anyway, it will be great to once again be able to eat good cheese and feast on pickled herrings.....

Paula Stella Teixeira

My story begins when I was told, as a very young child, what my name, Stella, meant. I have been fascinated by the stars ever since! I was born and spent my childhood under southern skies, and I remember identifying the Magellanic Clouds and the Coalsack, knowing these were famous astrophysical objects, but not knowing (yet!) what exactly they were. My family encouraged my interest, particularly my brother, who gave me a telescope when I was seven years old and who often took his little sister to science museums. My curiosity made me continue to wonder about the Universe, and so I grew up with a dream of becoming an astronomer.

I embarked on a path which began with a Physics undergraduate degree at the University of Lisbon, Portugal. I stayed on for an MSc in Astronomy and Astrophysics and enrolled in a PhD programme at the same university. At the beginning of my doctoral studies I was awarded a Smithsonian Predoctoral Fellowship, and off I went to the Harvard–Smithsonian Center for Astrophysics, in Cambridge Massachusetts, USA to carry out my research for the next five years. It was an extremely rewarding experience, both on a professional and personal level! I finished my PhD in the fall of 2008 and moved to Garching for an ESO Fellowship.

My research is primarily based on observational studies of low- and intermediate-mass star formation. I began working on ESO NTT near-infrared imaging data during my MSc, and progressively have been shifting to longer and longer wavelengths: during my PhD I analysed mid-infrared Spitzer data and ended up venturing into the (sub)millimetre realm with the Sub-Millimeter Array (SMA). I am interested in many aspects of star formation, namely, the collapse and fragmentation of filamentary molecular clouds, proto-binaries, the characterisation of young star-forming clusters, and the evolution of circumstellar discs and planet formation. I approach these topics from a multi-wavelength perspective.

ESO offers a wide spectrum of opportunities for me to expand my knowledge and horizons. Regarding my functional duties, I am involved with the second generation VLTI PRIMA instrument and

am part of the VISTA Science Verification Team. I am also co-organising a weekly meeting, the Informal Discussion, which has allowed me to interact with many visiting astronomers and learn about multiple aspects of the science being pursued at ESO and/or using ESO telescopes.

The future of astronomy is very promising, with ALMA coming online soon and the development of ESO's E-ELT. I am very fortunate to be able to pursue my childhood dream and hope to continue on this journey. One of my specific goals is to use these upcoming cutting-edge facilities, combining a multi-wavelength approach with stunning angular resolution!

Paula Stella Teixeira

Announcement of the ESO Workshop

Spiral Structure in the Milky Way: Confronting Observations and Theory

7–10 November 2010, Bahía Inglesa, Copiapó, Chile

Our knowledge of spiral arms in the Milky Way and the kinematics in the Solar Neighbourhood has increased significantly over the last few decades. Despite these advances, there is still no consensus on basic parameters of the spiral structure in our Galaxy, such as the number of major spiral arms and their location, the pattern speed(s) and amplitude, and the relation of the arms to the central bar. Major new facilities (e.g., ALMA, GAIA, LSST, VISTA and VST) will provide a wealth of data on the spatial and kinematic distributions of material in the Galaxy. Thus, it seems appropriate to perform a census of the current data for confrontation with theory and models of spiral structure, and thereby map out a path towards a consolidated view of the spiral pattern in the Milky Way.

The workshop will bring together observers and theoreticians, and thereby facilitate an in-depth discussion of the spiral structure in the Milky Way.

The main topics will be:
– Tracers of spiral arms in the Milky Way at any wavelength
– Kinematic indicators of the spiral pattern in our Galaxy
– Models and theory related to the Milky Way spiral structure
– Estimates of parameters for the spiral pattern in our Galaxy

Scientific Organising Committee:
Yuri Beletski (ESO), Leonardo Bronfman (Universidad de Chile), Giovanni Carraro (ESO), Ortwin Gehrard (Max-Planck-Institut für extraterrestrische Physik), Preben Grosbøl (ESO), Vladimir Korchagin (South Russia Federal University), Jorge May (Universidad de Chile), Naomi McClure-Griffiths (Australia Telescope National Facility), Lars-Åke Nyman (ALMA), Delphine Russeil (Observatoire de Marseille).

The workshop is planned for 3.5 days with four sessions for each of the full days. The first three sessions will contain long reviews (40 + 5 m) and some contributed talks (15 + 5 m). The last session of each afternoon will be devoted to discussions plus short summaries of selected posters. We aim for around 50 participants with a maximum of 70 as allowed by local facilities. Proposals for both contributed talks and posters are invited. Students are particularly encouraged to apply.

Further details are available at http://www.eso.org/sci/meetings/MW2010/.

The deadline for registration is 6 June 2010.

ESO

European Organisation
for Astronomical
Research in the
Southern Hemisphere

ESO Studentship Programme

The European Southern Observatory research student programme aims at providing opportunities to enhance the PhD programmes of ESO member-state universities. Its goal is to bring young scientists into close contact with the activities and people at one of the world's foremost observatories. For more information about ESO's astronomical research activities please consult http://www.eso.org/science/.

The ESO studentship programme is shared between the ESO Headquarters in Garching (Germany) and the ESO offices in Santiago (Chile). These positions are open to students enrolled in a PhD programme in astronomy or related fields. In addition, ESO will provide up to two studentship positions per year in Santiago for students enrolled in South American universities.

Students in the programme work on their doctoral project under the formal supervision of their home university. They come to either Garching or Santiago for a stay of normally between one and two years to conduct part of their studies under the co-supervision of an ESO staff astronomer. Candidates and their home institute supervisors should agree on a research project together with the ESO local supervisor. A list of potential ESO supervisors and their research interests can be found at http://www.eso.org/sci/activities/personnel.html. A list of current PhD projects offered by ESO staff is available at http://www.eso.org/sci/activities/thesis-topics/. It is highly recommended that the applicants start their PhD studies at their home institute before continuing their PhD work and developing their research projects at ESO.

ESO Chile students will have an opportunity to visit the observatories and to get involved in small projects aimed at giving insights into the observatory operations.

In Garching students may attend, if desired, and benefit from the series of lectures given to the PhD students enrolled in the IMPRS (International Max-Planck Research School on Astrophysics) PhD programme. Students who are already enrolled in a PhD programme in the Munich area (e.g., the IMPRS or at a Munich University) and wish to apply for an ESO studentship in Garching, should provide compelling justification for their application.

The Outline of the Terms of Service for Students (http://www.eso.org/public/employment/student.html) provides some more details on employment conditions and benefits.

Please attach to your application the following documents:
– a Curriculum Vitae (including a list of publications, if any), with a copy of the transcript of university certificate(s)/diploma(s);
– a summary of the Masters thesis project (if applicable) and ongoing projects, indicating the title and the supervisor (maximum half a page), as well as an outline of the PhD project, highlighting the advantages of coming to ESO (recommended 1 page, max. 2);
– two letters of reference, one from the home institute supervisor/advisor and one from the ESO local supervisor;
– a letter from the home institution that: i) guarantees the financial support for the remaining PhD period after the termination of the ESO studentship; and ii) indicates whether the requirements to obtain the PhD degree at the home institute are already fulfilled.

All documents should be submitted in English (but no translation is required for the certificates and diplomas).

Review of the received material, including the recommendation letters, will start on 15 June 2010. Applications arriving after this deadline will be considered until all the positions are filled. Incomplete applications will not be considered. All reference letters must be sent electronically to vacancy@eso.org.

Candidates will be notified of the results of the selection process in July 2010. Studentships typically begin between August and December of the year in which they are awarded. In well-justified cases, starting dates in the year following the application can be negotiated.

For further information please contact Christina Stoffer (cstoffer@eso.org).

Although recruitment preference will be given to nationals of ESO Member States (members are: Austria, Belgium, the Czech Republic, Denmark, Finland, France, Germany, Italy, the Netherlands, Portugal, Spain, Sweden, Switzerland and United Kingdom) no nationality is in principle excluded.

The post is open equally to suitably qualified male and female applicants.

Announcement of the Workshop

Science with ALMA Band 5 (163–211 GHz)

24–25 May 2010, Osservatorio Astronomico di Roma, Italy

There is increasing interest in observations at frequencies between 163 and 211 GHz (ALMA Band 5) for both Galactic and extragalactic science. A key application is high resolution imaging of the water line at 183 GHz in Galactic and nearby extragalactic sources. In addition, the 158 micron line of C^+ from objects at redshifts between 8.0 and 10.6 will appear in the band, opening up the possibility of probing the earliest epoch of galaxy formation.

The recent launch of Herschel and the imminent commissioning of ALMA offer complementary approaches: Herschel will allow spectroscopy free from absorption by water in the Earth's atmosphere, but at low spatial resolution, whereas ALMA observations will provide very high spatial resolution.

The European Union is funding the production of six Band 5 receivers for ALMA through the FP6 Enhancement Programme, together with the development of advanced phase correction and mapping techniques to support these challenging observations. The receivers will be delivered to ALMA in 2010–2011. The ALMA Project will be seeking proposals for enhancement of the instrument in the near future. These are likely to include the development of a full set of Band 5 receivers (66 + spares).

The aims of the workshop are:
– to assess the potential of ALMA Band 5 for both Galactic and extragalactic applications;
– to inform the community of the opportunities for observing with the initial set of Band 5 receivers;
– to develop synergies with the Herschel mission;
– to discuss technical approaches to the production of a full set of receivers;
– to evaluate approaches to calibration and data reduction for the band.

The primary output will be a science case for a full set of Band 5 receivers on ALMA, to be submitted to arXiv.

Scientific Organising Committee:
Paola Caselli (Leeds), Jose Cernicharo (Madrid), Robert Laing (ESO, chair), Roberto Maiolino (Rome), Leonardo Testi (ESO), Fabian Walter (Heidelberg).

SIXTH FRAMEWORK PROGRAMME

The workshop will take place at the Osservatorio Astronomico di Roma on 24 and 25 May 2010. There will be a small number of invited reviews, together with ample time for contributed papers and discussion. We anticipate a small, focused meeting with approximately 50 participants.

Limited financial support (primarily for young researchers from EU institutions) will be available from the EU ALMA Enhancement Programme. There will be no registration fee.

Further details are available at http://web.oa-roma.inaf.it/meetings/AlmaBand5/Home.html.

Credit: ESO/Ueli Weilenmann

Adriaan Blaauw, former Director General (1970-74), visited Paranal in February 2010 and is shown (centre) next to one of the VLT Unit Telescopes and in discussion with the current Director General, Tim de Zeeuw (right) and the Director of the La Silla Paranal Observatory, Andreas Kaufer (left).

Announcement of the Workshop

HTRA-IV: Era of Extremely Large Telescopes

5–7 May 2010, Aghios Nikolaos, Crete, Greece

The goal of the fourth High Time Resolution Astrophysics (HTRA) workshop is to explore the current and future state of observations of all different types of astronomical sources featuring variability at the second and/or subsecond time scales. The three-day workshop has been planned to offer the community the opportunity to present contributions in different thematic areas covering science, instrumentation and future observing facilities. Selected science topics include: isolated neutron stars; X-ray binaries; white dwarfs and ultra-compact binary systems; stellar oscillations; flare stars; extragalactic transients (GRBs); and planet transits/occultations. Contributions in other science topics related to the field of HTRA are equally welcome.

The focus of the HTRA-IV workshop is on optical studies in all of the above science areas. In particular, the major emphasis will be on optical observations and on the potential of HTRA with the next generation of Extremely Large Telescopes (like the European Extremely Large Telescope, the Thirty Meter Telescope and the Giant Magellan Telescope) to make discoveries beyond our current state of knowledge and expectations. However, the workshop will also focus on multi-wavelength HTRA studies (radio, X-rays and gamma rays) both with present (XMM, CHANDRA, FERMI) and future (e.g., IKO and SKA) observing facilities.

The purpose is to create a unique opportunity for interaction between the HTRA community and the wider astronomical community. This will stimulate discussions on the exploitation of the scientific potential of future facilities, on the development of their instrumentation, and on a number of technical and engineering aspects related to their design and operation.

Invited speakers include: Felix Aharonian (Dublin Institute of Advanced Studies), Werner Becker (Max-Planck-Institut für extraterrestrische Physik), Tomaso Belloni (INAF–Astronomical Observatory of Brera, Merate), Vik Dhillon (University of Sheffield), Isobel Hook (University of Oxford), Michael Kramer (Jodrell Bank Centre for Astrophysics), George Pavlov (Penn State University), Ron Remillard (Massachusetts Institute of Technology), Andrea Richichi (ESO) and Jürgen Schmitt (Hamburg Observatory).

Scientific Organising Committee: Cesare Barbieri (University of Padova, Dept. of Astronomy), Giovanni Bonanno (INAF–Astronomical Observatory, Catania), Vik Dhillon (University of Sheffield), Dainis Dravins (Lund Observatory), Gottfried Kanbach (Max-Planck-Institut für extraterrestrische Physik), Nikos Kylafis (University of Crete, FORTH), Tom Marsh (University of Warwick), Roberto Mignani (University College London–Mullard Space Science Laboratory), Andy Shearer (National University of Ireland, Galway), Aga Slowikowska (Institute of Astronomy, University of Zielona Gora).

The workshop is organised as part of the OPTICON-funded European Network for High Time Resolution Astrophysics with the European Extremely Large Telescope (E-ELT).

Details and registration information can be found at http://www.htra.ie/.

Beyond 2009: ESO at the Closing Ceremony of the International Year of Astronomy

Claudia Mignone[1]
Pedro Russo[1,2]
Lars Lindberg Christensen[1]

[1] ESO
[2] IAU

The International Year of Astronomy (IYA 2009) officially closed with a ceremony held at the University of Padova where Galileo Galilei taught physics. A brief description of the ceremony and the contribution of ESO are presented.

On 9 and 10 January 2010 the International Year of Astronomy (IYA 2009) reached its official close with a ceremony that took place in Padova, Italy, in the Aula Magna of the University of Padova, where Galileo Galilei taught experimental physics and astronomy between the end of the 16th and the beginning of the 17th century (see the image on the Astronomical News section page).

Figure 1. Chart from iya1001 Press Release. This diagram shows a selection of the projects taking place during the International Year of Astronomy, highlighting the huge diversity of activities, programmes and initiatives that characterised this unique venture.

As a celebration of Galileo's first observations of the skies through a telescope and of the subsequent 400 years of discoveries, the IYA2009 was launched by the International Astronomical Union (IAU) and the United Nations Educational, Scientific and Cultural Organization (UNESCO) under the theme "The Universe, Yours to Discover". After a long year, rich both in global projects and grass-roots initiatives, the organisers of the event gathered from all over the world to recount some of the multitude of experiences collected during this amazing venture that brought astronomers, amateurs and the general public together in 148 countries worldwide.

Around 280 people attended the closing ceremony, including eminent scientists from the Italian and international astronomical communities. Among the many astronomers present at the event was Franco Pacini from the Observatory of Arcetri, originator of the year of astronomy concept back in 2002. He pointed out the potential of astronomy as a truly global scientific discipline that unites researchers in the quest for answers to some of the most fundamental questions that humankind has ever asked.

Former ESO Director General Catherine Cesarsky, Chair of the IYA2009 Working Group and IAU President during most of IYA2009, reviewed the steps made in the organisation of what turned out to be the largest network ever built in science. "*Over the past 12 months we have seen astronomy enter the public's imagination and inspire people to ask the grandest questions,*" she said. "*The International Year of Astronomy 2009 has been an unforgettable journey and I am pleased to see that many of the projects will continue.*"

The ceremony featured a massive retrospective of many projects and activities conducted throughout the year (see Figure 1), from the great success of global events such as 100 Hours of Astronomy and From Earth to the Universe, to the creative effort of prodigious initiatives that have come from individual countries. The highlights were presented by the key organisational figures of IYA2009, including Pedro Russo and Lars Lindberg Christensen from the IYA2009 Secretariat at ESO Headquarters, as well as by some of the national Single Points of Contacts (SPoCs) who reported on the activities organised in several developing countries.

In the spirit of the theme of the ceremony, bearing the ambitious title, Beyond 2009, this survey of past activities and events was not intended as a nostalgic collection of memories, but instead as a solid base for future enterprises in public outreach of astronomy and science in general (see the logo in Figure 2). Many of the projects of IYA2009 will continue in the following years either unchanged or in a slightly changed form; several other initiatives significantly helped to pave the way for a network of researchers and educators focused on the communication of astronomy, especially in developing countries where a strong astronomical community is not yet present.

ESO's presence at the ceremony

The International Year of Astronomy 2009 has been a global celebration of the four centuries of revolutionary discoveries achieved through the use of the telescope. Ever since Galileo's very first observations of the sky with a more powerful tool than the human eye, the instruments used by astronomers have changed and evolved ceaselessly. Looking further, Roberto Gilmozzi from ESO gave an extensive overview of astronomy after the IYA2009, focussing on the telescopes of tomorrow and particularly on the European Extremely Large Telescope (E-ELT) which will become "the world's biggest eye on the sky". Along with a description of the main science drivers that led to the concept of extremely large telescopes, such as the search for Earth-like exoplanets and for the first stars and galaxies that formed in the Universe, Gilmozzi's talk highlighted how telescopes have grown in dimensions ever since Galileo's time and how the E-ELT, with its 42-metre primary mirror, would be a natural extension of this time-honoured tradition. The revolutionary design of this outstanding observatory and the timeline of the projects were also presented, followed by a look at the distant future, and the possible projects astronomers are planning even beyond the ELTs.

Although the main part of IYA2009 is over, it leaves an important legacy for the worldwide astronomical community including an impressive network for the future with ESO education and public outreach at its focal point.

Figure 2. Beyond IYA Logo. The logo of Beyond IYA, the signature that labels the legacy projects continuing after 2009.

In Memoriam Karin Horn-Hansen

Tim de Zeeuw[1]

[1] ESO

Karin Hansen, as she was known at ESO, was born in Lyngby in Denmark and began work in the Personnel Department in July 1991 where she was involved in the recruitment process and health insurance. In 1993 she moved to Finance Services and in 1997 became secretary to the Head of Administration. She moved to the Office of the Director General in September 2007 where she continued to act as the contact point at ESO for all matters related to Council. Karin was known for her excellent performance, complete reliability and high motivation, carrying out the complex and demanding tasks in support of Council, the Finance Committee and senior management, always maintaining excellent relationships with her internal and external contacts. She was diagnosed with a serious illness in mid-2008, but seemed to recover and returned to ESO part-time in the spring of 2009 and was married in June. Unfortunately the illness returned, and Karin passed away peacefully on 29 December 2009. She was a remarkable person,and will be remembered with great affection by many.

In Memoriam Nelson Montano

Roberto Tamai[1]

[1] ESO

Nelson Montano, Head of the Maintenance Department of the La Silla Paranal Observatory, died suddenly on 10 March 2010, at the age of 42 years.

Nelson joined ESO at the Paranal Observatory in May 1999 as a mechanical engineer. His warm, indefatigable character, as well as his well-organised personality helped to propel him to the position of Head of the Maintenance Department of the La Silla Paranal Observatory in 2004. For the first time in an astronomical observatory, an engineer succeeded in putting into practice abstract theoretical maintenance concepts, achieving superb results. The worldwide astronomical community has been impressed by this achievement.

Nelson was recognised not only in the astronomical community, but also around the world in the industrial environment field, and he participated as an invited speaker at international industrial maintenance conferences.

Nelson will be remembered by his colleagues and friends at ESO not only for his dedication, commitment and professionalism but also for his generous, open and friendly personality that was deeply appreciated by all. He will be dearly missed by his wife and son.

Personnel Movements

Arrivals (1 January–31 March 2010)

Europe	
Abad, José Antonio (E)	Mechanical Engineer
Bargna, David (GB)	IT Infrastructure Specialist
Esselborn, Michael (D)	System Analyst
Gago, Fernando (E)	Control Engineer
Hammersley, Peter (GB)	Systems Scientist
Kalaitzoglou, Dimitrios (GR)	Electrical Engineer
Märcker, Matthias (D)	Fellow
Marrero Hernandez, Juan Antonio (E)	Mechanical Engineer
Muckle, Christian (D)	Site Safety Engineer
Ridings, Robert (GB)	Mechanical Engineer
Rushton, Anthony (GB)	Fellow
Smolcic, Vernesa (HR)	Fellow
Zilker-Kramer, Irmtraud (D)	Administrative Assistant
Chile	
Alarcon, Javier (RCH)	Telescope Instruments Operator
Berger, Jean-Philippe (F)	Staff Astronomer
Calisse, Paolo Gherardo (I)	Test Scientist
Carrasco, Mauricio (RCH)	Student
Cortes, Alejandra (RCH)	Safety Officer
de Wit, Willem-Jan (NL)	Operations Astronomer
Drass, Holger (D)	Student
Fulla Marsa, Daniel (E)	Commissioning Scientist (JAO)
Kublik, Basilio (RCH)	IT Infrastructure Specialist
Küpper, Andreas (D)	Student
León, Angélica (RCH)	Telescope Instruments Operator
Leon Tanne, Stéphane (E)	System Astronomer
Villard, Eric (F)	Commissioning Scientist (JAO)
Wiklind, Tommy (S)	Operations Astronomer

Departures (1 January–31 March 2010)

Europe	
Baginski, Isabelle (D)	Administrative Assistant
Blondin, Stéphane (F)	Fellow
De Silva, Gayandhi Manomala (AUS)	Fellow
Dinjens-D'Lazarus, Mary (NL)	Administrative Assistant
Gieles, Mark (NL)	Fellow
Heymann, Frank (D)	Student
James, Gaël (F)	Fellow
Kubas, Daniel (D)	Fellow
Chile	
Almeida, Pedro Viana (P)	Student
Argomedo, Javier (RCH)	Software Engineer
Castizaga, Jorge (RCH)	Master Cook
Ruppert, Jan (D)	Student

Image next double page:
A VISTA mosaic of the central region of the Milky Way formed from images in *Y*, *J* and *Ks* bands. The image is about 2.0 by 1.5 degrees in size and the total exposure time was 80 seconds. See ESO Press Release eso0949 for more details.

Annual Index 2009 (Nos. 135–138)

Subject Index

Astronomical News

Author Index

ESO, the European Southern Observatory, is the foremost intergovernmental astronomy organisation in Europe. It is supported by 14 countries: Austria, Belgium, the Czech Republic, Denmark, France, Finland, Germany, Italy, the Netherlands, Portugal, Spain, Sweden, Switzerland and the United Kingdom. ESO's programme is focused on the design, construction and operation of powerful ground-based observing facilities. ESO operates three observatories in Chile: at La Silla, at Paranal, site of the Very Large Telescope, and at Llano de Chajnantor. ESO is the European partner in the Atacama Large Millimeter/submillimeter Array (ALMA) under construction at Chajnantor. Currently ESO is engaged in the design of the 42-metre European Extremely Large Telescope.

The Messenger is published, in hardcopy and electronic form, four times a year: in March, June, September and December. ESO produces and distributes a wide variety of media connected to its activities. For further information, including postal subscription to The Messenger, contact the ESO education and Public Outreach Department at the following address:

ESO Headquarters
Karl-Schwarzschild-Straße 2
85748 Garching bei München
Germany
Phone +49 89 320 06-0
information@eso.org
www.eso.org

The Messenger:
Editor: Jeremy R. Walsh
Design: Jutta Boxheimer; Layout, Typesetting: Jutta Boxheimer and Mafalda Martins; Graphics: Roberto Duque
www.eso.org/messenger/

Printed by Peschke Druck
Schatzbogen 35, 81805 München
Germany

ISSN 0722-6691

Contents

Front Cover: A section (14 × 19 arcminutes in size) from a large colour composite image of the Orion Nebula region (M 42 and M 43) taken with VISTA — the Visible and Infrared Survey Telescope for Astronomy. The image was formed from exposures in *Z*, *J* and *Ks* filters and shows a region north of M 43, which is relatively featureless in the optical, with an abundance of embedded outflow sources associated with young low mass stars. Features appearing in blue are reflection nebulae and in red are emission of molecular hydrogen. See ESO Press Release eso1006 for more details.